Active Power Balancing in Multi-Terminal DC Systems

Zur Erlangung des akademischen Grades Doktor-Ingenieur (Dr.-Ing.)
Genehmigte Dissertation von Dipl.-Ing. Sebastian Weck aus Heidelberg, Deutschland
Tag der Einreichung: 1. Februar 2022, Tag der Prüfung: 6. Juli 2022

1. Gutachten: Prof. Dr.-Ing. Jutta Hanson
2. Gutachten: Prof. Dr.-Ing. Dirk Westermann
Darmstadt, Technische Universität Darmstadt

TECHNISCHE UNIVERSITÄT DARMSTADT

Fachbereich Elektrotechnik und Informationstechnik

FG Elektrische Energieversorgung unter Einsatz Erneuerbarer Energien (E5)

Active Power Balancing in Multi-Terminal DC Systems

Genehmigte Dissertation von Dipl.-Ing. Sebastian Weck

Tag der Einreichung: 1. Februar 2022
Tag der Prüfung: 6. Juli 2022

Darmstadt, Technische Universität Darmstadt

Bitte zitieren Sie dieses Dokument als:
URN: urn:nbn:de:tuda-tuprints-228781
URL: http://tuprints.ulb.tu-darmstadt.de/22878
Jahr der Veröffentlichung auf TUprints: 2022

Dieses Dokument wird bereitgestellt von tuprints,
E-Publishing-Service der TU Darmstadt
http://tuprints.ulb.tu-darmstadt.de
tuprints@ulb.tu-darmstadt.de

Erklärungen laut Promotionsordnung

S 8 Abs. 1 lit. c PromO

Ich versichere hiermit, dass die elektronische Version meiner Dissertation mit der schriftlichen Version übereinstimmt.

S 8 Abs. 1 lit. d PromO

Ich versichere hiermit, dass zu einem vorherigen Zeitpunkt noch keine Promotion versucht wurde. In diesem Fall sind nähere Angaben über Zeitpunkt, Hochschule, Dissertationsthema und Ergebnis dieses Versuchs mitzuteilen.

S 9 Abs. 1 PromO

Ich versichere hiermit, dass die vorliegende Dissertation selbstständig und nur unter Verwendung der angegebenen Quellen verfasst wurde.

S 9 Abs. 2 PromO

Die Arbeit hat bisher noch nicht zu Prüfungszwecken gedient.

Darmstadt, 1. Februar 2022

Dipl.-Ing. Sebastian Weck

Gewidmet meiner Familie

Vorwort und Danksagung

Die vorliegende Arbeit entstand während meiner Zeit als wissenschaftlicher Mitarbeiter am Fachgebiet Elektrische Energieversorgung unter Einsatz Erneuerbarer Energien an der Technischen Universität Darmstadt. Während dieser Zeit durfte ich das Themenfeld Lehre und Forschung kennenlernen.

Für diese Gelegenheit und für die wissenschaftliche Betreuung meiner Dissertation möchte ich mich bei Frau Prof. Dr.-Ing. Hanson herzlich bedanken. Das entgegengebrachte Vertrauen und die Freiheit zur wissenschaftlichen Entfaltung haben die Arbeit in dieser Form erst ermöglicht. Des Weiteren möchte ich mich bei Herrn Prof. Dr.-Ing. Westermann für die Übernahme des Korreferats und die guten fachlichen Diskussionen bedanken.

Mein herzlicher Dank gilt weiterhin meinen ehemaligen Kolleginnen und Kollegen am Fachgebiet und in den verschiedenen Forschungsprojekten. Der sowohl wissenschaftlich als auch privat sehr wertvolle Austausch während dieser Zeit hat mich maßgeblich geprägt und wesentlich zu Motivation und Inhalt dieser Arbeit beigetragen.

Darüber hinaus möchte ich mich bei meinen Eltern bedanken, die mir das Selbstvertrauen und die Inspiration mitgegeben haben, diese Arbeit anzugehen, und die mich stets bedingungslos unterstützt haben. Ebenso danke ich meinen Geschwistern und ihren Familien und meinen Schwiegereltern für das fortwährende Interesse an meiner Arbeit.

Schließlich gilt mein besonderer Dank meiner Familie, die mich während der letzten Jahre immer unterstützt und mir die notwendige Freiheit für die Fertigstellung der Arbeit gegeben hat.

Heidelberg, im November 2022 Sebastian Weck

Abstract

The present work deals with active power balancing in embedded multi-terminal dc systems. The derived controller and grid control concept is able to achieve a significant improvement in power transmission deviations and excitation of oscillatory modes in the case of a converter outage.

Starting point for the design is the derivation of control requirements based on an analysis of state of the art converter control and dc grid control concepts in the context of active power balancing. The basic requirements are subsequently developed into design principles for a generalized controller and a derived tiered grid control concept.

The controller is designed based on a continuous integration of constant voltage, voltage droop and constant power control. This is achieved by a construction of the control characteristic and the subsequent gain scheduling of the individual loops as well as the PI control gain.

Finally, the grid concept is described and simulated on a number of benchmark cases in order to show the effectiveness of the proposed controller and grid concept. Results show, that the defined control objectives can be achieved, i.e. the controller implements the grid concept, the system is stable for all operating points and power transmission deviations and the excitation of oscillatory modes is kept at a minimum.

Keywords: HVDC, MTDC, Active power control, dc voltage control

Kurzfassung

Die vorliegende Arbeit behandelt das Thema Wirkleistungsgleichgewicht in Multi-Terminal HGÜ-Systemen. Es wird ein Regelungskonzept sowohl auf der Umrichter- als auch auf der Netzebene vorgeschlagen, das im Falle eines Umrichterausfalls den Einfluss auf das umgebende Drehstromnetz in Bezug auf den Leistungsfluss und Generator-Oszillationen minimiert.

Aufbauend auf einer Analyse bestehender Konzepte zum Erreichen eines Wirkleistungsgleichgewichtes werden Anforderungen für das Regelungskonzept aufgestellt. Diese gelten als Grundlage für den Entwurf eines allgemeingültigen Reglers und den hierauf aufbauenden Netzkonzepten.

Die Umrichterregelung basiert auf einer Verallgemeinerung der existierenden Konzepte in einer Regelstruktur, die sowohl eine Wirkleistungs- und Spannungsregelung als auch dezentrale Konzepte zur Gleichspannungsregelung umsetzen kann. Hierfür wird eine kontinuierliche Regelcharakteristik erzeugt, die durch eine Parameter-Adaption des Regelkreises und PI-Reglers umgesetzt wird.

Schlussendlich wird das Netzregelungskonzept beschrieben und anhand von Simulationen in Benchmark-Netzen verifiziert. Die Ergebnisse zeigen, dass die Regelungsanforderungen erfüllt werden. Das Netzregelungskonzept wird durch die Regler der Umrichter des HGÜ-Systems umgesetzt, das System ist für alle Betriebszustände stabil und die Wirkleistungsabweichungen und die Anregung der Schwingungsmoden werden auf ein Minimum beschränkt.

Schlüsselwörter: HGÜ, MT-HGÜ, Wirkleisungsregelung, Gleichspannungsregelung

Table of Contents

List of Figures

List of Tables

Abbreviations

ac	Alternating current
APB	Active power balance
AVM	Average value model
AVR	Automatic voltage regulator
dc	Direct current
DC-GIL	Dc gas insulated line
EMT	Electromagnetic transients
FB-SM	Full-bridge submodule
GC-APC	Generalized continuous active power controller
GOV	Turbine governor
GVD	Generalized voltage droop
HB-SM	Half-bridge submodule
HVDC	High voltage dc
ICC	Inner current controller
IGBT	Insulated gate bipolar transistors
IGCT	Integrated gate-commutated thyristor
LCC	Line-commutated converter
MMC	Modular multi-level converter

MPOPF	Multi-period OPF
MTDC	Multi terminal dc
OHL	Overhead line
OPF	Optimal power flow
PCC	Point of common coupling
PLL	Phase locked loop
PSS	Power system stabilizers
RES	Renewable energy sources
SCOPF	Security-constrained OPF
SRF	Synchronous reference frame
THD	Total harmonic distortion
TSO	Transmission system operator
VSC	Voltage source converter
XLPE	Cross-linked polyethylene

Symbols

Symbols related to AC and HVDC systems

V_{ac}	Voltage of the ac grid
V_{dc}	Voltage of the dc grid
I_{dc}	Direct current
$n_{\text{SM}}^{(\pm)}$	Number of submodules in a MMC (positive or negative arm)
C_{SM}	Submodule capacity
$\text{SM}_n^{\pm}$	n-th submodule on positive/negative arm of a MMC
S	Apparent power
P	Active power
Q	Reactive power
f	Ac grid frequency
$\boldsymbol{Y}_{\text{dc}}$	Dc system admittance matrix
CE	Capacitive energy in the dc system
C_{p}	Equivalent node capacity in the dc system

Symbols related to VSC control

d	Subscript for direct axis in Park-Transformation
q	Subscript for quadrature axis in Park-Transformation
i_{dq}	Measured current in pu in Park-Transformation
v_{dq}	Measured voltage in pu in Park-Transformation
i_{dq}^{*}	Reference current in pu in Park-Transformation
v_{dq}^{*}	Reference voltage in pu in Park-Transformation
k	Droop gain
Δ	Indicator for a deviation from the reference value
max, min, lim	Superscript for maximum, minimum and limit respectively
$D_{P/V}$	Static gain used in the generalized droop concept, for power and voltage respectively

Symbols specific to GC-APC

Γ	Control angle in degree
γ	Normalized control angle in pu
c_{max}	Scaling coefficient for the calculation of the control angle
$db^{\pm n}$	n-th threshold point for positive/negative plane, used to specify the dead-bands
$db_{\text{p/n}}$	Positive/negative transition points for smoothing of the characteristic
c_{r}	Continuity coefficient to calculate the transition points $db_{\text{p/n}}$
$\boldsymbol{P}$	Points to construct the Bézier curve
t	Scaling parameter to construct the Bézier curve
$K_{P/V}$	Power/voltage gain for the scheduling of the PI controller
K_{P}	Proportional gain for the PI controller
T_{i}	Integral time constant for the PI controller
$e_{(P/V)}$	Error signal for the PI controller (P/V corresponding to the power and voltage droop loops)
$c_{P/V}$	Scheduling gains for the power and voltage loop respectively

Symbols related to OPF

c	Subscript corresponding to converter values
P_{loss}	Active power losses
f_{obj}	Objective function of the OPF
α, γ	Constant and quadratic factor used for loss evaluation of HVDC converters
x, x^t, x^c	State vector of the OPF problem x and corresponding state vectors for time and contingencies

1. Preface

This work deals with the active power balancing in multi-terminal dc systems. The motivation for the topic is first given in section 1.1. Then the main contributions of the work are introduced in section 1.2. Finally, section 1.3 gives an outline over the approach chosen for this work.

1.1. Motivation

Climate concerns and advances in technologies are causing massive changes in the way energy is produced, documented by recent reports by the International Energy Agency's World Energy Outlook 2020 [1.1]. Renewable energy sources count among the most economical and ecological solutions available in the year 2020. The ever increasing integration of renewable energy sources into the electrical power system, however, brings along massive changes in the way power systems need to be designed and run. This is caused by increased regional imbalance and volatile energy generation. The power system operators adapt to these changes in their network planning outlooks, e.g. the most recent European and German network development plan, see[1.2] and [1.3] respectively.

One solution proposed for long-distance transmission of electrical energy is using high-voltage dc technology. This is already state of the art for point-to-point systems and can be extended to multi-terminal systems more and more in the future, one option being to construct embedded systems, i.e. an overlay grid over the existing ac transmission grid. These systems have a distinct influence on the stability of the ac system, as highlighted by Cigré in [1.4].

In addition, because the systems are composed of power electronic converters, the control plays a crucial role. The stable and optimal control of the dc voltage being one of the key tasks, which is achieved by an active power balancing strategy implemented in the system's converters.

1.2. Main Contributions

The control of (embedded) multi-terminal hvdc systems is not standardized to the same degree as for ac systems. One field of research is the control of active power between all converters of a dc system, which is highly linked to the control of a constant dc voltage. While the methodologies are not as mature as those for ac systems, there exist a high number of publications investigating this topic. The most generally recognized are summarized in the Cigré Technical Brochure *Control Methodologies for Direct Voltage and Power Flow in a Meshed HVDC Grid* [1.5].

The work presented in this document aims to follow up on the concepts proposed in the Cigré Technical Brochure. Furthermore, it aims to integrate into one common control methodology the most crucial findings presented in research on the topic, such as the preferred use of continuous control characteristics and generalized droop formulations. This shall be accomplished while still complying as closely as possible with the simple droop constant based concepts proposed in [1.5], so that experience gained in and further developments based on these concept are still applicable.

To summarize, the main premise of the work is to include the following criteria in one comprehensive as well as simple to understand and implement concept for the task of balancing the active power in the dc system:

1. Conformity with state of the art concepts

2. Continuous operation for the complete control characteristic

3. Generalized concept for the control that achieves all control objectives

These criteria present the key design objectives, which lead to the design of the control concept proposed here.

The proposed converter control concept is motivated by the possibility to achieve an advanced and more flexible control concept for the entire grid. A grid control concept made possible by the proposed controller is consequently proposed in a second step. This grid control concept utilizes the fact, that, in contrast to ac systems, the power flow is known due to the controllability of the converters and the absence of generation and consumption assets in the dc transmission systems. It is based on the principle, that in the case of a converter outage the majority of active power used for active power balance shall be provided in the same region as the faulted converter.

1.3. Outline of the Thesis

The design of the proposed concepts is approached with the following structure:

Chapter 2 introduces the state of the art for dc systems to build the basis for the subsequent analysis.

Chapter 3 expands on the analysis of the control of dc systems in regard to active power transmission and balancing.

Chapter 4 describes the models used to simulate the system and a benchmark system used for the simulation cases.

Chapter 5 introduces a generalized continuous active power balancing controller.

Chapter 6 shows the design concept for a tiered dc grid control, based on the introduced converter control.

Chapter 7 summarizes the approach chosen in this work and gives an outlook on possible further research.

2. Fundamentals of Ac/Dc Power Systems

Electrical power grids have historically been constructed in three-phase alternating current (ac) technology. Its initial triumph over direct current (dc) technology was due to its advantages in transformation of voltage levels, power generation with three-phase synchronous generators and the ability to decouple voltage magnitude and active power transfer. These advantages made it possible to form large synchronously operating grids, increasing system reliability and security by enabling shared power reserves in case of generation loss. Ac technology comes with its own disadvantages however, one being the necessity to provide reactive power in order to alternate the electrical and magnetic field of the grid's components.

With constant advances in the enabling technologies, dc technology has become technically and economically viable, and is increasingly introduced into the synchronous grid. The preexisting ac components in conjunction with the introduced dc devices form a novel, hybrid power grid combining the strengths of both technologies, which we will term ac/dc power system in this work. Transmission systems based on dc technology, called high voltage dc (HVDC) systems, play an important role here, because they are part of the power grid itself, therefore interacting very directly with the ac system.

This chapter gives an overview over the application of dc technology with focus on HVDC transmission systems in accordance with the scope of this work. It further aims to give deeper insight into the electrical equipment and control of HVDC systems. The chapter is structured as follows:

Section 2.1 gives an overview over the application of dc technology in synchronous power grids and of HVDC transmission systems in more detail.

Section 2.2 introduces the electrical equipment and control of voltage source converters.

Section 2.3 deals with the structure and control methods for HVDC transmission systems.

2.1. Application of Dc Technology in Synchronous Power Grids

The recent success of dc technology is closely coupled to the advances made in power electronics. The major enabling component is the power converter, which converts ac to dc quantities and vice versa. This conversion allows for the connection of dc components to the synchronous power grid. The connection of components of different or even varying frequency is furthermore enabled by combination of two conversion steps. The application of power electronic converters is manifold, encompassing all fields of electrical power supply, ranging from generation and load to transmission and compensation devices. Figure 2.1 gives a rough overview over the application of dc technology in synchronous power grids.

Assets using dc technologies in the form of power converters can be classified into two types: Grid interfacing power converters are mainly used to connect dc or variable frequency units to the synchronous ac grid. These can be consumption or generation units, and in some cases act as both, for example power converters for storage units. Moreover, the converters offer an increased controllability at the grid connection as a beneficial side effect. For transmission and compensation type assets on the other hand, the controllability aspect is crucial, allowing more freedom in control of active and reactive power as compared to ac technology components. The dc side plays a more minor role in this type of asset. These assets also differ, in the sense that they are part of the power transmission grid itself, as opposed to dc connected consumption or generation units.

2.1.1. High Voltage Dc Transmission Systems

HVDC transmission is a dc technology that utilizes power converters in order to transmit power in dc systems. Two or more power converters are connected to the synchronous grid on the ac side and to an interconnecting dc transmission system on the dc side. The dc transmission system consists of overhead lines or cables. The power converters can be line- or self-commutated technology. The system is termed multi terminal dc (MTDC), if more than two converters are connected to one dc transmission system.

Active power flow in HVDC systems is controllable, i.e. the transmitted active power is not related to ac voltage angle differences as is the case in ac grids but is chosen by the operator. Furthermore, a HVDC system does not require reactive power in the interconnecting transmission system, making HVDC especially suitable for long range power transmission and for cable connections. HVDC systems decouple their connection points when they are part of two

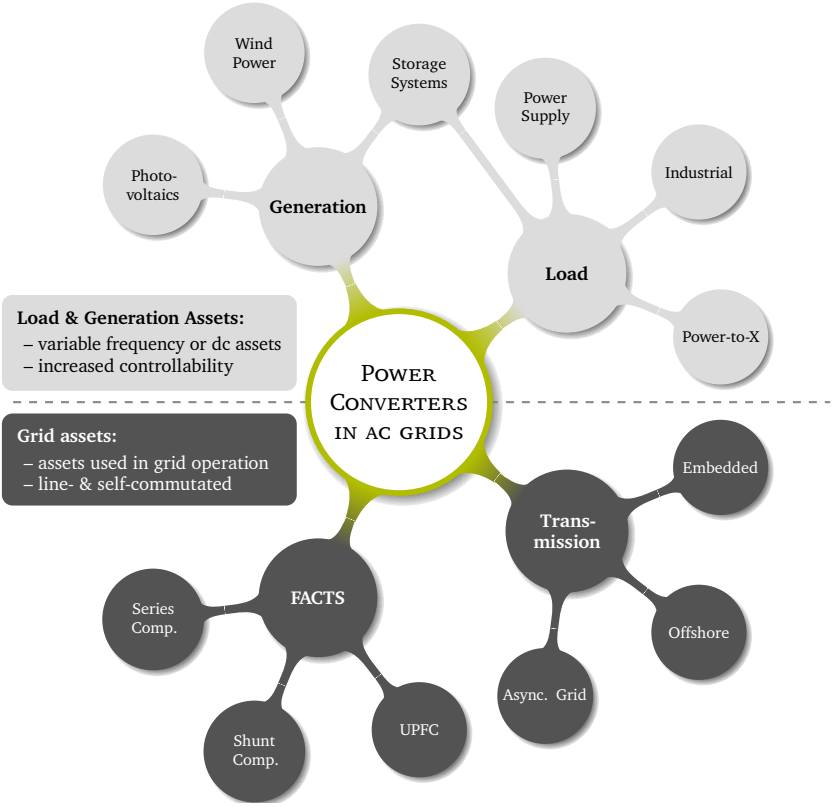

Figure 2.1.: Overview over dc technology applications in ac power grids.

unconnected ac grids. The two connected grids can thus have different electrical frequency and don't share short circuit power. Typical use cases for HVDC that arise from these advantages include the coupling of two asynchronous grid areas or electricity markets and the connection of remote or offshore energy sources. Another use case is the application of HVDC transmission parallel to a synchronous grid area. This is called an overlay system or alternatively embedded HVDC. In this work, we will use the term embedded HVDC.

2.1.2. Impact on the Ac System

HVDC systems have a big impact on the connecting ac grid for a variety of reasons. Firstly, due to the ability to control the power flow over the dc transmission path, the transmission system operator (TSO) is able to use the HVDC system to full capacity, or any other operating point that is beneficial to the power system. Due to the nature of the power electronic converters, this can be done with very low time constants compared to conventional grid components. Secondly, an embedded HVDC system does not contribute to the difference of voltage angles in the ac grid because of its decoupling effect. This means that for a given active power transfer, the resulting differences in voltage angles in an ac/dc system will be smaller compared to a "pure" ac system. Finally the power converters have an impact regarding reactive power and harmonics at their point of connection. While line-commutated converters need reactive power compensation and harmonic filters at the converter station, modern multi-level self-commutated converters do not need any of these measures and can provide reactive power compensation (see e.g. [2.1, 2.2]).

HVDC systems, especially in self-commutated technology, enable possibilities for the TSO, that are not present in an ac system. This includes but is not limited to fast active and reactive power control. The former enables an increase of operating efficiency and the ability to provide curative action by adaption of the HVDC's operating point following contingencies. The latter enables stationary and dynamic reactive power compensation comparable to STATCOM (see [2.2, 2.3]).

On the other hand, the introduction of power converters into the ac grid comes with its own challenges. In addition to questions regarding the hardware, there are also challenges regarding system operation of ac/dc power systems, e.g. an extended (n-1) criterium of the ac/dc system and small-signal stability of the power converters in high-frequency ranges.

2.2. Voltage Source Converters for HVDC

HVDC systems basically come in two fundamentally different converter technologies. The first variation is called line-commutated converter (LCC) technology. LCC uses thyristors as switching devices and is usually run as a current source converter, which means, that the dc current is held constant, and the voltage is variable. The second variation is the self-commutated converter technology. This technology is usually implemented as voltage source converter (VSC), i.e. the dc voltage is held constant and the current is variable. For this technology, VSC is the common abbreviation and will be used throughout this work.

Although LCC-HVDC is a mature, proven and reliable technology and achieves unrivaled power ratings for the transmission systems, it doesn't lend itself to very well to MTDC systems, apart from few existing, very simple and radial connections. VSC-HVDC on the other hand is very well suited, because the constant dc voltage allows for the connection of an arbitrary number of converters to the dc transmission system. It furthermore offers superior controllability of active and especially reactive power flow compared to LCC-HVDC, making it particularly suitable for embedded HVDC systems. [2.2] gives a very detailed overview over this field, and can be referred to for further information.

2.2.1. Converter Topology

Converters used in VSC-HVDC operate by connecting the dc voltage V_{dc} to the ac line voltages V_{ac} in a manner, so that the constant dc voltage translates to the sinusoidal ac voltage. The VSC thus acts as an ac voltage source. The power electronic switches used in VSC-HVDC components consist of a self-commutated switching device with an anti-parallel diode. Insulated gate bipolar transistors (IGBT) are used as switching device, with research investigating other options as well, e.g. the integrated gate-commutated thyristor (IGCT). The electrical circuit connecting V_{dc} to V_{ac} and the way the sinusoidal voltage form is achieved depends on the converter topology.

2.2.1.1. Two-level Converters

The earliest and most basic topology for VSC consists of one power electronic switch for each phase and each polarity. In this way, the converter can generate either the voltage on its positive or its negative pole, with no intermediate levels. This converter technology is consequently called two-level converter. For this topology, a smoothing capacitor is placed on the dc side between the two poles

of the converter, which also acts as an energy source. The ac-side sinusoidal voltage is achieved using pulse-width modulation of the converter voltage and implementing a reactance on the ac side. This results in a sinusoidal converter current, albeit with comparatively high total harmonic distortion (THD). This topology is widely used for grid interfacing inverters in RES generators because of its simplicity. It is however limited by the complexity to construct power electronic switches for very high blocking voltages and by its high losses due to high switching frequencies. For HVDC transmission systems, two-level converters are less suited compared to and largely superseded by more modern multi-level topologies in recent installations due to these disadvantages.

2.2.1.2. Three-level and Multi-level Topologies

In order to improve the harmonic performance of the converter, the number of voltage levels that the converter can generate is to be increased. The three-level converter achieves this by using a voltage divider on the dc side capacitor and clamping diodes in the converter topology. This concept allows for a smoother ac voltage wave and can be extended to multi-level topologies. However, this comes at the cost of increasing complexity of the converter with increasing voltage levels and most importantly doesn't address the necessary high blocking voltages of the switching devices because at the maximum voltage level, all switches are connected in series.

2.2.1.3. Modular Multi-level Converter

The modular multi-level converter (MMC) is a converter topology first proposed by Marquardt in 2002. This technology uses multiple submodules, which are connected modularly in series, hence the name of the technology. Very high converter voltages and a very high number of voltage levels can be achieved by this modular design. The reason for this is mainly that the blocking voltage of each power electronic switch is based on its corresponding submodule capacitor voltage, as opposed to former technologies, where a stack of switches has to withstand rated dc voltage. As of 2022, this converter technology can be seen as the state of the art for VSC-based HVDC connections, with research focusing on submodule types and the switching devices used in the MMC.

MMC: Topology In the MMC, V_{ac} is connected to V_{dc} by the converter "arms". For each phase, there is an upper and a lower phase arm connecting the positive and negative dc pole respectively. Thus, there are 6 identical arms in the

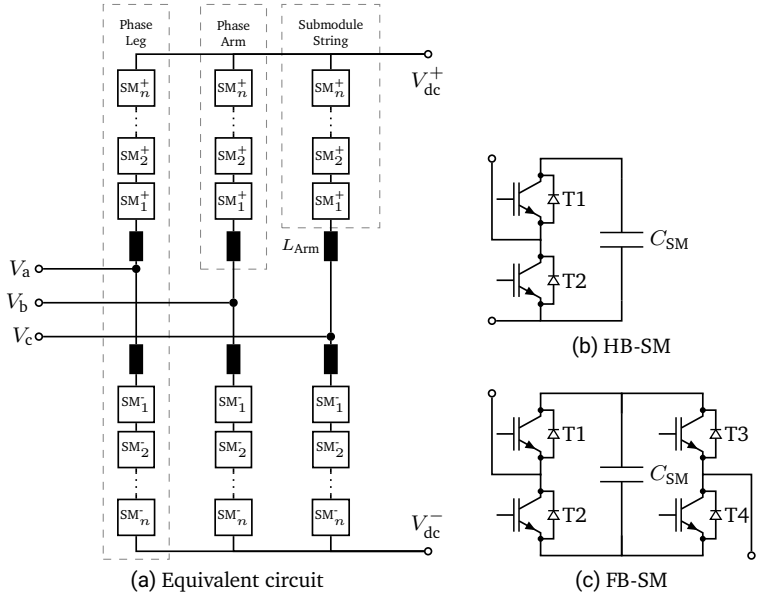

(a) Equivalent circuit

(b) HB-SM

(c) FB-SM

Figure 2.2.: Equivalent circuit of the topology of the Modular Multilevel Converter and submodule types.

converter, each consisting of N_{SM} series-connected, independent submodules and an arm reactance L_{Arm}, which can be located at the dc-side or ac-side connection of the arm. The upper and lower arm form the converter phase leg, connecting the dc poles. The equivalent circuit of the MMC is depicted in figure 2.2a. The MMC topology is very widely used and is employed by all major manufacturers.

MMC: Submodules The MMC's arms are made up of series-connected, independent units, which are called submodules. There are a number of submodule types, which are a topic of research. The different submodule types differ in two main characteristics. These are the number and polarity of achievable voltage levels and the ability to block the submodule in case of submodule failure or dc-side short circuit. The main submodule types, that are also used in opera-

tional MMCs are the half-bridge and the full-bridge submodule. The half-bridge submodule (HB-SM) consists of two switches with anti-parallel diodes and a submodule capacitor C_{SM}. As the name implies, these are connected as in one half of an H bridge. The equivalent circuit of the HB-SM is shown in figure 2.2b. Depending on the state of the switches, the HB-SM can generate a submodule voltage V_{SM} equal to the voltage over the capacitor V_{C}, or zero voltage making the HB-SM a unipolar cell with one voltage level. The HB-SM can not be blocked and results in the MMC behaving as a passive 6-pulse bridge in case of a dc-side short circuit. There is however only a single operational switch for each state, which results in low losses. The full-bridge submodule (FB-SM) consists of four switches and the capacitor in H bridge connection. The equivalent circuit is shown in figure 2.2c.

In contrast to the HB-SM, the FB-SM is bipolar, i.e. it can generate one voltage level V_{C} in positive and negative polarity. In addition, the FB-SM can be blocked in the case of a dc short circuit. These advantages come at the cost of increased converter losses, because there are always two conducting switches for each state. Other concepts for submodule types try to retain the positive operational characteristics of the FB-SM (bipolarity and blocking capability), while lowering the amount of active switches per state and thus the submodule losses. For an overview of proposed submodule types, see [2.2].

MMC: Operating Principle The MMC generates the sinusoidal ac-side voltage V_{ac} by switching the state of the switches in the respective arm for each phase. The ac and dc voltages depend on the voltage level and polarity of the active switches $n_{\mathrm{sm}}^{\pm}$ for the upper and lower arm. V_{ac} results from the difference and V_{dc} from the sum of the arm voltages. The corresponding equations for each converter leg are given in (2.1a) and (2.1b). For the HB-SM, this results in a maximum of V_{ac} when all submodules of the lower arm are active, and all submodules of the upper arm are short-circuited. Lower peak voltages can be achieved by using less active submodules on the lower arm and more on the upper arm.

The basic operation of the MMC described above is ruled by the balancing of ac and dc powers. This principle can be translated to a power flow for each sub-module or submodule string (e.g. converter arm), in which the total power determined by all voltages v and i in a submodule over one period T of the fundamental frequency equates to zero, resulting in the integral given in equation (2.1a). In frequency domain, this equates to the sum of ac and dc powers for all harmonics given in equation (2.1b), with the voltage $\hat{v}_h$ and

current $\hat{i}_h$ magnitudes for each harmonic with harmonic order h and voltage-current phase angle $\cos\varphi_h$.

$$\int_{t}^{t+T} vi\, d\tau = 0 \tag{2.1a}$$

$$V_{\mathrm{dc}} I_{\mathrm{dc}} + \frac{1}{2} \sum_{h=1}^{\infty} \hat{v}_h \hat{i}_h \cos\varphi_h = 0 \tag{2.1b}$$

The power balance principle given in above equations governs the operation of the MMC and determines the equations for the combined system, such as the power balancing of the total system and the balancing of individual capacitor voltages. A detailed description of the behavior and the governing mathematical equations of the MMC are found in [2.2], including the derivation of voltage and current magnitudes, the sizing of its components as well as further topics.

2.2.2. Converter Controls

VSC-HVDC is very flexible and fast in its provision of active and reactive power. The converters can furthermore provide auxiliary services. There is, however, no inherent (mechanical) behavior of any kind, as typically seen with e.g. synchronous machines. All operational features have thus to be controlled actively. This requires a complex control system with different modes for each required control mode. Requirements for the control of VSC for HVDC are given in Cigré report [2.4].

Traditionally methods derived from the control of inverter-interfaced drives have been used for HVDC converters. These use a cascaded control structure in a rotating synchronous reference frame (SRF), which is synchronized to the grid voltage by a phase locked loop (PLL). This kind of control method results in the converter acting as a current source. It has the advantage, that the currents can be controlled and consequently be limited to permissible magnitude directly by the control system. However, the controllability as well as the synchronization comes at the cost of an indirect control, which has the effect, that the converter cannot transiently provide power, for example reactive power in the event of a short circuit.

In order to overcome this limitation, a number of alternative approaches have been proposed (see e.g. [2.5]). These methods try to overcome the limitations of the traditional cascaded control system by avoiding the inner control loop, the synchronization by the PLL and/or the usage of the SRF altogether. A number of different terminology has been used to dub these control methods, such as virtual synchronous machine, power synchronization control and fast voltage control. Often, these control methods cause the converter to act similar to a voltage source. Consequently, these control methods are usually superior when interfacing ac grids with little or no inertia. This enables voltage provision, e.g. for black start scenarios or grids without synchronous machines. The advantage of inherent voltage support comes with the challenge of the limitation of the the converter current, which has to be appropriately addressed.

In order to characterize the different methods for the control of converters for HVDC (or other power electronically interfaced assets for that matter), the terms grid feeding converter for the former method and grid supporting for the latter method(s) can be employed. This emphasizes the purely current providing characteristics of the cascaded control system in contrast to the advanced control methods.

2.2.2.1. Control System Overview

The control system of a VSC can be divided into fundamental parts, that can be defined regardless of the individual method employed. The inputs of the control system are the measurements at the VSC's ac and dc terminals, and the reference values, that are handed down from the upper levels of the dc system control (for details of HVDC system control hierarchy, see section 2.3). The actual measurements and reference values used depend on the control method and usually include the ac- and dc-side voltages and currents, as well as additional signals like grid frequency or voltage measurements at remote buses. A simplified representation of the hierarchical structure of the VSC control system for grid feeding converters is shown in figure 2.3[2.2]. The major parts are the inner and outer control structures, furthermore the converter requires synchronization and signal pre- and post-processing (not depicted). Synchronization consists solely of the PLL for grid feeding converters. Pre-processing consists of signal conversion to SRF by Park-Transformation and calculation of powers from voltage and currents. Post-processing consists conversion from SRF to time domain by inverse Park-Transformation and if needed compensation of time-delays of the control structure. The inner and outer parts of the control structure is discussed in the following.

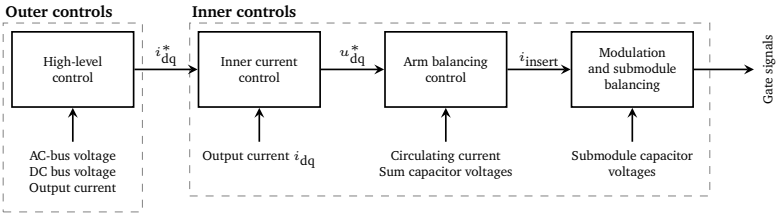

Figure 2.3.: Overview of control system for VSC, adapted from [2.2, 2.4].

2.2.2.2. Inner Control Loops

The part of the converter control system that are responsible for the internal processes of the VSC is defined as *low-level* or *inner control*. These include the generation of gate impulses for the power electronic switches of the VSC from given (voltage) reference values as well as the control of interior physical quantities, e.g. capacitor voltage balancing or circular current suppression in MMCs. Compared to the other parts of the control system, the inner control loops are very system specific. The required loops thus vary for each converter topology and can be manufacturer specific as well.

2.2.2.3. Outer Control Loops

The term *high-level* or *outer control* loops describes the parts of the VSC's control system that generate the voltage reference for the VSC. The actual control parts used here depend on the control method and on the functionality of the converter. The various control methods differ primarily in the way, the voltage reference signal is generated. For grid-feeding converters with inner current control, the PLL aligns the SRF to the ac-side voltage, i.e. the q-axes voltage v_q. The d-axes current i_d of the park-transformed SRF thus corresponds to active current, because it is in phase with the line voltage. The q-axes current i_q consequently corresponds to reactive current.

The converter control can achieve different tasks using either i_d or i_q. The different control loops for outer control are summarized in table 2.1.

Table 2.1.: Overview over outer control loops of grid-feeding VSC-based HVDC converters.

Control Base	Control loop	Control variables
Active current i_d	Active power control	P
	Dc voltage control	V_dc
	Dc voltage Droop	P, V_dc
	Frequency control	f
Reactive current i_q	Reactive power control	Q
	Ac voltage control	V_ac
	Ac voltage droop	Q, V_ac
Others	Harmonic compensation	I_h

2.3. HVDC Transmission Systems

As introduced in section 2.1, HVDC transmission systems are formed by connecting multiple power converters to a common dc transmission system, e.g. consisting of cables or overhead lines. The possible complexity of HVDC transmission systems ranges from simple point-to-point connections to proposed MTDC super grids spanning entire continents with high numbers of converters.

Regarding the terminology, it is important to distinguish simple point-to-point connections from MTDC systems, which can be defined as HVDC systems with three or more converters connected to one common dc transmission system. The term MTDC includes point-to-point connections with so called *tapping*, i.e. one ore more converter stations on the direct transmission path, as well as radial and meshed grid structures of higher complexity. The differences between these structure types are fuzzy, because grid structures and control methods are very similar. The terms MTDC and dc grid can be used interchangeably. In this work, MTDC will be used as the more general term to label all dc system types mentioned above, while the term dc grids shall be confined especially to larger, more complex structures.

Point-to-point HVDC systems can be described as state of the art. VSC-MTDC systems however are still a new field of research, with only a few installations operating as of 2019. The greater controllability of HVDC systems compared to ac systems comes at the cost of an increased complexity regarding construction and topology as well as additional requirements for control, protection,

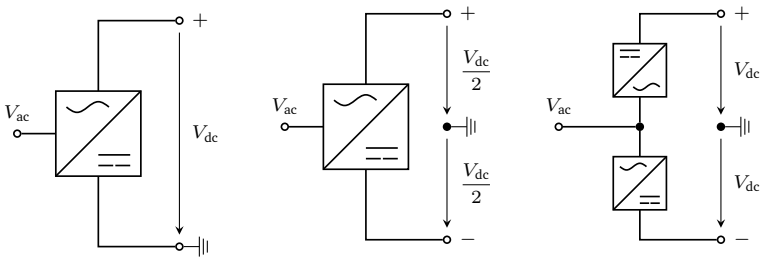

(a) Asym. Monopole (b) Sym. Monopole (c) Bipole

Figure 2.4.: Possible pole configuration for VSC-HVDC systems.

regulation and standardization.

The following sections give a general description of the relevant topics, for a more detailed overview, see [2.1, 2.2, 2.4, 2.6].

2.3.1. System Topology

System topology in the context of HVDC systems describes the way the converters and the ac and dc systems are connected. The system topology of HVDC systems can be divided by the use of voltage levels for the interconnection of the converters (i.e. pole configuration) and the type of conductor and the structure of the dc transmission system interconnection(i.e. transmission medium and dc system interconnection respectively).

2.3.1.1. Pole Configuration

Power converters by definition have a positive and negative pole. Both are connected by the converters specific topology to the phases of the ac system. The term pole configuration in this context describes the manner of connection of the converter(s) to the dc system. Depending on the number of converters used per configuration, it is called a *monopole* or *bipole*, when one or respectively two converters are used. Figure 2.4 gives a schematic overview over possible configurations. [2.1] gives a detailed overview over these configurations. The configurations below can be extended, when very high voltage or power ratings shall be achieved by using series or parallel connection of converters.

The asymmetric monopole (figure 2.4a) is the most basic pole configuration and has been used for the first VSC installations. The VSC's positive pole is connected to the positive pole of the dc system. The negative pole is connected to earth, which can be a dedicated metallic return path, or physical earth if regulation allows for it. This configuration, especially using a physical earth connection, has the advantage of a simple system design, both logically and physically. Only one conductor and at where applicable one metallic return path are needed. However, V_{dc} is limited by the insulation of the positive pole.

The symmetric monopole (figure 2.4b) is similar to the asymmetric monopole in converter station layout. Both VSC's poles are connected to a dc conductor with the voltages $+\frac{V_{\mathrm{dc}}}{2}$ and $-\frac{V_{\mathrm{dc}}}{2}$ respectively. Thus, the voltage seen by the VSC is again V_{dc}. This has the effect that, for a given V_{dc}, the conductors need to withstand only half voltage or, from another viewpoint, for a given conductor (e.g. a high voltage cable), the admissible voltage for the converter is doubled compared to the asymmetric monopole. The symmetric monopole, however, has the disadvantage of needing a symmetric dc system. This makes it unsuitable for(long) cable systems because the voltage can become unsymmetrical due to impurities in the cables.

In bipole configuration (figure 2.4c), the converter station consists of two VSCs. Each VSC is connected as an asymmetric monopole as depicted. The common dc connection of the converters is connected to earth. Again, this can be a metallic return conductor if desired. With bipole configuration, the earth return is only ever used when the two conducting poles of the dc system have asymmetrical voltages. The bipole configuration has the advantage of continued operation of one pole in case of the outage of one converter.

This configuration enables the option to forgo the metallic return conductor. In case of an outage, the link can then be operated with the remaining converter and conductor while the other conductor is used as return path.

2.3.1.2. Transmission Medium

The power transmission in HVDC systems is done via the same technologies available for ac systems. This includes mainly overhead lines (OHL), mass-impregnated (MI) or extruded cross-linked polyethylene (XLPE) cables and dc gas insulated lines (DC-GIL). Overhead lines are cost-effective and can have a high current and voltage rating due to their comparatively simple insulation design and good thermal characteristics. They also have low series resistance, which equals low losses. These attributes make them a very good choice. However, overhead lines are suspect to exterior influences, such as lightning strikes.

They are more importantly visible from afar, which is especially true for high voltage ratings, which causes regulatory and political problems.

Cable systems are very well suited for dc systems when compared to ac systems, due to no reactive power needed. Cables have been the standard for offshore HVDC systems. Still cables suffer from high construction costs and technical difficulties regarding the insulation when compared to OHL. This is especially true for land cables, where there additionally exists the need for a high number of cable joints, which has an effect on both reliability and construction costs. The costs for land cables compared to OHL are expected to be much higher. Land cable systems also have a high environmental impact because of large needed corridors and soil heating through thermal losses.

The third option is DC-GIL, which is a promising albeit still unproven technology. It is characterized by low thermal losses and construction costs comparable to cable systems. However, long distance transmission systems and the use of environmentally sustainable insulation gas are still subject to additional research.

The need for a transmission medium suitable for long-distance land based HVDC systems in densely populated areas has also led to the concept of mixed systems, e.g. mixed cable and OHL. This is mainly done out of regulatory and political rather than technical reasons. While this solution can bring advantages in regards to construction and maintenance cost, it poses its own challenges, e.g. in the form of transient overvoltages introduced to the dc system and the resulting physical phenomena [2.1].

2.3.1.3. DC System Interconnection

The interconnection of the converters obviously plays a crucial role in the design of HVDC systems, as it allows for power transfer between the converters. In this context, system interconnection can be a simple point-to-point connection, or alternatively some kind of dc grid structure. Details regarding technical and economical characteristics of these interconnection types are provided in CIGRÉ technical report *HVDC Grid Feasibility Study* [2.6].

The most straightforward method is using point-to-point interconnections, i.e. using a direct connection of two converters. For two terminal systems, point-to-point naturally is the only option. While technically possible, creating a grid-like MTDC system using point-to-point connections will result in a very high number of converters, raising construction costs and space needed. This effect becomes more prominent with increasing number of MTDC converters (for details, see [2.6]).

For dc transmission systems it is thus sensible to construct MTDC structures, consisting of dc substations connected to (multiple) lines instead of multiple individual point-to-point systems. Each converter connects to the same dc system, reducing the need for additional converters for each dc transmission path. This is enabled by the VSC's constant V_{dc}, which leads to a dc system with a voltage profile resulting from the power transfer over the transmission paths. While MTDC grids offer technical and economical advantages over multiple point-to-point connections, they come at the cost of a loss of controllability, as the resulting stationary voltage vector $\mathbf{V}_{\mathrm{dc}}$ and line currents $\mathbf{I}_{\mathrm{dc}}$ are only determined by the admittance matrix of the dc system $\mathbf{Y}_{\mathrm{dc}}$ through $\mathbf{V}_{\mathrm{dc}} = \mathbf{Y}_{\mathrm{dc}}\mathbf{I}_{\mathrm{dc}}$. Thus, the voltage profile and line currents can only be influenced using the converters power and voltage setpoints, but not controlled directly.

Grid structures of MTDC systems can be categorized further into radial and meshed grids. As the name implies, radial grids are constructed in a way, so that there is always one transmission path between each two converters in a grid. This results in minimum required paths for the systems. In a meshed system, there are more than one transmission path between each two converters, forming meshes as is common in the ac transmission grid. Radial grids offer an economical and easily controllable solution, while meshed systems offer an increased flexibility and security regarding line outages. It is consequently possible to build systems, where large parts of the grid are constructed in a radial manner with meshes in crucial areas [2.1].

2.3.2. Control of HVDC Systems

From an operator's point of view, the flexibility and controllability of HVDC systems offer great possibilities. These come with the need for an increased effort for control and protection systems however. In addition to the control systems of the individual converter stations, which are already complex in nature, the system operator needs to ensure an appropriate operation of the entire HVDC system, taking into account the ac system(s) it is connected to as well. The tasks of a HVDC system control operation include the control of the converters active and reactive power provision and a number of auxiliary services that the converters can provide. The system operator furthermore has to ensure secure operation in cases of failure inside the HVDC system, requiring specialized protection systems and emergency control schemes (see also [2.1, 2.2, 2.4]). The hierarchical control system of MTDC systems is discussed more in detail in chapter 3.

2.3.2.1. Control of Active Power

The transmission of active power can rightfully be considered the most important task of an HVDC system. This makes the control of the converters' active power operating points one of the main challenges. In addition, the control of active power is also responsible of ensuring secure system operation due to its connection to the power balance in the dc system and therefore V_{dc}. Because of the importance to this work's research focus, the control of active power in HVDC systems is specifically discussed in chapter 3.

The provision of active power to the ac grid as an auxiliary service can stabilize frequency, which is described in a section below.

2.3.2.2. Control of Reactive Power

The VSC's flexibility regarding reactive power provision enables system operators to utilize the converter stations as reactive power compensation units. This compensation can be very effective, when the reactive power provision is considered in the design phase of the converter, e.g. by slight over-dimensioning of the power capability of the converter. The converter stations can in this way act similar to STATCOM, regardless of the state or type of the connected dc system. The reactive power provision has very little impact on the dc side of the HVDC system, other than incurring additional losses in the converters.

The topic can to be subdivided into separate parts: stationary and dynamic reactive power provision of HVDC systems. For stationary time frame, the reactive power provision can be fixed to a given value, which is determined by optimal power flow calculation or through a market based approach. Another option is controlling V_{ac} at the point of common coupling (PCC), either using a fixed reference voltage or a $Q(V)$-characteristic. In a dynamic time frame, the system converters can be used to provide reactive current support for voltage drops during short circuits. This is usually achieved by a droop characteristic with a dead-band. Another way to achieve dynamic voltage support is the use of grid-forming type converter controllers, which cause the converter to have some direct voltage supporting behavior similar to that of synchronous machines.

The behavior of reactive power support of HVDC systems is fundamentally very similar to that of power electronic interfaced generation units. This is true for both stationary and dynamic time frames. It also results in very much comparable regulations and standards for HVDC systems.

2.3.2.3. Auxiliary Services

HVDC systems can provide services which go beyond basic active or reactive power provision [2.1]. In contrast to STATCOMs without an integrated energy source, HVDC systems also offer the possibility to provide auxiliary services using active power. The capabilities are especially pronounced when the HVDC is spanning two or more separate, asynchronous ac systems, enabling active power transfer between the grid areas. Exemplary auxiliary services can be:

- Frequency support in case of load/generation imbalance. Converters can deliver active power to provide primary control and/or virtual inertia, using the energy contained in the converters' capacitors and the dc system or a neighboring system if applicable. The former is limited to small boosts of energy, because the energy in the dc systems electrical field is small as opposed to the energy held in rotating masses of the ac grid. The latter can be very effective and is able to couple the electrical frequencies using control rules.
- When coupling two or more ac systems, HVDC systems have enhanced black-start capability due to being able to supply the system with active power. HVDC systems can even power entire ac systems when the total available power rating is large enough. Both tasks require converter controllers to be of grid forming type in order to generate a reference frequency and angle for the ac system.
- Power oscillation damping can be done by both active and reactive power modulation. Active power modulation is proven to be more effective [2.7].

In addition, HVDC systems can provide most auxiliary services a STATCOM can provide. However, there are limitations to the capabilities of an HVDC system's converter station related to interactions with the dc system when compared to a STATCOM, e.g. with active harmonic cancellation techniques, that can propagate harmonics to the other converter(s).

2.3.3. Protection and Security in HVDC Systems

Protection and security of HVDC systems is a very broad topic, which is one of the major fields of current research. Only a coarse and non-exhaustive overview can thus be given in this work. The field encompasses hardware- and control-based protection schemes as well as system security and stability issues, both for the HVDC system and the resulting ac/dc power system.

Protection of HVDC systems is very special due to the changed physics in dc and the fact, that power electronic valves are sensitive to overvoltages or -currents. Very fast and reliable protection systems are necessary to protect the power electronic equipment from both ac- and dc-side influences. Very prominent fields of research regarding the protection of HVDC systems include dc-side short circuits and transient overvoltages. The clearing of dc-side short circuits presents a major challenge, especially for MTDC systems, because of absent zero crossings of the short-circuit current. This necessitates specialized solutions ranging from dedicated dc circuit breakers to control based short-circuit clearing strategies. Specialized circuit breakers come in different technical implementations, including resonant, power electronic or hybrid power electronic/mechanical designs. A control based approach tries to leverage the ability of FB-MMCs to force V_{dc} to become zero or slightly negative in order to extinguish the short circuit. After short-circuit clearing and removing the faulted branch with disconnectors if required, the voltage can be restored. Transient overvoltage in HVDC systems usually occurs due to lightning strikes into OHLs in the dc system. The effects are aggravated when the dc transmission system is a mixed OHL/cable system due to traveling wave phenomena [2.1].

Security of HVDC systems can be subdivided into the topics stability, power quality and reliability. In the context of HVDC, the combined ac/dc system needs to be taken into account for stability assessment. Usually, stability for the HVDC system alone is mostly a control related topic, as there are no active elements inside the dc system but the converters. On the other hand the classical stability issues of the ac system can often be alleviated with HVDC (see also section 2.3.2). There are certain fields of stability however, where dc systems affect the stability or power quality of the ac system. One example are hybrid ac/dc OHLs, i.e. an ac and dc circuit on one OHL. Determining the interactions between and the effects on the two respective systems' stability, power quality and protection is still a scope of research. Another example are high frequency oscillations, that can occur between different components in grid areas with high shares of power electronic elements. This effect combines topics from both classical small-signal stability, in this case for relatively high frequencies, and power quality. The field is consequently sometimes termed harmonic stability. Because the electrical power systems become increasingly dominated by power electronic devices like photovoltaics, wind power generators and HVDC, this topic is of crucial interest for TSOs and DSOs alike. Detailed information on the topics mentioned here is found in [2.1, 2.2, 2.8].

3. Control of Active Power Flow in HVDC Systems

The primary role of HVDC systems is the transmission of active power, with other purposes of the converters such as reactive power support being side effects, albeit welcome ones. The active power transmitted over the HVDC system can be controlled by the converters. For VSC-HVDC systems, the active power provision of the converter can be controlled very flexibly and independently from the reactive power provision. The (steady state) magnitudes depend only on the references supplied to the local controller.

The purpose of active power provision for VSC-based HVDC systems is twofold. First and foremost it fulfills the (main) purpose of transmitting the power over the transmission medium. Moreover however, because the dc voltage is the synchronizing element in the dc system, its voltage level depends on the active power balance in the dc system, i.e. the converters aggregated active power provision. Some kind of power balancing scheme is required to achieve a stable equilibrium point of the dc voltage. The systems thus requires a control structure which is able to achieve both an appropriate active power transmission as well as a stable control of its dc voltage. In addition, the control must ensure permissible operation regarding voltage and current limits for all converters.

This chapter aims to provide an introduction and a broad overview over the control of active power in MTDC systems. The chapter is structured as follows:

Section 3.1 analyses the requirements and provides a categorization for active power control strategies.

Section 3.2 describes active power control from an overall ac/dc system wide perspective.

Section 3.3 describes active power control from the perspective of dc voltage control.

Section 3.4 discusses the current state of the art and establishes requirements for further development.

3.1. Requirements and Categorization of Active Power Control Strategies

While this work focuses on HVDC applications, the control structure for these systems is very much shared with MTDC distribution or microgrid applications. Here, the requirements are more general, as there are usually dc generation or consumption units feeding directly into the dc system. [3.1] provides an extensive literature review for existing control strategies for dc networks. The control aspects identified as most common here are the control of dc voltage and load sharing, which determine the basic operation of the grid. Furthermore, important identified dynamic aspects are the mitigation of dynamic interactions between the grid's components, the performance of transitions between grid connected and islanded operation as well as the response to contingencies. Finally, stationary metrics identified are the balance of storage energy, the power sharing of converters and die minimization of transmission losses.Furthermore, [3.2] divides the control of dc systems in 4 distinct levels, which shall also be applied similarly in this work:

- **Local levels:**
  - **Level 0:** Local converter controls, see section 2.2.2 (e.g. voltage and current control)
  - **Level 1:** Local, decentralized active power control loop
- **Global levels:**
  - **Level 2:** Centralized active control loop, providing the reference for the local controls
  - **Level 3:** Global control loop, supervising the active power transmission in and exchange with the connected ac grid

The requirements given above can be fulfilled in different ways. The control strategies are categorized into active load sharing and master- slave / droop based strategies. In active load sharing strategies, control of active power is achieved directly in the global levels and passed to the local levels over a communication link. In master-slave and droop based strategies, the control is layered, the local levels providing a stable and independent control, while the global levels provide a system wide coordination of the active power flow in the dc system and the power exchange with the ac grid. Various control concepts have been proposed for the control of dc microgrids, including rule based (deterministic or fuzzy) or optimization based strategies [3.3–3.8].

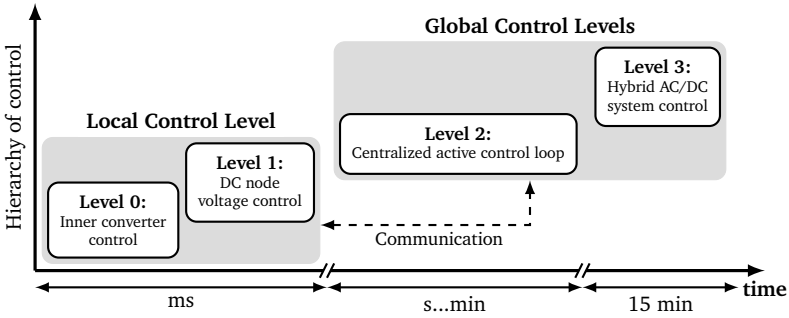

Figure 3.1.: MTDC hierarchical control structure and time frames, based on [3.9].

The layered control implemented in master-slave and droop based strategies is usually seen as the method of choice for MT-HVDC systems, as it provides a good combination of security and system stability and reliability by using the communication-less local control with coordinated control of power flows inside of internal and ac and dc combined power system. This is seen very much analogous to the active power control in ac transmission systems. Rouzbehi et. al. give a detailed overview of the analogies of ac and dc power system control and the respective control hierarchies in [3.10]. In [3.9], the hierarchical control structure is discussed, as well as time frames, in which the individual levels operate (see figure 3.1). The global levels are the overarching control structure, responsible for the ac and dc system-wide active and reactive power flows. The values relevant are passed to the local controllers over a communication link. The local controllers are responsible for the independent control of not only the converter power, but also the decentralized control of the dc voltage. For this each local controller relies solely on local measurements. In addition, measurements relevant to the overall system behavior are fed back to the global control.

This hierarchical control structure, which is described here in general, is mostly adapted when talking about control of MTDC systems. The terms are often inspired by the terms used in ac grids, such as primary control for local levels and secondary and tertiary control on the global levels. For example, Egea-Alvarez, Beerten etc al. in [3.11] define tertiary control for ac and dc combined control (similar to level 3) and secondary control as the dc network

specific control (level 2) on a global level and primary control as local converter control (level 1). A similar approach has been taken by Rouzbehi, Miranian et al. in [3.12]. Van Hertem et al. propose a hierarchical control structure as well in [3.13]. In addition, control actions for MTDC systems are often divided into central and local actions, such as by Sass, Sennewald et al. for preventive and corrective actions in [3.14] (see also section 3.2.2). All approaches fit very well with the general categorization of control levels described above.

3.2. Global Level Control: Active Power Transmission

The main driver for the introduction of MTDC into ac power systems is its suitability for transmission of active power, especially when significant distances need to be covered. In addition, VSC-based systems provide additional benefits (see chapter 2). This aspect of active power transmission is not only global to the MTDC system but, as mentioned, to the resulting hybrid ac/dc power system. This means, that the control of the converters making up the MTDC system needs to be embedded tightly into the operation of the ac system. This includes taking into account all economic and technical boundary conditions, essentially including the MTDC system into the dispatch procedure of the existing grid. The control concepts discussed in this section can be attributed to level 4 of the control strategy categorization introduced in section 3.1.

For the scope of this work, the following three aspects are shortly highlighted in the following sections:

- Economic aspects of MTDC system active power control
- Dispatch of MTDC based on ac/dc wide optimization of active power flow
- Security aspect of MTDC dispatch planning

The aspects of operator ownership and global control is discussed in [3.13] in detail.

3.2.1. Market Driven Active Power Transmission

The active power control of a MTDC system is usually tightly coupled to economic considerations. As a very top level layer, the active power of the converters can be integrated into the energy market. This is especially true for HVDC systems forming asynchronous grid interconnections. It also applies to converters in

MTDC systems spanning multiple market regions of a future hybrid power system.

In this market driven operations, the active power transmission is determined by the electricity prices in the respective market region. This enables the operator of the system to leverage price differences. For embedded systems inside one contiguous market region, this is not yet applicable. This could become more relevant in the future, e.g. when a nodal pricing inside the market regions is introduced, enabling the MTDC to actively control the active power transmission based on price levels at the system's converters ac connection.

As is applicable in today's ac grids, the active power order $P_{\mathrm{c}}^{\mathrm{ord.}}$ for the converters is the fundamental basis for the subsequently performed technical dispatch of the MTDC system.

3.2.2. Optimal Power Flow Driven Active Power Transmission

The determination of active power operation points for the converters – and thus the MTDC system as a whole – is often integrated into the dispatch procedure within the operators. This is usually done by integration of the converters active power setpoint P_{ac}^{*} as well as the dc system's constraints into a combined ac/dc optimal power flow (OPF) formulation. This also enables to ensure permissible operation of the MTDC system by adding the system's limitations, such as dc voltage limits $V_{\mathrm{dc,min}}$ and $V_{\mathrm{dc,max}}$ as well as converter maximum power $S_{\mathrm{c,max}}$.

Calculating the MTDC operation point in an OPF enables the operator to integrate the MTDC using a system wide viewpoint. The operator is also able to use economic as well as technical objectives for the OPF. As an example, an embedded MTDC can be used for the minimization of losses of the combined hybrid ac/dc system or for avoiding congested ac lines, both of which are independent of the generator dispatch. On the other hand, the MTDC can be incorporated into the overall optimization of generator costs. The topic of hybrid ac/dc OPF has been scope of work of numerous publications, such as by Baradar et al. [3.15–3.17], Rimez et al. [3.13, 3.18, 3.19], Wiget et al. [3.20, 3.21], Sass, Sennewald et al. [3.14, 3.22], Aragüés-Peñalba, Beerten et al. [3.23, 3.24], Meyer-Huebner et al. [3.25–3.28] and others [3.29–3.33]. The topic is also relevant for smart grid and microgrids, see [3.8] for an extensive review of OPF studies applied there.

The OPF is usually formulated as a non-linear non-convex optimization problem and solved using solvers from the interior-point family (e.g. [3.24, 3.28, 3.34]), with other solvers used as well (e.g. [3.22, 3.29]). The general formulation of the OPF problem is given in equations (3.1) as a function of the state

vector x of the combined system (see [3.28] for details).

$$\min_x f_{\text{obj}}(x) \tag{3.1a}$$

subject to

$$g(x) = 0 \tag{3.1b}$$
$$h(x) \leq 0 \tag{3.1c}$$

with $g(x)$ and $h(x)$ being the equality and inequality constraints considering the entire ac/dc system. The minimum set of constraints associated with the dc system is

$$g_{\text{DC}} = [\mathbf{P}_{\text{dc}} + \mathbf{P}_{\text{ac}} + \mathbf{P}_{\text{loss}}] \tag{3.1d}$$
$$h_{\text{DC}} = \begin{bmatrix} \mathbf{P}_{\text{c}}^{2} + \mathbf{Q}_{\text{c}}^{2} - \mathbf{S}_{\text{c,max}}^{2} \\ \mathbf{V}_{\text{dc,min}} - \mathbf{V}_{\text{dc}} \\ \mathbf{V}_{\text{dc}} - \mathbf{V}_{\text{dc,max}} \end{bmatrix} \tag{3.1e}$$

With the vector of dc powers and losses respectively defined by

$$\mathbf{P}_{\text{dc}} = \mathbf{V}_{\text{dc}} \times (\mathbf{Y}_{\text{dc}} \cdot \mathbf{V}_{\text{dc}}) \tag{3.1f}$$
$$\mathbf{P}_{\text{loss}} = \alpha + \gamma \cdot (\mathbf{P}_{\text{c}}^{2} + \mathbf{Q}_{\text{c}}^{2}) \tag{3.1g}$$

Additional constraints and other formulations are possible as well.

From the point of view of interior-point solvers, the OPF in electrical power systems is of special interest, as the calculations can become challenging when considering large networks. The topic is covered in this field in publications dedicated to solving these large problems, solving optimization problems with millions of state variables. The large number is a result of extending the optimization problem to multiple points in time, uncertainties due to forecasting as well as considering security constraints. These additional dimensions multiply not only the number of state variables and constraints of the original problem, but also multiply by each other when integrating more than one dimension, e.g. considering contingencies over a given number of time steps, resulting in the reported very large optimization problems (see e.g. [3.35, 3.36]).

3.2.2.1. Integration of Security Constraints

The handling of contingencies presents one of the major tasks for generator dispatch. This is also reflected in the converter dispatch for MTDC systems. The (n-1)-principle needs to be tackled for the combined hybrid ac/dc system. The possibilities are to handle the ac and dc system separately or to use a joint (n-1)-security principle. This is reflected in OPF formulations used for the dispatch of controllable assets in the system, termed security-constrained OPF (SCOPF). The SCOPF is scope of many publications (e.g. [3.21, 3.22, 3.26, 3.33, 3.37]).

In SCOPF, the optimization problem is extended to include the contingencies by incorporating a set of x^{c} state variables corresponding to each contingency into the state vector x. The optimization problem is then solved, yielding an operating point, which is secure in regards to all constraints given and also to all contingencies considered. This way, the (n-1)-principle is ensured.

In order to handle contingencies in the system, the SCOPF can consider two possible strategies:

Preventive constraint handling uses a pre-contingency dispatch, that ensures secure post-contingency operation by having a security margin. In case of a contingency, the network is still secure without additional action. The preventive SCOPF is employed for systems with and without dynamically controllable components such as embedded MTDC or storage.

Curative constraint handling utilizes the flexibility of MTDC systems or storage units (or other assets) to allow a post-contingency adaption of operating points. This brings the system dynamically to a secure state. The curative SCOPF is also termed corrective in many publications.

Both preventive and curative (here: corrective) SCOPF are used by Sass et al. in [3.14, 3.22], also describing the integration of the resulting operating points into a hierarchical control scheme. The publications also employ an automated corrective actions implemented on the local converters level of the MTDC. Here, an evolutionary algorithm is used to solve the SCOPF problem. Similarly, Meyer-Huebner et al. show in [3.26, 3.28], that the flexible curative action of MTDC systems and storage units can greatly increase the utilization of the ac system in the pre-contingency dispatch.

3.2.2.2. Integration of Multiple Time Periods

Optimal power flow for the dispatch of the converters, often in conjunction with other controllable assets in the hybrid ac/dc system, is often extended by a time dimension. Analogous to SCOPF, the state vector x is expanded by identical state vectors x^{t} for each point in time that is to be considered. This can for example be used to perform a day-ahead dispatch using hourly data as input. Parameters such as generator costs, state of charge of storage units and a forecast for RES energy production and for expected load can be included in order to achieve an optimal dispatch for the entire time range. Time related constraints can be incorporated as well, such as maximum ramping of generators. This kind of OPF is usually labeled multi-period OPF (MPOPF), more seldom dynamic OPF.

Meyer-Huebner et al. report solving of optimizations over a time horizon of 24 hours in 1 hour steps incorporating MTDC as well as storage units for an exemplary network. Kourounis et al. introduce an MPOPF solver in [3.35], that solves problems for time periods of 8760 hours for IEEE 118 bus network and of 720 hours for PEGASE13659 (i.e. with >13k busses), each with hourly data. Similarly, very high dimensions are reported in [3.36, 3.37]. While these publications do not include MTDC systems, this shows the capabilities of modern solvers and hardware to be able to handle the optimization of hybrid ac/dc grids of realistic size.

3.2.2.3. Integration of Uncertainties

In addition to contingencies and time coupling, uncertainties introduced by forecasted renewable energy sources (RES) production and loads can be incorporated, using the so called stochastic OPF. Here, a number of scenarios taken from a probability distribution are used and incorporated as x^{s} into the OPF problem. System operators can thereby gain a more reliable result in systems with high penetration of RES. For an example of an Stochastic OPF, see [3.38].

3.3. Local Level Control: Active Power Balancing

As introduced before, VSC-MTDC systems are connected to a dc circuit with constant V_{dc}. This allows for the connection of an arbitrary number of converters to one common dc circuit. The voltage level V_{dc} is determined by the energy stored in the dc circuit's capacities (including the converters' internal capacities). As shown in [3.10], the energy stored in the MTDC system's capacitors CE is given by equation (3.2a).These capacities are charged and discharged depending

on the power balance of the dc circuit, given by equation (3.2b). V_{dc} is therefore the synchronizing element in the dc system, much like the frequency in ac systems. However, it is not a global parameter, i.e. it is different for each converter in the system.

$$CE = \sum_{p=1}^{N_{\mathrm{cap}}} \frac{1}{2} C_p V_{\mathrm{dc},p}^2 \tag{3.2a}$$

$$\Delta P_{\mathrm{dc}} = \sum_{q=1}^{N_{\mathrm{conv}}} P_{\mathrm{dc},q} + P_{\mathrm{loss,dc}} \tag{3.2b}$$

Equation (3.2a) gives the total capacitive energy CE in the dc circuit, determined by the sum of individual energies over all capacitive elements N_{cap}, with the corresponding capacities C_p and dc voltage $V_{\mathrm{dc},p}$. Equation (3.2b) gives the excess power ΔP_{dc}, determined by the sum of active power P_{dc} over all converters N_{conv} and the active power losses $P_{\mathrm{loss,dc}}$.

V_{dc} is directly dependent on ΔP_{dc} and thus the converters' active power provision. V_{dc} needs to be kept constant for steady state operation by using the MTDC control system (see section 3.1), i.e. ΔP_{dc} needs to be controlled to zero. On local control scope, the corresponding control is termed direct voltage control. On the global dc system scope, this is called active power balancing, sometimes also active energy balancing. As the three terms relate to the same control action, they are mostly directly interchangeable. For this work, the term active power balancing (APB) is used to describe the synchronizing control of converter active power transmission based on the measurement of the dc voltage. While active power transmission is the primary task related to active power systems in MTDC systems, APB nevertheless plays a vital role in keeping the system stable and in the determination of the active power operating point of the converters in case of a contingency.

For steady state operation, the active power transmission and APB of the MTDC is usually ensured by the global levels of the control hierarchy, see figure 3.1. The two objectives are reconciled by giving appropriate references for P_{ac}^* and V_{dc}^*. The role of APB control is to ensure stable operation for deviations from the calculated operating point. Those can be deviations from modeling, intermittent feed in, e.g. from RES feeding a MTDC directly, such as offshore wind farms. More importantly, the deviations can be caused by contingencies in the dc system, such as converter outages, which significantly disturb ΔP_{dc} in the system. Here, a fast and secure control is needed to ensure stable and permissible system

operation. While a new operating point can be supplied by the global control levels, the local control levels are responsible for the control of V_{dc}, and therefore APB, in order to eliminate the risk of communication failure.

APB control has two aspects:

Converter control strategies are the local control structures generating new reference points for deviations from the operating point provided by the global layers.

Dc grid control strategies are strategies that combine a set of converter controls to achieve APB for the dc system.

The basics of both aspects have been established in publications, such as Barker et al. in [3.39] and Vrana et al. in [3.40], and has been published by Cigré Working Group B4.58 in [3.9]. The described control principles are also part of relevant literature, such as [3.13, 3.41]. The control strategies on converter and grid level are described in more detail in section 3.3.1 and section 3.3.2 respectively.

3.3.1. Converter-level Control Strategies for Active Power Balancing

The need for a communication-less control at converter level arises from the requirements presented in section 3.1. The local control is designed to allow quick response in order to achieve stable operation in the event of a contingency, i.e. mainly converter outage. While the task is easy enough in point-to-point HVDC links, where there is exactly one converter controlling V_{dc}, this doesn't suffice for MTDC systems. Some kind of power sharing needs to be implemented in order to achieve stability for every converter outage (when the primary master controller fails).

As discussed in section 3.1, the options for dc system control mainly include active load sharing (on global levels) and master-slave/droop based (on local level) methods. Active load sharing is mostly not envisioned for MTDC transmission systems, although still mentioned as an option in [3.13]. The second option are master-slave methods, that implement a traditional voltage controller as master, with a fallback slave if the master fails to achieve the desired V_{dc}, due to an outage or overloading.

Droop methods implement a distributed control using a linear relationship between two electrical values. The formulation for MTDC systems can be done in two different formulations as shown in table 3.1 (see [3.42]). The basic representation is shown in equation (3.3), with the corresponding control block

Table 3.1.: Generic representation of droops: Mathematical formulation and control block diagram. Variables are the droop gain k, measured values x and y and the set points x^* and y^*.

$$y = y^* + k\,(x - x^*) \qquad (3.3) \qquad\qquad x = x^* + \frac{1}{k}\,(y - y^*) \qquad (3.4)$$

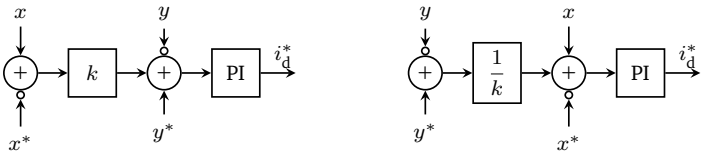

Basic Representation | Alternative Representation

diagram in table 3.1. In MTDC systems, V_{dc} is usually used as y, and the x being either current i or active power p, both defined as positive in direction of the ac grid (from dc to ac). Because i and p can be measured at ac or dc side, this results in 4 possible combinations for the formulation of the droop equation. Furthermore, as equation (3.3) can be reformulated as equation (3.4), this equates to another possible control diagram shown in table 3.1, resulting in four more variations for droop control in MTDC systems.

The droop equation can be interpreted as such: The reference value y^* is increased by a value $\Delta y^*(\Delta x)$, in this case the linear relationship $\Delta y^* = -k\Delta x$ (note the negative sign here). For example, with $y = V_{dc}$ and $x = P_{ac}$, this means that each converter adapts its voltage setpoint V_{dc}^* by an amount ΔV_{dc}^* depending on the deviation of the active power scaled by the droop constant, i.e. $\Delta V_{dc}^* = -k\Delta P_{ac}$. Vice versa, with the alternate formulation given in equation (3.4), it means that the power setpoint P_{ac}^* is adapted by ΔP_{ac}^* depending on the voltage deviation scaled by the inverse droop constant, i.e. $\frac{1}{k} V_{dc}^*$. This formulation is physically very intuitive: the power from the dc system is increased, when the voltage is to high, and vice versa.

The possible implementations for the droop controller are summarized in [3.42]. The control action is linear for current based droop methods ($x = I$) and k can be interpreted as a resistance. If k acts on V_{dc} as in equation (3.4), this variant also doesn't require a PI controller, as the reference value i_d^* can

be calculated from the control value I_{ac} or I_{dc} respectively. All other implementations require a PI controller to generate the reference value i_d^*. For power based implementations ($x = P$), the control becomes non-linear, but also more interpretable from a power system's and global control hierarchy's perspective [3.40]. This is especially true, when looking at the implementation with P_{ac}, as here ac values are compared to dc values. On the other hand, control of active power is normally measured from the PCC, which is also the case for normal active power control (converter controlling P_{ac} only). Thus, using P_{ac} for the power based droop can have advantages, if a generalization of the controller is desired.

The droop control described by equations (3.3) and (3.4) can be drawn on the P-V or the I-V plane, with V usually on the y-axis, and P or I in the x-axis. Power based droops give a linear characteristic in P-V and a non-linear one on the I-V plane. The same is true vice versa for current based droop control. An overview over the characteristics and limits of each droop control method can be found in [3.40] and [3.9]. From here on, following the standard conventions, the concepts are presented for formulation (3.4) with the variant $y = V_{dc}$ and $x = P_{ac}$ only, i.e. the droop equation is

$$P_{ac} = P_{ac}^* + \frac{1}{k}\left(V_{dc} - V_{dc}^*\right) \tag{3.5}$$

For this type of control, a PI controller is always necessary to obtain the reference value i_d^* for the current.

For the introduction of the concepts, the converter limits are omitted and the figures are presented for the deviations in ΔP-ΔV plane. For a detailed representation, including current, power and voltage limits, refer to the Cigré technical brochure [3.9].

3.3.1.1. Basic Concepts

Droop control concepts derived from the simple droop formulation given in equation (3.5) are defined as the basic converter control concepts. More advanced concepts can be derived from these basic control concepts. Figure 3.2 shows an overview over the basic control strategies, presenting the corresponding characteristic and control block diagram.

Voltage droop: Positive droop constant Voltage droop control describes the linear relationship between ΔP_{ac} and ΔV_{dc}. The characteristic is linear in its corresponding plane, see figure 3.2a. The PI controller ensures that in steady

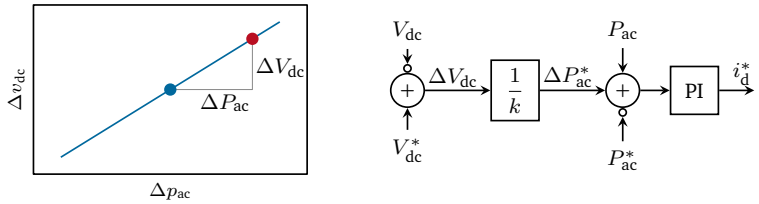

(a) Voltage droop control

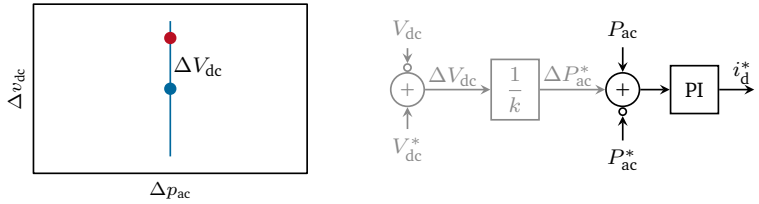

(b) Constant power control

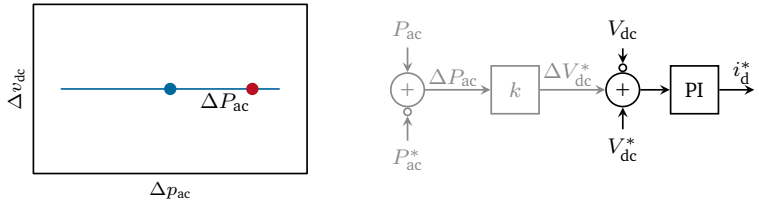

(c) Constant voltage control

Figure 3.2.: Basic control concepts: Characteristics and block diagrams. Blue dot corresponds to the steady state setpoint, red dot to the new operating point after voltage deviation.

state, the error is zero. This implies, that there is a deviation of V_{dc} from its setpoint, which is given by the droop equation $\Delta V_{\mathrm{dc}} = k\Delta P_{\mathrm{ac}}$.

Constant power: Infinite droop constant Constant power control uses an infinite droop constant, i.e. $k = \infty$. Because we use the formulation given in equation (3.5), this equates to a zero gain for ΔV_{dc}, thus effectively negating its influence on the control, i.e. resulting in $\Delta P_{\mathrm{ac}} = \frac{1}{\infty}\Delta V_{\mathrm{dc}} = 0$ for all ΔV_{dc}, with the characteristic shown in figure 3.2b. The ineffective part of the control diagram is grayed out. Using P_{ac}, this concept is equivalent to normal power control.

Constant voltage : Zero droop constant Constant voltage control uses a zero droop constant. Using equation (3.5), this means, that very small deviations in voltage lead to infinite ΔP_{ac}, because for $k = 0$, $\frac{1}{k}$ becomes infinite. In reality, this is not feasible for implementation, as is pointed out in [3.9]. However, it can be interpreted using the basic droop formulation of equation (3.3). Here, $k = 0$ simply yields $\Delta V = 0$ for all ΔP_{ac}. This interpretation is shown in the characteristic and its corresponding block diagram in figure 3.2c. This interpretation also shows that this concept is equal to traditional dc voltage control, as symbolized by the grayed out parts.

3.3.1.2. Advanced Concepts

The basic concepts introduced are sufficient for a stable operation of MTDC systems. However, in order to achieve serviceable grid control strategies, more flexibility is needed, mostly to gain access to “tiered” solutions for back-up schemes (i.e. solutions with more than one control layer). The advanced concepts proposed are piece-wise compositions of the basic concepts. This has the effect, that the control block diagrams are not as straightforward, as switching between different control concepts is needed in some way, such as dead-bands or clamping (e.g. for V_{dc}). While allowing for greater flexibility, this piece-wise approach also has its drawbacks. For one, the switching introduces non-linearities and more importantly discontinuities in the droop gain required to achieve the desired characteristic. This has been shown to lead to undesirable behavior in [3.43]. An overview of the P-V characteristics resulting from the advanced concepts are shown in figure 3.3.

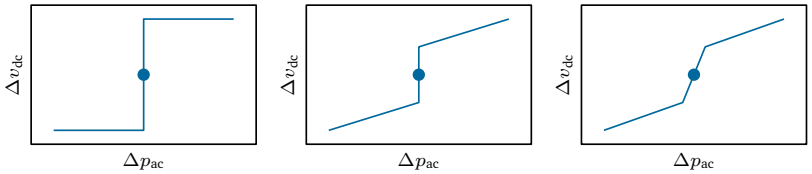

(a) Voltage margin control. (b) Dead-band droop control (c) Undead-band droop control

Figure 3.3.: Advanced control concepts, piece-wise linear, composed of basic control concepts for each dead-band.

Voltage margin control In voltage margin control mode, the converter operates in constant power control in a certain band around its setpoint. When there is significant voltage deviation, the controller switches to constant voltage control. This control mode is usually realized by clamping of the voltage at a certain voltage level. This results in the characteristic shown in figure 3.3a.

Dead-band droop control Dead-band droop control employs droop mode outside a dead-band around the steady state setpoint. Inside the dead-band, the controller is in constant power control. The characteristic is shown in figure 3.3b.

Undead-band droop control Undead-band droop control again operates with a dead-band around the steady state setpoint. The controller operates in droop control inside as well as outside the dead-band, with two different droop constants k, resulting in the characteristic shown in figure 3.3c. Because all basic control concepts can be derived from droop control, undead-band droop control presents the most generalized form of all control concepts. All other concepts can be seen as a special implementation of this variant. In addition, concepts not shown here can also be implemented, such as constant voltage control inside the dead-band and droop control outside.

3.3.1.3. Nonlinear Continuous Droop Control

The discontinuities of the advanced, composite control concepts can lead to undesired oscillations. Therefore, there have been efforts to design control

methods that do not rely on switching between different modes of operation. For example, Marten et al. have shown the unstable behavior in [3.43] and proposed a continuous droop method to cope with this phenomenon [3.44]. The continuous characteristic is calculated by a combination of two sigmoid functions as given in equation (3.6).

$$P(V) = \frac{P_{\text{max}} - P^*}{e^{h_{\text{left}}(V - V_{\text{min}})} + 1} + \frac{P^* - P_{\text{min}}}{e^{h_{\text{right}}(V - V_{\text{max}})} + 1} + P_{\text{min}} \tag{3.6}$$

The proposed continuous droop control is able to emulate the basic control concepts by parameterization of the sigmoids. Slight limitations exist for dead-band and undead-band droop methods, which cannot fully be implemented due to the characteristic of the sigmoid functions.

3.3.1.4. Generalized Droop Controller

The basic and advanced concepts have in common, that having constant power and constant voltage control cannot be achieved with the same control structure. This is due to the fact, that infinite gains are numerically infeasible for the control structure. Coming back to the formulation of the droops, the gain associated with k or $\frac{1}{k}$ can only achieve either constant voltage or constant power respectively. In order to overcome this, several generalized formulations have been proposed. These are designed to provide the possibility to achieve all control modes with one control structure. Generalized concepts include the generalized voltage droop proposed by Rouzbehi et al. in [3.12, 3.45] and a generic primary control structure proposed by Berggren et al. in [3.46]. In addition, the continuous droop control described above can also be seen as a generalized form of the droop formulation.

Generalized voltage droop With the generalized voltage droop (GVD), Rouzbehi et al. describe a droop formulation which can be parameterized to achieve any basic control concept. The GVD formulation can be done for current based [3.45] or power based [3.12] formulation. The equation for GVD is given in equation (3.7) with the parameters α, β and γ. Constant power control is achieved for $\alpha = 0$, constant voltage for $\beta = 0$, conventional voltage droop for $\alpha, \beta, \gamma \neq 0$.

$$\alpha V_{\text{dc}} + \beta P + \gamma = 0 \tag{3.7}$$

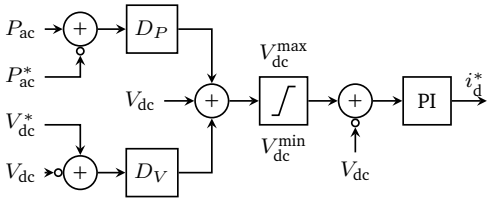

	D_P	D_V
Const. P	1	0
Const. V	0	1
Droop (P)	D_P	1
Droop (V)	1	D_V

Figure 3.4.: Generic primary control: Control block diagram and table of parameters required to achieve conventional basic control concepts. Based on [3.46].

Generic primary control structure Berggren et al. propose a straightforward control structure in [3.46], implementing both ΔP_{ac} and ΔV_{dc} in parallel, each with a gain D_P and D_V respectively. This generic control structure is shown in figure 3.4, including a table of parameter sets to achieve the basic control concepts. This structure very well discusses the interchangeable nature of the two formulations. For steady state operation within limits, the PI controller ensures zero error and thus the relationship given in equation (3.8a).

$$0 = \Delta P_{ac} D_P + \Delta V_{dc} D_V \tag{3.8a}$$

$$\Delta V_{dc} = \frac{D_P}{D_V} \Delta P_{ac} \tag{3.8b}$$

The relationship to the droop formulation in equation (3.5) is shown by reordering to equation (3.8b), with the simple relationship $k = \frac{D_P}{D_V}$. An important statement of the publication is furthermore, that there is need for tuning the PI controller based on the parameters chosen to maintain desired control performance. This statement applies to all droop related concepts, as soon as the control structure changes its gains.

3.3.2. Dc Grid Control Concepts

The local levels of converter controls, i.e. the converter primary control structures, must be coordinated over all converters of a MTDC system to form a dc grid control concept. For this, the converter level control concepts are combined to achieve a stable voltage control for all contingencies. The concepts here again largely follow the Cigré methodology [3.9]. All grids concepts essentially follow

the same pattern as with the converter concepts. Basic grid control is comprised of the basic converter concepts. The advanced grid concepts make use of the dead-bands of the advanced converter concepts to achieve a “tiered” control concepts including a back-up control (see section 3.3.1).

3.3.2.1. Basic Grid Control

These control concepts implement the dc grid control with only one mode of operation, i.e. neither a distinction between steady state and disturbed operation nor a back-up.

Centralized voltage control This concept uses a master concept, with exactly one converter in constant voltage as the voltage controlling instance. All other converters of the MTDC system are operated in constant power mode. This concept, while simple to implement, has several drawbacks. For one, the voltage controlling converters take up all power fluctuations, which equates to stress for the converter as well as the connected ac system. This becomes more pronounced with increasing network sizes. Furthermore, there is no back-up for the voltage control for large disturbances. These disadvantages make this concept infeasible for all but the simplest MTDC systems.

Distributed voltage control This concept employs a several, or even all, converters of a MTDC in voltage droop control. This means, that the voltage control is distributed over all these converters, the power shared depending on the droop constant of each respective converter. As V_{dc} of each converter is not a global value (opposed to the frequency), this power share is not exactly determined. Due to the nature of droop control, there will always be a steady state deviation after a contingency.

3.3.2.2. Advanced Grid Control Concepts

The advanced concepts described in the following make use of the advanced converter control concepts, and thus can make a distinction between e.g. steady state and disturbed operation. This also implies a back-up voltage control.

Centralized voltage control with centralized back-up Here, in addition to a central master converter in constant voltage mode, a dedicated converter in voltage margin control is employed as backup. Thus, if the master voltage

controller is overloaded or fails, the converter takes over the voltage control. This concept is equivalent to the master-slave principle. It has the advantage of very clear distinction of responsibility, because there can always be exactly one converter in voltage control.

Centralized voltage control with distributed back-up This concept uses dead-band droop control to achieve a distributed back-up for a central voltage controlling converter. In contrast to the centralized back-up, the consequences for large disturbances are shared by multiple converters, which can be beneficial, especially for larger networks. On the other hand, in contrast to distributed voltage control, the voltage deviation for small disturbances and steady state is zero, because of the voltage controlled central converter.

Distributed voltage control with distributed back-up With this concept, the undisturbed voltage control as well as the back-up is shared by multiple converters. For this, undead-band droop control is employed, with different droop constants and dead-bands for the converters, depending on which role they shall take. This is the most general of the grid control concepts. As already discussed in section 3.3.1 for undead-band droop control, the other concepts described in this section can be derived from this concept as a special case. This makes the concept very flexible and also enables further research to tie in with the general idea presented.

3.3.2.3. Pilot Node Concept

As mentioned, V_{dc} is a parameter local to each individual converter. Berggren et al. have proposed the so called pilot node concept for MTDC systems [3.47]. Here, one node in the system is designated the “pilot node”, with all converters controlling the voltage at that pilot node. This introduces communication and undermines the local character of the hierarchical level. However, it allows for a very efficient calculation of droop constants to achieve exact power sharing in the case of disturbances.

3.3.2.4. Optimization-based Control Strategies

Dc grid control concepts, which operate on the local control levels receive their parameters and setpoints from the hierarchical MTDC control system. This can be leveraged to employ an optimization not only on the global level, but also

directly on the local control level. This is achieved by optimizing the parameters of the converter control, e.g. the droop gain parameter k of all converters employing the basic control concept (see section 3.3.1). The optimization is performed with an objective, which can be chosen by the operator. A common formulation is an optimization of control parameters with the objective to minimize the transmission losses in the complete ac/dc system.

This kind of parameter optimization has been proposed in the context of the GVD in [3.48] as well as for the continuous droop in [3.14]. Optimization of droop controls is also a research topic in the scope of dc microgrids [3.6]. The concepts seem very promising, as they bridge the gap between the very fast response achieved by the local control level and the subsequent (slower) update received from the global control levels.

3.4. Discussion of State of the Art Control Concepts

In this section, the state of the art on MTDC control and the possibilities for further development are discussed, with focus on the local control levels, as these will be the focus for the remainder of this work. For this we will first evaluate the requirements for MTDC system control already discussed in section 3.1. In [3.9], the requirements for the local control are defined for MT-HVDC systems specifically. The requirements here focus on a stable, reliable and redundant control concept, which can achieve energy and power balance of the dc system and being easy and flexible to dispatch and schedule. This shall be done without the risk of hunting between the controlling converters, while being able to control the dc voltage and the load of the converter in admissible limits. Finally, the concept shall be interoperable both between the converters and with other control loops inside the local control, e.g. Power Oscillation Damping.

Most of those requirements apply to the local control level. With the concepts described in this chapter, the requirements for both global and local control levels are satisfied. Still, from the above analysis of the state of the art, especially in section 3.3, additional requirements for the local control level can be derived:

- Provide a control structure that can be generalized and parameterized to achieve at least the concepts described in section 3.3.1.
- The control characteristic shall be as continuous as possible in order to avoid unstable operation at the discontinuities.
- Allow good flexibility regarding power sharing of the individual converters,

such as asymmetric characteristics, i.e. different behavior for positive and negative deviations of the control variables.

- Ensure adequate performance of the PI controller over the entire range of the control characteristic.

Most of these additional requirements can probably be fulfilled by the basic and advanced control concepts from [3.9], e.g. control performance and flexibility. However, hard switching between control modes is an integral part of the advanced concepts, so discontinuities in the gain cannot be avoided. Moreover, an infinite gain is problematic from the point of view of control implementation. Thus, different structures are required to implement constant power and constant voltage in a single controller.

These challenges are partly overcome in some of the publications included in section 3.3.1.2. The continuous droop concept for example eliminates the discontinuities of the composite characteristics. It can be seen as a generalized structure and provides a good degree of freedom. However, concepts like undead-band droop control cannot be replicated with it. Moreover, the concepts break with the original idea of droop. The connection from the droop constants of the conventional concepts to the parameters of the continuous is possible, but not straightforward. Research aiming in the direction of droop control will thus not be easily reproducible.

Generic primary control on the other hand gives a generalized control structure able to implement the basic concepts in one control, and also discusses the control performance to some degree. Still, the controller is mathematically equivalent to the basic concepts and the advanced concepts are not as straightforward. The same is true for the generalized voltage droop.

In this work, we will bridge the gap between the basic and advanced concepts and the additional requirements that have been identified. The following chapters establish a methodology for the modeling and assessment of hybrid ac/dc systems (chapter 4), the converter level design of a controller (chapter 5) and the derived grid control concepts (chapter 6).

4. Modeling Requirements for HVDC System Simulations

The simulation of hybrid ac/dc systems requires appropriate models, which have to be adapted to the scope of the investigations. The level of detail for these models can range from very high for electromagnetic transient or hardware in the loop studies to very low for steady state power flow or optimal power flow studies.

High level of detail includes detailed modeling of each subcomponent for the converters as well as high fidelity line modeling of lines and other components in the ac and dc system. While this kind of model fidelity is able to capture the behavior of the converters in a realistic way, it also requires a high computational effort, which is not feasible for each specific application. This is why the model fidelity needs to be adapted to the time constants of the investigated phenomena and to the component in focus of the respective study. In this work, a system model with medium level of detail has been used.

This chapter presents the modeling of the power system used in this work and introduces the benchmark system used to create the simulation cases:

Section 4.1 gives an overview over the abstraction levels for converter models and discusses the level of detail needed for this work.

Section 4.2 deals with the converter model that implements the required level. The model description includes the converter station and the corresponding control loops.

Section 4.3 deals with the modeling of the hybrid ac/dc system as a basis for the creation of the network models used in the subsequent analysis. This includes the applied dc system topology, transmission system models for ac and dc, as well as the generator models.

Section 4.4 presents the benchmark system and the corresponding simulation cases used in later system assessment. For this, currently available benchmark systems are discussed and the benchmark system is designed.

4.1. HVDC Converter Model Abstraction Levels

As described above, the models of HVDC converters can have various levels of details depending on the use case. High level of details includes a detailed representation of all station equipment, such as surge arresters, circuit breakers, disconnectors and more. This level of detail has to be extended to all control and protection systems, in order to capture the relevant interactions with the electrical system. In order to standardize the model level of detail, Cigré has published a guide in [4.1]. This guide introduces 7 types of converter models, which equate to the respective scope. The types range from full physical models, over a number of models with details appropriate for electromagnetic transient (EMT) simulations, to simplified models for phasor simulations (type 6) and loadflow calculations. For a detailed description and discussion of the different model types, the reader is referred to the original guide.

As discussed in chapter 3, the scope of this work is APB control in MTDC grids. The APB control is part of the outer control, furthermore the focus will be on the active power flow in the hybrid ac/dc power system and on the interaction with the electro-mechanical dynamics of the ac system. From this, we can conclude, that the implementation of a type 6 phasor domain model is the appropriate choice. Considering phasor domain for the simulation yields the best trade-off between model fidelity and computing times. It also has the advantage of simplifying the control design regarding the inner control loops and thus also making the methods independent of the actual converter technology used.

For these reasons, for the remainder of this work, phasor simulation of the converter and the ac/dc system in general will be considered. The model for the type 6 simplified average value model, including the required control, is described in section 4.2.

4.2. Modeling of HVDC Converters

This section deals with the modeling of the converters that make up the MTDC system of the simulation models. The converter model is discussed first, followed by the electrical components and the control system needed for the phasor simulation of the converter.

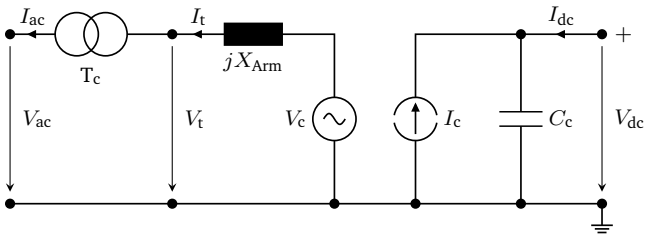

Figure 4.1.: Structure of the simplified average value model [4.1], including the converter substation.

4.2.1. Converter Model Structure

The type 6 simplified average value model (AVM) discussed in section 4.1 consists of decoupled ac- and dc-side elements. The dc side is modeled by a current source feeding a capacitor, the ac side is modeled by a three-phase voltage source connected in series to the arm reactance. The ac voltage source operates at fundamental frequency only, i.e. no switching harmonics are modeled. The general layout of the model is shown in figure 4.1. The ac and dc side of the model are coupled using the power balance of the converter given in equation (4.1), i.e. the powers flowing through the converters are directly coupled without any dynamic behavior.

$$P_{ac} + P_{dc} + P_{loss} = 0 \tag{4.1}$$

In addition to the converter, the substation connecting to the ac grid comprises a transformer and the PCC terminal, with measurements for the control system (see section 4.2.2).

4.2.2. Modeling of the Converter Control System

The control system of the converter is modeled as described in [4.1] as well. As the AVM is based on a the fundamental frequency ac voltage, the control system introduced in figure 2.3 in chapter 2 is realized only up to the inner current controller (ICC), generating v_c as the reference for the voltage source. The dc current reference is determined by the power balance formulation given in equation (4.1). The inner control loops, e.g. arm balancing control, are omitted

due to the usage of the AVM for phasor domain simulation. An overview over the control structure is shown in figure 4.2.

4.2.2.1. Control System Inputs

The inputs used in the control system are measured inside the converter substation at different points. The location of the input value measurement points are specified in figure 4.1. All measured values are converted to per unit and are subsequently used for the converter control loops. The control system takes the following input signal:

- Voltage v_{t} and current i_{t} measured directly at the converter terminal.
- Voltage v_{ac} and current i_{ac} measured at the PCC.
- Dc voltage v_{dc} measured at the dc terminal.

4.2.2.2. Control System Structure

The simplified control has the following structure:

Preprocessing & Synchronization: Encompasses the transformation to dq reference frame, calculation of AC powers at PCC and the PLL.

Outer control loops: High level control loops to determine the required converter reference currents.

d-axis control: This block realizes control loops related to active power and generates the d-axis reference current i_{d}^{*}. This control block the most significant for this work, as it comprises the APB control.

q-axis control: Realizing the reactive power related control action and generates the q-axis reference current i_{q}^{*}. This control loop is out of scope for this work and will mostly be neglected.

Current limiter: Limits the reference current i_{dq}^{*} to the admissible total current for the converter. Here, the limitation is used with equal scaling of the dq values and set to 1 p.u.

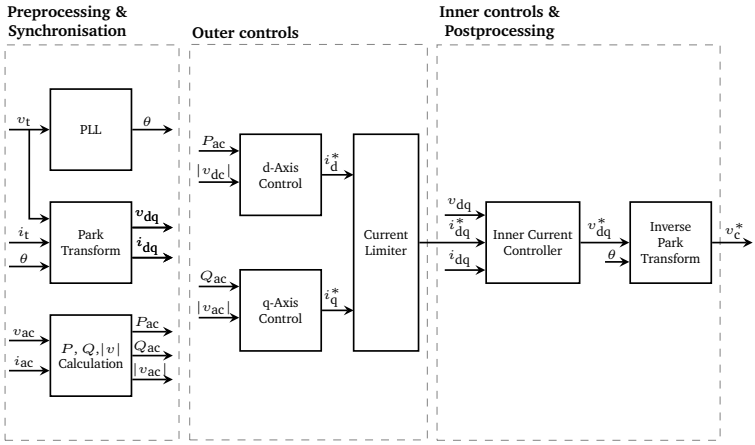

Figure 4.2.: Structure of the control system based on [4.1].

Inner control loops: Here, the inner control loops consists only of the ICC, creating the voltage reference v^*_{dq} from the measured and reference currents i_{dq} and i^*_{dq} and the terminal voltage v_{dq}. All other inner control loops can be neglected for the phasor domain AVM.

Postprocessing: Comprises transformation to the reference values for the converter voltage source.

4.3. Modeling of the Multi-Terminal Dc System

This section deals with the modeling of the ac and dc components needed in addition to the converters. For this, the component models used are introduced and discussed.

4.3.1. Dc System Topology

The topology of the embedded MTDC system is described in section 2.3.1. For the simulation, one topology has to be selected. MTDC in general can be built with all topologies, however, while the symmetric monopole is used for offshore

systems a lot, the bipole seems to be the most plausible solution. On the other hand, the simulation of bipole systems in network models tends to complicate showing basic principles. This is caused by the fact, that bipole systems have the advantageous effect of being able to take some of the power when an outage occurs.

The scope of this work is to show the basic principles and the power flows and their deviations in the network. The influence of the topology on the results, on the other hands is negligible, when the worst case is considered, which is the outage of the whole substation. For that reasons, the decision was made for an asymmetric monopole topology for the MTDC system.

4.3.2. System Interconnection

The system interconnection, i.e. the lines between the terminals of the ac and dc systems, is done in a straightforward way:

- For the ac system, overhead lines with a phase-to-phase voltage of $380\,\mathrm{kV}$ are used, with the parameters based on a basic tower geometry.
- The dc system is connected using cables with operating voltage of $320\,\mathrm{kV}$, with parameters taken from [4.2]. While an embedded MTDC system would likely be constructed with overhead lines or using mixed transmission media, the influence is negligible, so this straightforward approach is used.

4.3.3. Generator Model Ratings

The generators in the model are based on standard generators of the power system software used. They are modeled including the generator transformer and controls including excitation system (automatic voltage regulator, AVR) and turbine governor (GOV). There are no power system stabilizers (PSS) used in this work.The ratings and parameters of the generators as well as the control system variables are given in Appendix A.

4.4. Benchmark Systems for Hybrid Ac/Dc Systems

The topic of appropriate benchmark systems exists for all applications. For ac grids, there are numerous benchmark systems defined by different entities, such as the IEEE. However, for dc systems, the level of standardization is not as far

advanced. Still some benchmark systems for ac/dc systems are available. This section discusses the existing benchmarks and introduces the benchmark system used to construct the simulation cases for the further analysis.

The following requirements are defined for the benchmark system for this work:

1. Embedded HVDC: The system shall be able to show the effects of a MTDC system, with all or most terminals in a contiguous ac grid area. Preferably, there should be a clear power transmission direction, as would be expected in a lot of real-life scenarios.

2. Included dynamics: The system shall be designed for (at least) phasor simulation, i.e. dynamics of at least the systems generators need to be included.

3. Minimum working example: The system shall be designed to intuitively describe a test case with exactly as much components as needed, as shown with the two area system presented in Kundur's *Power System Stability and Control* [4.3]. The reasoning is, that this makes it possible to understand the fundamental physical processes.

4.4.1. Analysis of Existing Benchmark Systems

There exist a number of benchmark systems for MTDC systems, each tailored to a specific usecase. Most notable here is the CIGRÉ B4 DC grid test system, which has been published in [4.4] in 2013, and more recently in [4.5], where it is more deeply analyzed. In addition, Sass et al. have published a system for mixed ac/dc system in [4.6].

The Cigré system can be used to model a number of scenarios. However, when looking at embedded MTDC systems, there is no application given there, that satisfies the need for a dynamic benchmark system, i.e. a certain number of nodes in one ac area. The second benchmark, while more tailored towards OPF and (n-1) line contingencies, includes an embedded MTDC and has one specified scenario including a power flow direction. It is not considered for this work because of the requirement for a minimum working example. It would nevertheless be an interesting option for further research, if a dynamic model is available.

4.4.2. Power System Model Used in this Work

For the reasons laid out above, a novel fundamental benchmark system has been designed to show the effects in a very intuitive way in a minimal system. However, because there are some requirements on the system, a certain number of components is required. The fundamental design principles are

Long distance power transmission: the benchmark shall depict the scenario of an ac system subjected to a significant power transmission, which is taken partly by the MTDC system and partly by the ac system.

Generators: There shall be generators present in all regions of the system, possibly showing (small) oscillatory behavior. This is done to be able to evaluate, albeit on a very basic level, the effect on the small signal behavior of the system.

MTDC converters: There shall be a number of converters in the same region, with the distances between the converters noticeable, but small compared to the main power transmission axis.

A power system model has been designed to meet these criteria. The model has the following features:

- There are 2 main regions, northern, and southern. In addition, there is a middle region, which is not part of the active power transmission, but plays a role for reactive power compensation and can have connections to the MTDC system.
- The main regions have 2 horizontal terminals each. Again, there is a horizontal midpoint terminal, which can be connected with the MTDC system.
- The regions are connected by overhead lines as discussed in section 4.3, the vertical lines sum up to 400 km and the horizontal lines within the regions to 50 km.
- The western and eastern terminals each have generators attached. In addition, there are components that achieve the vertical power transmission:
  - An additional RES generation unit is connected to the northern terminals.
  - A load is connected to the southern terminals.

- At the vertical middle terminals, there are two shunt reactive power compensation units, which provide the reactive power necessary for the long vertical lines.
- The MTDC network can be connected to all terminals present in the system.
  - Depending on the simulation case, only some of the converters are in effect.
  - The network is interconnected by a simple, radial dc system.

The MTDC is the element defining the simulation case. All other components stay the same for each case. A naming scheme in the form of $<N_{\mathrm{N}}><N_{\mathrm{M}}><N_{\mathrm{S}}><\mathrm{r}>$ is used, where N_{N} represents the number of converters in the northern region, analogous for $<N_{\mathrm{M}}>$ and $<N_{\mathrm{S}}>$, the "r" part stands for system interconnection, i.e. radial as meshed systems are not investigated. For example, if the simulation case has 2 converters at the main terminals in the north-west and north-east, none in the middle region and two on the main terminals in the southern regions, with a radial interconnection, the simulation case is labeled *202r*.

For the network elements, the labeling has the form $< Element >_{<Location>}$, with the converters C, the generators G, the loads L, RES W, the terminals T and the ac and dc lines respectively $\mathrm{L_{ac}}$ and $\mathrm{L_{dc}}$. The location is given by north N, south S, east E, and west W as well as the middle components M.

The resulting model is depicted in figure 4.3, with the "optional" converters in gray. The model shown here, is modified to construct cases based on the needs of the simulations. Each simulation case has a specifically tailored, distinct operating point.

4.4.3. Simulation Cases for System Assessment

A number of simulation cases are defined for the assessment of grid concepts performed in chapter 6. The case names correspond to the introduced naming scheme and each is tailored to the concept, which shall be presented. The active power setpoints for all cases are presented in p.u. in table 4.1. The load flow for each of the simulation cases is presented in more detail in Appendix B.

Case 202r This case presents the case with the least components needed to show the desired effects. Only the eastern and western terminal at the northern and southern region have connected converters. The converters have a active power setpoint which is about half of the rated power.

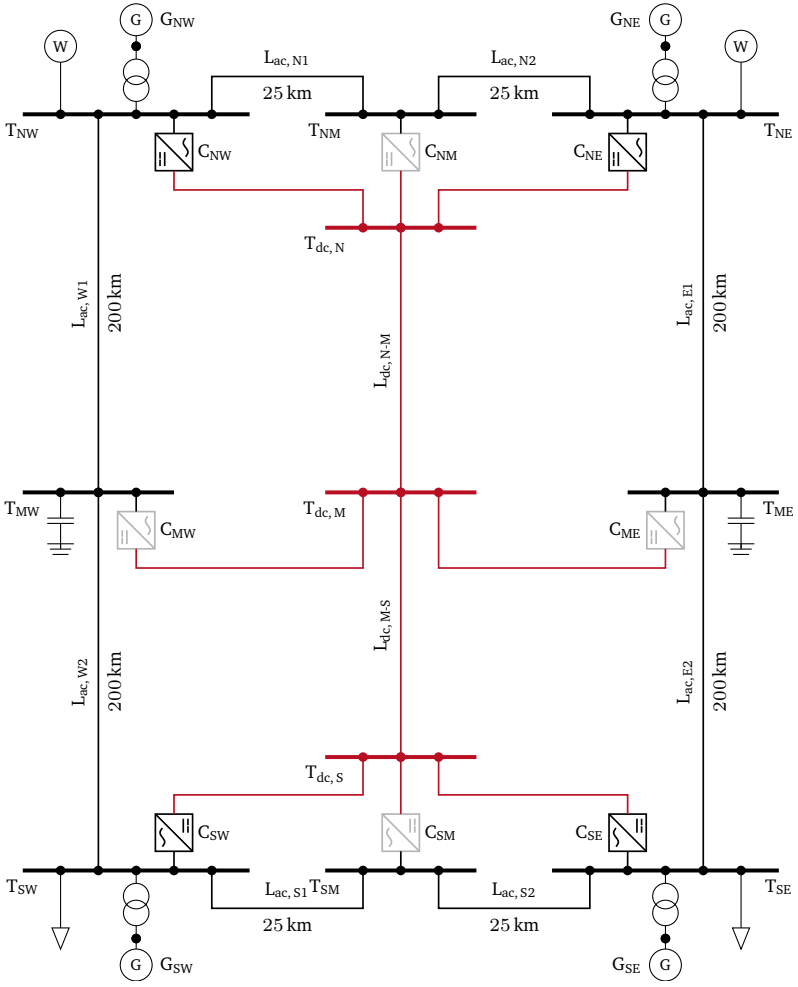

Figure 4.3.: General model of the power system used in this work including line lengths. The gray units represent the optional converters of the MTDC system.

Table 4.1.: Active power setpoints of the converters for each case.

Case	Active power setpoint P_{ac}^{*} in p. u.							
	C_{NW}	C_{NM}	C_{NE}	C_{MW}	C_{ME}	C_{SW}	C_{SM}	C_{SE}
202r	-0.47	–	-0.49	–	–	0.47	–	0.47
303r	-0.63	-0.66	-0.63	–	–	0.63	0.63	0.63
222r	-0.78	–	-0.78	0.11	0.15	0.625	–	0.625

Case 303r For this case, the three northern and southern converters are in effect each. The scenario is tailored to have more than two remaining converters in any respective region for a converter outage. The converters are more loaded in comparison to case 202r to show the effect, when no individual converter can fulfill power balancing by itself.

Case 222r This case has the northern and southern converters like in case 202r, but adds the two converters at the middle terminals. This case is designed to show how intermediate converters can take part in power transmission in case of on outage in one of the main reasons. The converters have high loading for the main regions and low loading for the middle region.

4.4.4. Oscillatory Modes of the System

The model has two distinct regions with a long transmission line. It is expected to have some sort of oscillatory behavior, which can be used to evaluate a possible impact of a dc grid control concept.

A pre-study regarding the small-signal stability of the system has been performed to get the relevant oscillatory node, i.e. modes of the system with low bandwidth in the relevant frequency range. For this, the system small-signal equations are analyzed, taking into account the electrical system as well as the incorporated controls of the ac generators. In addition to the frequency and damping of all oscillatory modes of the system, the calculation also yields the participation factors for all components of the grid and the control system. The components with higher participation factor contribute more to the mode, enabling a root of cause analysis. The results are filtered for modes with low damping ratio and high magnitudes, i.e. modes which will also impact the dynamic behavior after a converter outage, which essentially acts as the excitation

Table 4.2.: Summary of least-damped oscillatory modes in the relevant frequency range.

Mode	f	T	Damping ratio	Damping time constant	Participating components	
	Hz	s	%	s	Group 1	Group 2
1	1.24	0.80	6.09	2.10	G_{NE}, G_{NW}	G_{SE}, G_{SW}
2	1.55	0.64	8.64	1.18	G_{NE}	G_{NW}
3	1.46	0.68	9.46	1.15	G_{SE}	G_{SW}

impulse for the oscillations.

The results summarized in table 4.2 show, that there are low-damped modes with participation of the generators. Most notably, mode 1 represents the generators of the southern and northern terminals swinging against each other with a period of $0.8\,\mathrm{s}$. This is a north-south oscillation which is expected in this benchmark system. This kind of slow oscillatory mode is also a characteristic feature of many real world grids with low meshing and high transmission distances.

Modes 2 and 3 are nodes with participation of the eastern and western generators, i.e. represent a east-west or “horizontal” oscillation. As the distance on this axis is much lower, these are more damped compared to mode 1.

Observing the three least damped modes, the system is expected to have significant oscillations when excited, which should be influenced by the APB strategy used by the MTDC system. The oscillation as well as the influence of the MTDC system is clearly observed in the dynamic simulations of the system, see chapter 6.

5. Proposed Generalized Continuous Active Power Controller

After the identification of the general requirements in chapter 3, this section deals with the design, implementation and verification of a controller, which aims to fulfill these requirements. The controller is labeled the generalized continuous active power controller, GC-APC, after the two most crucial features, that it implements.

The section is structured as follows:

Section 5.1 introduces the control principles that build the basis for the later implementation of the GC-APC.

Section 5.2 presents the implementation of the control principles into a control structure and presents the resulting control characteristics.

Section 5.3 gives details on the time domain performance of the proposed controller.

Section 5.4 finally summarizes the findings of this section.

5.1. Control Principles

This section presents the principles and methods used in the design of the GC-APC. First, the requirements are adapted into design criteria. Subsequently the methods for the generalization, the specification for the characteristics and a way to achieve continuous characteristics are presented.

5.1.1. Design Criteria for the Active Power Controller

Looking at the requirements defined in section 3.4 we can see that most of them apply to the converter controller. This is especially true for the additional requirements introduced there. Out of those, flexibility of power sharing needs

to be implemented into the grid control concept. The others, namely the generalized structure, the continuous control characteristic as well as the appropriate performance need to be implemented on the controller side.

This leads to the design criteria defined for the GC-APC:

Generalized control: The GC-APC shall consist of one and only one control structure, that achieves all control concepts that can be of use in a given grid control concept.

Flexible Parameterization: To achieve an intuitive design of the grid concepts, an intuitive parameterization shall be possible.

Continuous Operation: The GC-APC shall avoid hard switching between control modes as well as between linear sections of the characteristic. If possible, this includes limits for e.g. dc voltage.

Consistent Control Performance: The control performance of the controller shall be independent of the current operating point.

The following sections follow these criteria and present the proposed solutions.

5.1.2. Generalized Approach to Power Control

One first and crucial criterion is the implementation of a generalized, i.e. unified approach for the converter concepts introduced in section 3.3. This means, that the concepts constant voltage, constant power, and the corresponding droop concepts, i.e. V-control with P-droop (V-P-droop) and P-control with V-droop (P-V-droop), should actually be implemented in one controller.

The key challenge is already outlined in the Cigré report [5.1], which states that voltage control could be implemented with zero droop constant k, yielding infinite gain. Thus, it is concluded, that this concept needs a PI controller. This statement can be extended: We know, that equation (5.1a) and equation (5.1b) are equivalent.

$$u_1 \cdot G(s) + u_2 = y \tag{5.1a}$$

$$u_1 + u_2 \cdot G^{-1}(s) = y \cdot G^{-1}(s) \tag{5.1b}$$

This implies, that when converting from V-P-droop to P-V-droop, i.e. k to $\frac{1}{k}$, there is also a gain on the error signal equal to $\frac{1}{k}$. This means, that numerically

the equations $\Delta P = \frac{1}{k}\Delta V$ and $\Delta V = k\Delta P$ will become infeasible for $k \to 0$ and $k \to \infty$ respectively. This shows, that the concepts derived here cannot be applied if all droop concepts shall be incorporated in a generalized concept.

Berggren et al. have given a proposal how to handle this with the generic structure from [5.2](see section 3.3). The questions here would be, when we would switch between the gains D_P and D_V proposed there to implement V-P-droop and P-V-droop. The value, when to switch would depend not only on the gains, but also on the dynamics associated with the voltage and power closed loop, as you would want to switch in the region, where the dynamics are approximately the same. Failing to do this would invariably lead to a jump of controller bandwidth at the point of switching and thus a significant non-linearity in control behavior.

This work proposes a novel approach, which builds upon this idea. However, instead of arguing based on the gains of the system, we introduce a control angle Γ, which corresponds to the angle of the droop characteristic and therefore the participation in voltage control. We define $\Gamma = 0°$ if there is no participation at all (=constant P), and $\Gamma = 90°$ for full participation (=constant V). The values inbetween will correspond to the droop concepts.

For a more intuitive approach, we define a normalized control angle γ, which is expressed in per unit:

$$\gamma = \frac{\Gamma}{90°} \tag{5.2}$$

Furthermore, we define the intermediate participation in voltage control $\gamma = 0.5$ as the line through the voltage and power limits as given by equation (5.3a). Thus, γ is calculated as of equation (5.3b) with the change in power and voltage deviation $d\Delta P$ and $d\Delta V$ respectively. For a linear characteristic, it follows that $\frac{1}{k} = \frac{d\Delta P}{d\Delta V}$. Consequently, $\frac{1}{k}$ can be formulated as given in equation (5.3c).

$$c_{\text{max}} = \frac{P_{\text{max}} - P_{\text{min}}}{V_{\text{max}} - V_{\text{min}}} \tag{5.3a}$$

$$\gamma = \arctan\left(\frac{d\Delta P}{c_{\text{max}} \cdot d\Delta V}\right) / \frac{\pi}{2} \tag{5.3b}$$

$$\frac{1}{k} = c_{\text{max}} \cdot \tan\left(\frac{\pi}{2} \cdot \gamma\right) \tag{5.3c}$$

From this definition, the voltage droop definition $\Delta P = \frac{1}{k}\Delta V$ and derived concepts can be replicated very easily as shown in equation (5.4) for the extreme cases $k \to 0$ and $k \to \infty$.

$$\gamma\left(k \to 0\right) = \arctan\left(\frac{1}{c_{\max} \cdot 0}\right) / \frac{\pi}{2} = \arctan\left(\infty\right) / \frac{\pi}{2} = 1 \text{ (constant voltage)} \tag{5.4a}$$

$$\gamma\left(k \to \infty\right) = \arctan\left(\frac{1}{c_{\max} \cdot \infty}\right) / \frac{\pi}{2} = \arctan\left(0\right) / \frac{\pi}{2} = 0 \text{ (constant power)} \tag{5.4b}$$

This shows that all droop control concepts can now be logically expressed on a generalized scale in the range of $\gamma = (0, 1)$. A crucial observation is also the relationship of γ with the gains D_P and D_V used in generalized droop methodology from [5.2], which can be derived using the droop gain k with $k = \frac{D_P}{D_V}$ and equation (5.3c). When rewritten as in equation (5.5a), the gain can be calculated directly from γ as given in equations (5.5b) and (5.5c). This relationship preserves the values for the gains at the extreme case, i.e. $D_P(y = 1) = 0$, $D_P(y = 0) = 1$ and correspondingly $D_V(y = 0) = 0$, $D_V(y = 1) = 1$. However, in the range $\gamma = (0, 1)$ the gains are continuously updated without a hard switching between control modes. This effect is used for the design of the GC-APC proposed in section 5.2.

$$\frac{1}{k} = \frac{D_V}{D_P} = c_{\max} \cdot \tan\left(\frac{\pi}{2} \cdot \gamma\right) = \frac{c_{\max} \cdot \sin\left(\frac{\pi}{2} \cdot \gamma\right)}{\cos\left(\frac{\pi}{2} \cdot \gamma\right)} \tag{5.5a}$$

$$D_V = c_{\max} \cdot \sin\left(\frac{\pi}{2} \cdot \gamma\right) \tag{5.5b}$$

$$D_P = \cos\left(\frac{\pi}{2} \cdot \gamma\right) \tag{5.5c}$$

The control angle γ can also be interpreted as a continuous measure for the derivative of the characteristic, which is important for gain scheduling of the associated PI controller.

5.1.3. Construction of Continuous Characteristics

As discussed in chapter 3, the droop formulated in equation (5.6a) can also be interpreted as adding an additional offset ΔP^* to the reference power P^*. Equations (5.6b) and (5.6c) show the restructuring of the classical droop equation (5.6a). $\Delta P^*\left(\Delta V\right)$ is the offset to the reference power P^* in dependence on the voltage deviation ΔV, which is equal to $\frac{1}{k}\Delta V$ in this case.

$$\Delta P - \frac{1}{k}\Delta V = 0 \tag{5.6a}$$

$$P - \left(P^* + \frac{1}{k}\Delta V\right) = 0 \tag{5.6b}$$

$$P - \left(P^* + \Delta P^*\left(\Delta V\right)\right) = 0 \tag{5.6c}$$

Once this observation is made, it is not important, how this additional value ΔP^* is calculated, as long as the resulting characteristic in the P-V-plane is achieved as desired by the operator. That means that $\Delta P^*\left(\Delta V\right)$ can be any value, e.g. obtained by any mathematical equation or lookup table. If desired, additional variables could be introduced for the calculation of ΔP^*, which is however not done in this work. Note that for this implementation, the derivative of the characteristic at the corresponding operating point is still crucial for the gain scheduling, as discussed in section 5.1.4.

Being able to calculate ΔP^* flexibly is key for the construction of continuous characteristics. In principle, it can take any form, as long as the derivative of the resulting characteristic is positive (in the reference frame chosen in this work). In order to comply with the existing concept, an approach is chosen, that uses the existing undead-band concept as a basis. As stated previously, the undead-band concept is the most general and all other concepts can, in principle, be derived.

The construction of the continuous characteristic is done using a straightforward approach based on the specification of linear dead-band regions and subsequent "smoothing" of the switching between these linear regions. For this the following steps are performed:

1. Specification of dead-bands in order to achieve the individual linear regions of the characteristic.

2. Specification of a smoothing factor to avoid the discontinuities between the linear regions.

3. Interpolation of the characteristic in between the linear regions to achieve a continuous characteristic without hard switching.

4. Incorporation of the voltage and power limits into the continuous characteristic.

These steps are described in the following sections.

5.1.3.1. Specification of the Dead-bands

The specification of the dead-bands is done by selection of a the dead-band using either ΔV or ΔP as threshold and the droop constant k. This implementation is not straightforward, as the choice here depends on the kind of approach chosen, i.e. using a power or voltage based droop (see section 3.3.1). The introduction of the control angle γ solves this by enabling any linear region in the sense of an (un)dead-band to be expressed using two of three values ΔV, ΔP, γ. With the constraints $\frac{\Delta V}{\Delta P} \geq 0$ (=positive derivative of the characteristic), the dead-bands can be freely selected. We will define all dead-bands based on ΔP and ΔV for this work, because a direct interpretation of the linear regions of the characteristic is possible this way.

The n^{th} dead-band will thus be defined by the threshold point db^n, which is a tuple $(\Delta P^n, \Delta V^n)$ seen from the current operating point of the converter. The linear region for db^n is thus defined by the regions between the threshold points db^n and the previous threshold db^{n-1} or the steady state operating point for the first one. The corresponding control angle γ is calculated using equation (5.3b), defining the derivative of the characteristic for the corresponding linear region for db^n.

5.1.3.2. Avoiding Discontinuities by Smoothing of the Characteristic

In order to avoid the discontinuity associated with the switching between the linear regions defined by the dead-band points, an approach based on interpolation is chosen. This interpolation shall be done between the threshold values between the linear dead-bands. For this, transition points db^n_{n} and db^n_{p} are introduced at negative and positive side of db^n respectively. The two transition points are used as starting point and end point for the interpolation between the linear region. We introduce a continuity coefficient c_{r} for the calculation of these points, that determines the location of the transition points. c_{r} is defined in the range of $c_{\text{r}} = (0, 1)$ to determine which portion of the linear region is interpolated.

The calculation of the transition points is shown in equation (5.7). The resulting characteristics for different coefficients c_{r} is shown in figure 5.2.

$$db^n_{\text{n}} = db^n - c_{\text{r}} \cdot \frac{db^n - db^{n-1}}{2} \tag{5.7a}$$

$$db^n_{\text{p}} = db^n + c_{\text{r}} \cdot \frac{db^{n+1} - db^n}{2} \tag{5.7b}$$

In words, the interpolated non-linear region is defined by the mid-points $\frac{db^n - db^{n-1}}{2}$ between two dead-bands, scaled by c_r. For $c_\mathrm{r} = 1$, the entire range of the characteristic is interpolated and the non-linear regions touch each other. For $c_\mathrm{r} = 0$, no interpolation takes place, and the characteristic is equal to a conventional undead-band droop, consisting only of the linear regions. The choice of the coefficient c_r is a trade-off between a smoother characteristic for high c_r and interpretability and power sharing preciseness for lower c_r.

5.1.3.3. Method of Interpolation between Dead-bands

In the next step, the characteristic between the transition points is interpolated to achieve a smooth transition at the threshold point db^n. The following objectives are defined for this interpolation:

- At the starting and end points of the interpolation, i.e. db^n_n and db^n_p respectively, the derivative of the characteristic, i.e. γ shall be equal to the corresponding linear region.
- The characteristic shall be gradually interpolated from one linear regions to the next, i.e. smooth transition of γ.

The interpolation technique of quadratic Bézier curve fulfills exactly the above objectives (see [5.3]) and is consequently selected for the interpolation in this work. Quadratic Bézier curves are defined by three control points $\mathbf{P}_0$, $\mathbf{P}_1$ and $\mathbf{P}_2$ and a parameter t with $0 \leq t \leq 1$ which indicates the position of the interpolated point on the curve. $\mathbf{P}_0$and $\mathbf{P}_2$ are part of the resulting interpolated curve, while $\mathbf{P}_1$ is called the inflection point and determines the form of the curve.

The formulation for the Bézier curve in its quadratic polynomial form is shown in equation (5.8a). Notably, the derivative of the curve at the point $\mathbf{P}$ can also be directly calculated by forming the derivative of equation (5.8b), which is shown in equation (5.8b).

$$\mathbf{P}(t) = (\mathbf{P}_0 - 2\mathbf{P}_1 + \mathbf{P}_2)\, t^2 + (-2\mathbf{P}_0 + 2\mathbf{P}_1)\, t + \mathbf{P}_0 \tag{5.8a}$$

$$\frac{d}{dt}\mathbf{P}(t) = 2\,(\mathbf{P}_0 - 2\mathbf{P}_1 + \mathbf{P}_2)\, t + (-2\mathbf{P}_0 + 2\mathbf{P}_1) \tag{5.8b}$$

The resulting Bézier curve has two important properties:

1. The endpoints are part of the interpolated curve, i.e. the interpolated curve begins at $\mathbf{P}_0$ and ends at $\mathbf{P}_2$ exactly.

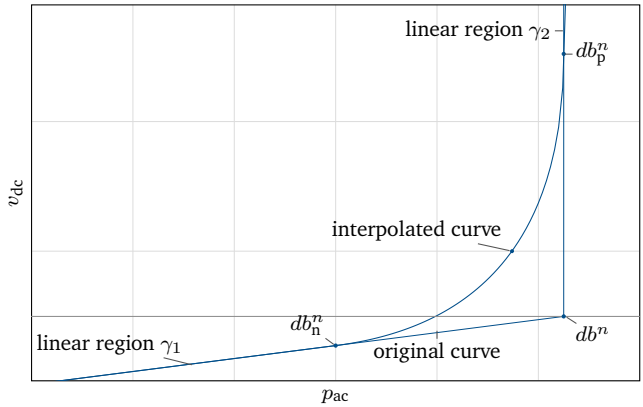

Figure 5.1.: Visualization of the proposed construction of the continuous characteristic.

2. The curve is tangent to the segments to $\mathbf{P}_1$, i.e. the tangents at the starting and endpoint meet at $\mathbf{P}_1$.

With the definition of the three control points of the Bézier curve to $db^n = \mathbf{P}_1$, $db_\mathrm{n}^n = \mathbf{P}_0$, and $db_\mathrm{p}^n = \mathbf{P}_2$, these properties of the Bézier curve show perfect correspondence to above requirements. The resulting interpolation is shown in figure 5.1 together with the corresponding threshold db^n and transition points db_n^n and db_p^n.

Moreover, because the curve is a quadratic function, the parameter t can be calculated from either ΔP or ΔV by solving equation (5.8a) for t. The other value can be subsequently calculated by inserting the resulting t into equation (5.8a). This procedure can be used to derive the required $\Delta P^* (\Delta V)$.

5.1.3.4. Incorporation of Voltage and Power Limits

The limitation of the voltage and the power of the system to certain values can be incorporated into the continuous characteristic. For this, the voltage limit Bézier curve db^lim is assigned with the point where the curve intersects the voltage limit V_lim, the negative point $db_\mathrm{n}^\mathrm{lim}$ is assigned according to above formula, and $db_\mathrm{p}^\mathrm{lim}$ is assigned to the limit for both power and voltage. This

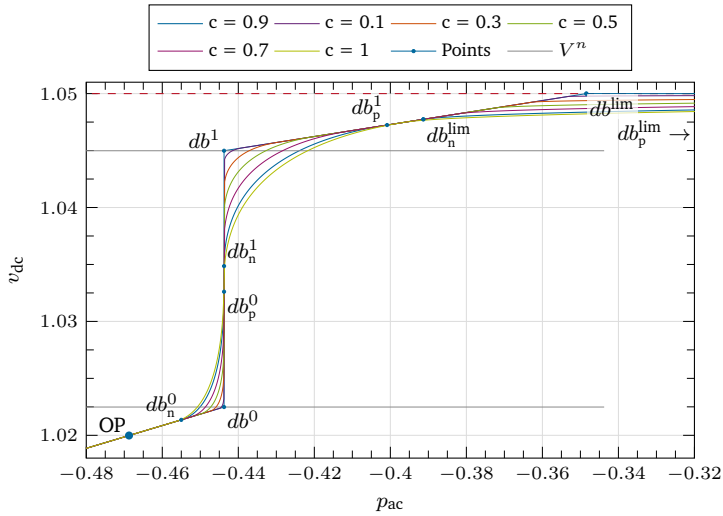

Figure 5.2.: Visualization of the dead-band interpolation using Bézier curves for two dead-bands. Curves for $c_r = (0.1, 0.9)$, points shown for $c_r = 0.9$.

way, the controller will provide maximum power at the upper voltage limit and minimum power at the lower voltage limit.

While the same could be done for the power limit, in this work it is not taken into account, as this increases the voltage deviation for an outage and decreases the effectiveness of power sharing.

An exemplary characteristic for positive ΔV_{dc} is shown in figure 5.2. Here, the relevant threshold and transition points are specified for a continuity coefficient c_r of 0.9. Furthermore the original and smoothed characteristics are shown for different coefficients c_r in the range of $(0.1, 0.9)$, showing the effect of the coefficient c_r, the interpolation and the incorporation of voltage limit.

5.1.4. Gain Scheduling of the PI Controller

As described in section 5.1.2, the performance of the controller is dependent of the derivative of the characteristic, and consequently of γ. When parameterizing the PI controller for a conventional droop concept with the droop gain k, the dynamics of the closed loop system is static, i.e. does not change in regards to the control system. The PI controller is then tuned to this particular dynamic. If the droop gain changes, the parameters have to be adapted to the new value. This is particularly significant, when using a generalized control concept, e.g. as introduced in section 3.3.1.4.

When a calculated characteristic is used, this still holds true, even if no actual gain k is used. The derivative of the characteristic at each given point describes the sensibility of the characteristic to a change in the measurement variable, i.e. it determines the dynamic, that the calculated value changes. The derivative thus presents a "virtual" gain that needs to be taken into account for the parameterization of the PI controller. Because the control angle γ presents a measure for the derivative of the characteristic of the controller, it can be utilized to achieve a gain scheduling.

To do this in a simple way, we define the PI controller in a serial form as given in equation (5.9a) with the proportional gain K_P and the integral time constant T_I. To implement the gain scheduling, we define two seperate gains K_V and K_P associated with the voltage and power droop concept respectively. Using the two tunable gains, the gain of the PI controller is calculated by linear interpolation as shown in equation (5.9b).

$$PI(s) = K_\mathrm{P} \cdot \left(1 + \frac{1}{T_\mathrm{I}}\right) \tag{5.9a}$$

$$K_\mathrm{P} = K_V \cdot \gamma + K_P \left(1 - \gamma\right) \tag{5.9b}$$

From this relationship, it can be seen that for pure voltage control, i.e. $\gamma = 1$, only K_V is in effect. Consequently, for pure power control, i.e. $\gamma = 0$, only K_P is in effect, with the droop concepts automatically calculating their gain according to the derivative of the characteristic in that particular operating point. The gain scheduling allows the operator to parameterize the PI controller based on the dynamic of the voltage and power loop independently.

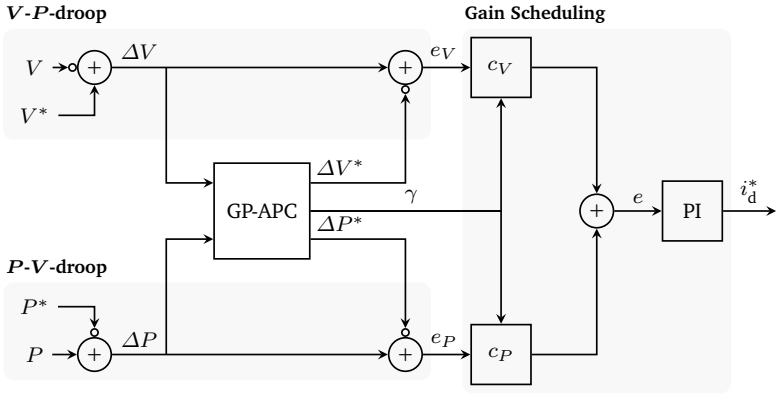

Figure 5.3.: Control structure of the GC-APC as a block diagram. Creation of the control characteristic and the control values is done in the central block.

5.2. Implementation of the Generalized Controller

Using the principles and methods defined in section 5.1, a controller can now be implemented. The challenge herein lies in the operation of voltage as well as power control in one structure. This section presents the implementation of the the GC-APC structure, the structure of the input parameters as well as the characteristic resulting from an exemplary set of parameters. The concept's control structure block diagram is shown in figure 5.3.

5.2.1. Controller Structure

The control structure is based upon the idea, that it is possible to run two control loops in parallel, V-P-droop conventionally defined by $\Delta V = k\Delta P$ and P-V-droop defined by $\Delta P = \frac{1}{k}\Delta V$. The loops equate to error signals e_V and e_P as given in equation (5.10). ΔV^* and ΔP^* are the offsets to the references as discussed in section 5.1.3, which are calculated by the GC-APC block.

$$e_V = \Delta V - \Delta V^*(\Delta P) \tag{5.10a}$$
$$e_P = \Delta P - \Delta P^*(\Delta V) \tag{5.10b}$$

The controller uses continuous characteristics defined by an input structure (see section 5.2.2), and calculates the values for $\Delta V^*\,(\Delta P)$ and $\Delta P^*\,(\Delta V)$ and their derivatives based on the measurements for P and V respectively, using the interpolation method shown in section 5.1.3. Based on the derivatives of the characteristic for a given voltage deviation, the control angle $\gamma\,(\Delta P, \Delta V)$ is calculated as discussed in section 5.1.2. The control angle is then used for two purposes: first, to schedule the gain of the PI controller as shown in section 5.1.4, second to also schedule the two droop blocks as given by equation (5.11), with the two gain scheduling factors c_V and c_P and the corresponding total error signal e.

$$c_V = c_{\text{max}} \cdot \sin\left(\gamma \cdot \frac{\pi}{2}\right) \tag{5.11a}$$

$$c_P = \cos\left(\gamma \cdot \frac{\pi}{2}\right) \tag{5.11b}$$

$$e = c_v \cdot e_v + c_P \cdot e_p \tag{5.11c}$$

As the control angle approaches 0, c_V goes to zero, with the V-P-droop becoming unstable while c_p approaches 1, which is appropriate for $\gamma = 0$. For $\gamma = 1$, the same applies vice-versa.

This gain scheduling allows for a continuous implementation of both loops in one controller. The presented control structure approach solves the problem, that one droop formulation cannot be applied by the basic formulas of the conventional concepts introduced in chapter 3. Here, both loops are active all the time, and are switched in a continuous fashion based on the calculated control angle γ.

It is important to keep in mind, that both loops of the GC-APC implement the identical continuous characteristic. This means, that both loops converge to zero for the steady state operating point, i.e. equation (5.11a) always converges to zero with both e_v and e_p equal to zero.

5.2.2. Input Structure

The characteristic defined by the GC-APC needs to have a structure, where the operator can easily parameterize the system. The dead-bands for this characteristic are based on the inputs of the dead-band threshold points db, as defined in section 5.1.3.1. For this work, the GC-APC is parameterized with the following inputs:

Table 5.1.: Exemplary parameterization for the GC-APC, taken from the case 202r for C_{NW}.

	V_{db}	P_{db}	V_{min}	V_{max}	P_{min}	P_{max}	c_r
	%	%	p.u.	p.u.	p.u.	p.u.	
db^0	0.25	2.5	0.95	1.05	−1.0	1.0	0.9
db^{+1}	2.5	2.5					
db^{+2}	5	50					
db^{-1}	-1	-40					
db^{-2}	-2	-60					

- A steady state dead-band db^0, which is symmetric to the negative and positive plane, V_{db}^0 and P_{db}^0. This ensures a stable and precise steady state operation point by avoiding a discontinuity. This steady state dead-band can be chosen very small, because it is not relevant for dynamic reaction.
- A number of dead-bands for each negative and positive plane. Two dead-bands are used in this work:
  - Positive plane: db^{+1}, db^{+2}
  - Negative plane: db^{-1}, db^{-2}
- Limits on voltage and power:
  - Voltage: V_{min}, V_{max}
  - Power: P_{min}, P_{max}
- Continuity factor c_r
- Parameters for the PI controller: K_V, K_P and T_I

The parameters can be freely chosen as discussed in the previous sections.

5.3. Dynamic Verification of the Controller Design

In order to evaluate the performance of the GC-APC, an exemplary controller design is verified. The following uses the parameter set for one converter taken

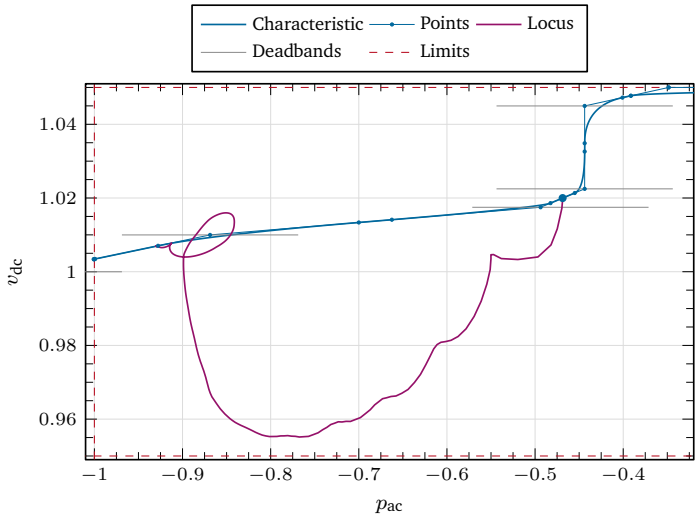

Figure 5.4.: Diagram of the exemplary characteristic in P-V-plane, including the construction points and dead-bands as well as the locus of the converter for the dynamic verification.

from grid 202r specified in table 5.1 as an exemplary case. The parameters for the PI controller are $K_V = 1$, $K_P = 4$ and $T_{\mathrm{i}} = 0.5\,\mathrm{s}$ to achieve a stable operation in roughly $0.5\,\mathrm{s}$, with acceptable transients. For the parameters chosen, the values for γ on the relevant negative plane can be calculated as $\gamma^0 \approx 0.29$, $\gamma^{-1} \approx 0.75$ and $\gamma^{-2} \approx 0.5\,\mathrm{pu}$ using equation (5.3b).

The characteristic corresponding to the exemplary parameter set as well as the locus of the converter voltage and power are shown in figure 5.4. The graph shows, that the controller achieves a new operating point located on the continuous characteristic.

In addition, the results of the measured values ΔV and ΔP as well as the values $\Delta V^*\,(\Delta P)$ and $\Delta P^*\,(\Delta V)$ calculated by the GC-APC are shown in figure 5.5 as timeplots over one second with the outage at zero seconds.

The signals for voltage and power are shown in figures 5.5a and 5.5b respectively. It can be seen, that measured and calculated value converge to the same value. Thus the corresponding error signals e_v and e_p converge to zero

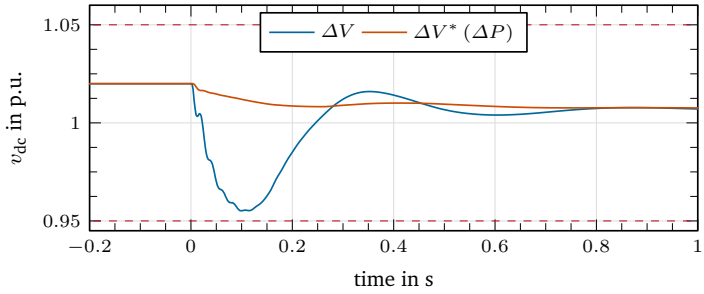

(a) Measured and calculated voltages

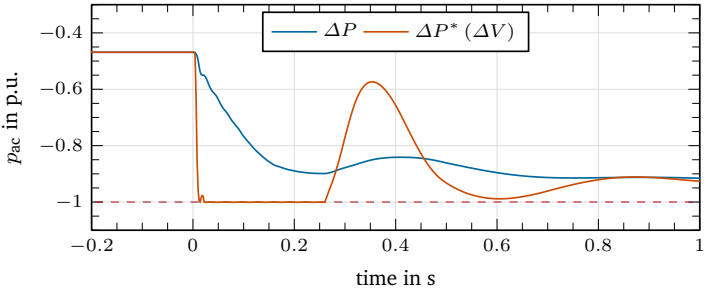

(b) Measured and calculated active powers

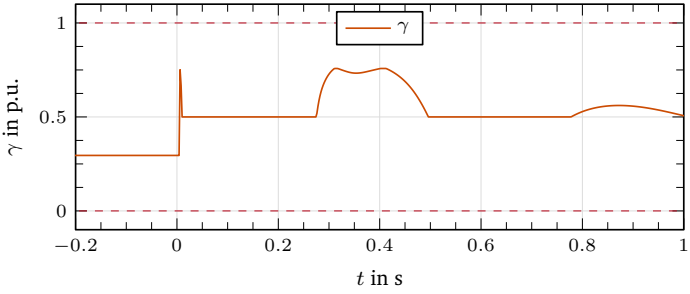

(c) Calculated control angle γ over time

Figure 5.5.: Dynamic verification of the GC-APC, using the exemplary parameterization of C_{NW} based on grid 202r, outage of C_{NE}. Measured values in blue, calculated values in red.

as discussed in section 5.2. Figure 5.5c shows the calculated control angle γ over the time range. The control angle equates to the calculated values for db^0 and db^{-2}. Also a deviation in direction of γ^{-1} is shown when the locus is in the region of db^{-1} (see also figure 5.4).

The verification shows that the controller achieves the design objectives with the proposed structure.

5.4. Summary for the Active Power Controller

This chapter has presented a generalized continuous active power controller (GC-APC) for the active power balance in MTDC networks. Starting from the definition of control principles for the design of the controller, appropriate methods are proposed. The generalization is achieved using a novel approach to droop control by definition of a control angle γ that achieves steady calculating of the values for the entire operational range. The nonlinear continuous characteristic is constructed by interpolating linear regions of the characteristic, avoiding hard switches between operation modes. Finally, an approach to gain scheduling based on the defined control angle γ is proposed.

In a second step, the GC-APC is implemented using these methods. For this, a control structure based on the calculation of the points on the characteristic and their derivatives as well as a parameter structure is introduced.

Finally, the GC-APC is verified using an exemplary parameter set. Results show, that the desired characteristic can be achieved and all design objectives are fulfilled.

6. Possible Derived Dc Grid Control Strategies

The requirements for the control of MTDC systems have been established in chapter 3 and a generalized controller has been designed based on these requirements. To achieve a desired power sharing of a MTDC system by means of the active power balancing control, the control characteristics of the individual converters in the system have to be coordinated to form a grid control strategy. In chapter 3, the grid control strategies for the conventional droop control are described, e.g. decentralized with decentralized back-up. This chapter establishes the grid control concepts leveraging the features provided by the GC-APC. The concepts are defined by the composition of characteristics in each region of the grid as well as by the concrete parameters chosen of the each characters.

The design and simulation of the dc grid control concept in this chapter is structured as follows:

Section 6.1 discusses the design of the grid control based on the requirements from chapter 3 and establishes the basic types of strategies for subsequent implementation.

Section 6.2 implements and analyses the dc grid control concepts for the benchmark systems discussed in chapter 4. For each system, it discusses the appropriate parameters and the resulting steady state characteristics for the converters, presents the results of the simulation of converter contingencies and analyses the impact of the outage on the ac system in comparison to conventional droop control.

Section 6.3 summarizes the results and discusses possible implications.

6.1. Control Strategies Design

This section discusses the design of the dc grid control. For this, the basic design principles are first established and developed into grid control concepts.

6.1.1. Basic Dc Grid Control Design

In contrast to ac networks, embedded MTDC systems are primarily transmission assets. There are neither generation nor load units inside the network aside from the converters. This means, that the transmission through the dc network has a certain profile which is – at least qualitatively – always known, because the converter setpoints are always known. Often, this transmission profile will have a certain "direction" that is determined by load and generation centers of the ac grid, e.g. the transmission along the north-south axis from wind generation to load centers, which is typical for Germany (and many other regions). In addition to this, the control shall distinguish between steady state and larg(er) disturbances.

In addition to the minimum requirements given in chapter 3, we define the following design principles:

Selectivity: The converters shall be able to react differently, depending on the current power and voltage deviations, i.e. the severity of the disturbance (steady state control, power fluctuations, large disturbance, etc.).

Directionality: The grid control concept shall be able to discern between positive and negative power balance, i.e. take into account the direction of power transmission.

Flexibility: The operator shall be able to select the control modes for the converters in a simple and intuitive manner.

The first design principle, *selectivity*, is implemented using tiers, which essentially correspond to a defined order in which to react to a disturbance. The tiers are defined by the parameters for the dead-bands of the controller in relation to each other. As described in chapter 5, the GC-APC can be parameterized by two of the three reference parameters voltage V_{db}, power P_{db} and control angle γ_{db} for each dead-band. For the purpose of this chapter, we will use the voltage and power to define each tier. Derived from the principles above, we define the tiers:

Tier 0: This zero level tier describes the behavior of the control in steady state. In order to avoid a change of parameters at the setpoint, the steady state tier is symmetric, i.e. with equal positive and negative values for the dead-band. As in conventional concepts, the converters responsible for voltage control can be freely assigned, and converters can but need not take part in voltage control.

Tier 1 to N: Each subsequent tier can be assigned in the same way as before. However, in order to comply to the *directionality* principle, there will be a distinction for each tier between positive (with suffix -p) and negative (with suffix -n) tier. The power provided and the corresponding voltage dead-band V_{db} can also be freely chosen depending on positive or negative tier.

- Tier 1-p: Parameters V_{db} and P_{db} for the reaction to positive deviations.
- Tier 1-n: Parameters V_{db} and P_{db} for the reaction to negative deviations.

The tiers can be very flexibly parameterized, fulfilling control principle *flexibility*. It is advisable to define the tiers using common dead-bands for the GC-APC for all converters[1]. The voltage dead-bands V_{db} are arguably the preferred option, as the deviation of the voltage is the main indicator for power imbalance. It is important to notice, that the tiers can be triggered slightly differently for each converter, because V_{dc} is a local measurement and the voltage deviation ΔV_{dc} can be different on the converters due to a changed power flow in the dc system.

For an exemplary grid control design, the following parameterization could be chosen:

- Tier 0 could be parameterized to allow only very small voltage deviations by assigning two or more converters with small values for V_{db}, but also only for a small power range P_{db}, designed to result in a high control angle γ_{db}, e.g. the converters control the voltage to a deviation of $V_{\text{db}} = 0.25\,\%$ using available power of $P_{\text{db}} = 5\,\%$. Converters not part of Tier 0 voltage control are assigned a value of $P_{\text{db}} = 0$ for this dead-band.
- If the power assigned in Tier 0 is not sufficient and the voltage deviation exceeds V_{db}, the controller will progress to the next higher tier. There,

[1] Note: The parameters of different (groups of) converters allow completely different voltage and power dead-bands. However, power sharing at the post-contingency operating point would not be very intuitive in this case.

additional converters could be added to the voltage control by assigning $V_{\mathrm{db}} = \pm 1.00\,\%$ to several more converters, including or not including the original voltage controlling converters. For the Tier 1-p, the voltage dead-band would be $V_{\mathrm{db}} = +1.00\,\%$, with a contribution $P_{\mathrm{db}} = +10\,\%$ for one subset of converters and zero contribution $P_{\mathrm{db}} = +0$ for another subset. For Tier 1-n, the subsets would be mirrored, with $V_{\mathrm{db}} = -1.00\,\%$ for all converters and $P_{\mathrm{db}} = 0$ and $P_{\mathrm{db}} = -10\,\%$ for the each respective converter subset.

6.1.2. One-tiered Control Strategy

One-tiered control is the basic control strategy implemented in the above framework. It is employed, when there shall be only a distinction between steady state and disturbed operation. Steady state is represented by the Tier 0, Tier 1 is subdivided into positive and negative plane, i.e. Tier 1-p and Tier 1-n. Although there can be two tiers, only one plane and consequently only one control tier is in effect for a given converter outage. For symmetric parameters, this concept equates to undead-band control. It is, however, asymmetric in nature due to the degree of freedom coming from the GC-APC.

The following example shall demonstrate the possible use case: Given a transmission grid with two regions, north and south, and north-south power transmission.

- In steady state, the voltage is controlled by Tier 0 with one converter in each region to distribute the stress at the PCC to both regions.
- In Tier 1-p, if the voltage deviation is positive, the southern converters, which take power out of the dc grid, shall contribute with all available power to voltage control with a small voltage deviation.
- In Tier 1-n, if the voltage deviation is negative, the northern converters, which provide power to the dc grid, shall contribute with all available power to voltage control with a small voltage deviation.

The resulting concept shall ensure that the active power transmission in the grid is maintained as good as possible for the outage of each converter.

If one of the northern converters fails, the energy balance in the grid will be negative (energy exported from the grid), and the voltage will drop. Thus the other converter(s) will take over power up to their capacity to maintain the transmission direction. As there is no second tier, there is also no back-up

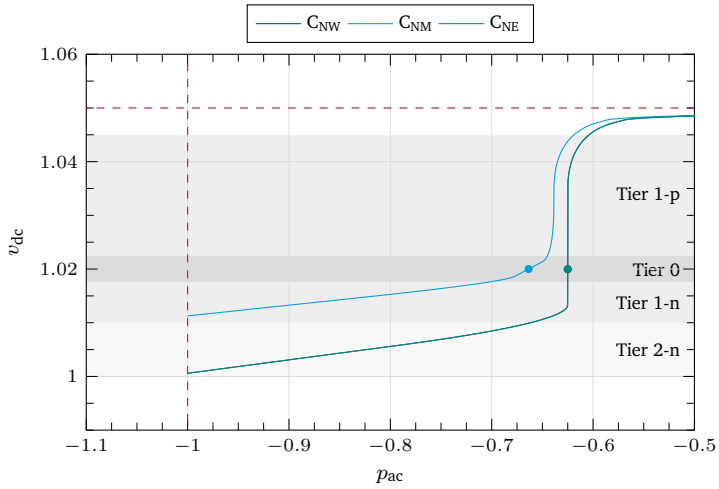

Figure 6.1.: Example for a two-tiered grid concept. Only the northern region is shown. Converter C_{NM} is active in Tier 0 and Tier 1-n, C_{NW} and C_{NE} in Tier 2-n with equal characteristics.

voltage controller as the southern converters do not contribute in Tier 1-n. They will still take over power, as the voltage limitation in the GC-APC activates, when $V_{dc,max}$ is reached.

If one of the southern converters fails, the dc grid concept operates vice versa. The southern converter acts as voltage controller to take out as much power as possible, controlling the voltage and maintaining the power transmission.

6.1.3. Multi-tiered Control Strategies

Two-tiered concepts is an extension of one-tiered strategies, adding more deadbands for each positive and negative plane and therefore another layer to the control strategy. This means, that in addition to the one-tiered example, the grid control concept can be parameterized to distinguish between the converters in the same region, or add a second layer of control from another region. In practice, this layering ensures, that the first layer participates with the maximum power provision to the power sharing scheme. The additional power needed

to balance the MTDC system is provided by the converter(s), which are part of the second layer. By assigning converters to the first, second layer or none at all thus enables the operator to achieve very flexible control of the power sharing in the MTDC grid for each positive and negative deviations.

An exemplary concept taken from the grid 303r is shown in figure 6.1. Here, the tiers of the northern converters are presented. In Tier 0, i.e. steady state control, converter C_{NM} is responsible for voltage control, the other two northern converters are active power controlled with γ equal to zero. The same is true for the first negative Tier 1-n. In the second negative Tier 2-n, the other 2 converters (same characteristic) are in shared, decentralized voltage control. For the positive plane, all converters do not contribute to APB. Here, the southern converters are active (see figure 6.9 on page 96). It is interesting to note, that the usage of a high interpolation factor c_r may cause the tiers to overlap and thus interfere with the grid control strategy.

The term multi-tiered concept expands the two-tiered concept to an arbitrary number of control tiers. Although there is no formal limitation on the number of tiers, in order to maintain a clear distinction between the tiers and to still have an intuitive design, the number of tiers should be limited.

The two-tiered control, i.e. negative and positive plane having two dead-bands each, is utilized for the results presented in this work in order to provide enough flexibility while limiting the complexity. An example for the complete grid concept with two tiers can be found in figure 6.2, where the concept for a grid with 4 converters is shown.

6.1.4. Vertical and Horizontal Control Tiers

If there are more than two regions (e.g. there is a middle region in above example), a distinction can be made between the way the tiers are designed. If power sharing between two converters takes place inside a region (e.g. for converter PCCs located near each other), the term horizontal tier is used. This enables to configure the grid concepts in a way, that the power in the case of a converter outage is balanced by other converters in the same region in a tiered fashion. If the power sharing is effective between multiple geographical regions (e.g. along the transmission path), the term vertical tier is used. Vertical tiers allow the converters in the intermediate region to help in APB, if the capabilities of the converters in the faulted region are exceeded.

As an extension to the Directionality requirement, it is considered desirable to compensate for the outage of a converter at a location as near as possible.

Table 6.1.: Parameters common for all investigated scenarios.

Parameter	c_r	K_P	K_V	T_I in s
Value	0.9	4	1	0.05

Thus, it is expected, that horizontal tiering is always more preferable to vertical tiering.

6.2. Implementation and Simulation of the Grid Concepts

This section presents the implementation of the concepts introduced in section 6.1 and the results of the contingency simulations. The implementation is done choosing appropriate parameters for each grid investigated. For detailed information on the grid models see chapter 4. A two-tiered control strategy is employed for all grids, with the control parameters common for all benchmark systems as given in table 6.1. The PI controller parameters for the voltage loop K_V and for the active power loop K_P are obtained by investigation of the responses for operation with very high and very low control angle γ respectively. A high value for c_r is chosen in order to have a smooth control characteristic. This may have some influence on the effectiveness of the power sharing in special cases. The impact is however not expected to be significant, which is also confirmed by the simulation results presented in this chapter.

6.2.1. Structure and Formatting of Results

The sections are structured by the grids investigated. For each system, a northern and southern converter is considered as a contingency. The results for the ac grid are presented to showcase the effectiveness of the proposed concept to minimize the influence of the converter outage on the power flow in the ac grid. The results for the southern contingency as well as the impact on the ac grid is only shown for selected cases to avoid redundancies in the documentation.

The results are summarized using bar plots of the pre- and post-contingency deviations for both northern and southern outage as well as in comparison to the conventional symmetric power sharing concept. Here, the converter power and the active and reactive power of the lines are presented.

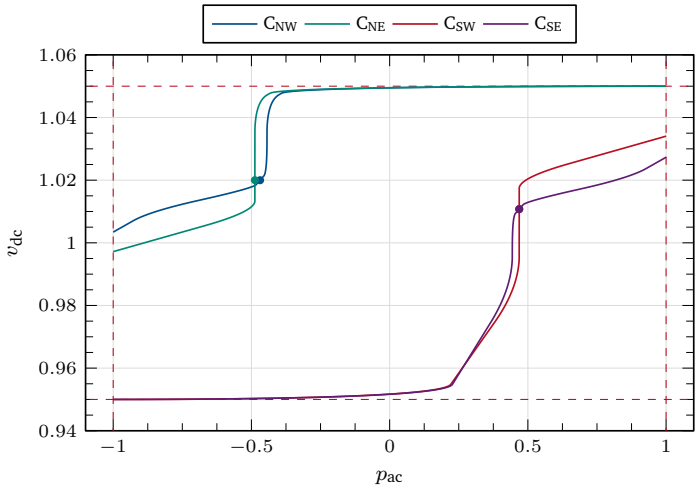

Figure 6.2.: Tiered converter characteristics for grid 202r and 202m resulting from parameters in table 6.2.

The results are presented with a color coding for the northern elements in variations of blue, the southern in red and the middle point in green. The simulation is shown for 6 seconds. This presents a trade off between the quick response by the converters and the slow response of the generators, so both can be observed.

6.2.2. Grid Concept for Grid 202r

First, the grid 202r is investigated. In the following, the parameterization will be explained and the results of the simulations are presented. For this grid, the results for the contingencies of both C_{NE} and C_{SE} are shown. The results are then compared to the results obtained by a conventional control concept, i.e. in this case distributed control with equal power sharing. In addition, the oscillations of the generators' angular speed ω_g and the terminal voltages V_t are discussed for the outage of C_{NE}, both in detail and in comparison to the conventional concept.

Table 6.2.: Parameter set for grids 202r and 202m. All values are in %. Converters are parameterized for tiered directional voltage control, relevant parameters (i.e. achieving the active power control) marked in bold for each dead-band.

		C_{NE}	C_{NW}	C_{SE}	C_{SW}
db^0	V_{db}^0	0.25	**0.25**	**0.25**	0.25
	P_{db}^0	0	**2.5**	**2.5**	0
db^{+1}	V_{db}^{+1}	2.5	2.5	**1**	1
	P_{db}^{+1}	0	2.5	**40**	0
db^{+2}	V_{db}^{+2}	5	5	**2**	**2**
	P_{db}^{+2}	50	50	**60**	**40**
db^{-1}	V_{db}^{-1}	-1	**-1**	-2.5	-2,5
	P_{db}^{-1}	0	**-40**	-2,5	0
db^{-2}	V_{db}^{+2}	**-2**	**-2**	-5	-5
	P_{db}^{+2}	**-40**	**-60**	-20	-20

6.2.2.1. Parameter Sets

The parameterization is performed based on the principles for the tiered control concept presented in section 6.1. The detailed parameters are summarized in table 6.2, with the parameters responsible to achieve the tiered control marked in bold. In figure 6.2, the resulting characteristics and the corresponding calculation points (see chapter 5) are shown.

The steady state tier is chosen very small with $V_{db}^0 = 0.25\,\%$ and $P_{db}^0 = 2,5\,\%$ and assigned to the converters C_{NW} and C_{SE}. These converters are furthermore assigned as voltage controller in the next tier, with $V_{db}^{+1} = 1\,\%$ and corresponding $P_{db}^{+1} = 40\,\%$ for the positive plane for C_{SE} and similarly $V_{db}^{-1} = -1\,\%$ and corresponding $P_{db}^{-1} = -40\,\%$ for C_{NW}. In a next tier, for $V_{db}^{+2} = 2\,\%$ and $V_{db}^{-2} = -2\,\%$ respectively, the other converters are assigned voltage controller with an absolute value of $40\,\%$.

The “inactive” tiers are assigned dead-bands of $V_{db}^{+1} = 2.5\,\%$ and $V_{db}^{+2} = 5\,\%$ (symmetrically on the negative plane). Between the active second tier and the

inactive tier, a small gap has been implemented to ensure selectivity. However, using the available two dead-bands, a third tier could easily be implemented with the converters of the opposite region. Here, the limit on the dc voltage will act as back-up tier and ensures a permissible operation if the active tiers are overloaded. It also supersedes the values of the northern converters because they already operate near the limit.

6.2.2.2. Converter Results for Outage of C_{NE}

A converter outage of C_{NE} triggers the power imbalance in the embedded MTDC system at $t = 0$. The response of the other converters is shown in figure 6.3. The PI controller is parameterized to achieve a stable operation in roughly $0.5\,s$, with low transients. The converters act as follows:

Figure 6.3a shows the converter voltage in p.u.. The voltage drops to about 0.95 p.u. and recovers without major oscillations to a steady state with small voltage deviation as expected for droop control. The voltage drop over the line (i.e. the difference of voltage levels) stays essentially constant during and after the fault.

Figure 6.3b shows the power provision, also in p.u.. Converter C_{NW}, which is the voltage controller in this tier (negative deviation) adjusts it's power provision to about 0.95 p.u.. The southern converters transiently do a small adjustment (according to their characteristic, and recover almost perfectly to their pre-fault values, with a slight deviation at C_{SE}, due to the steady state control parameter P^0_{db}.

Figure 6.3c shows the time behavior as a locus in the P-V plane as well as the converter characteristics as dotted lines, as introduced in section 5.3. The adaption of the converters to the new operating point can be very well observed, with the post-outage operating point lying on the characteristic as designed.

The simulation shows, that the converters act according to the control scheme. Only the converter assigned to the voltage control tier has a significant contribution, while the other converters are more or less in constant power control. Furthermore, the control is stable and sufficiently fast.

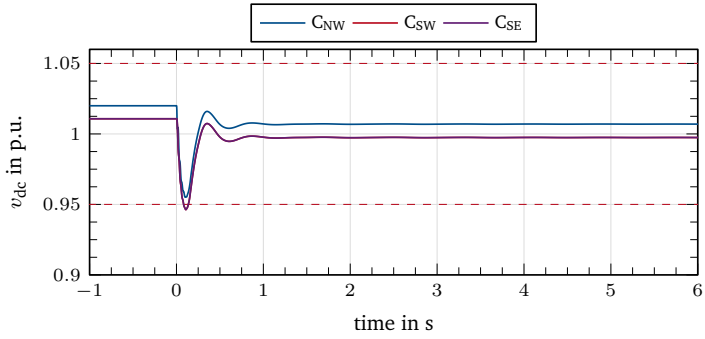

(a) Timeplot of converter V_{dc}

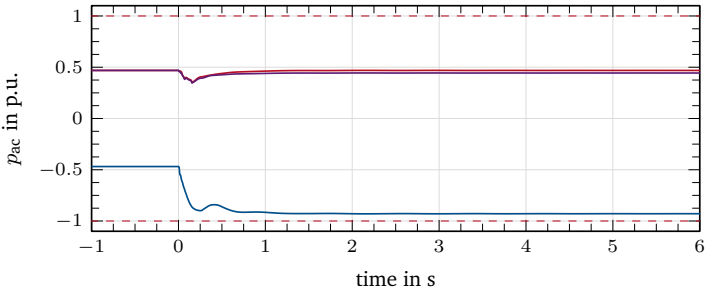

(b) Timeplot of converter P_{ac}

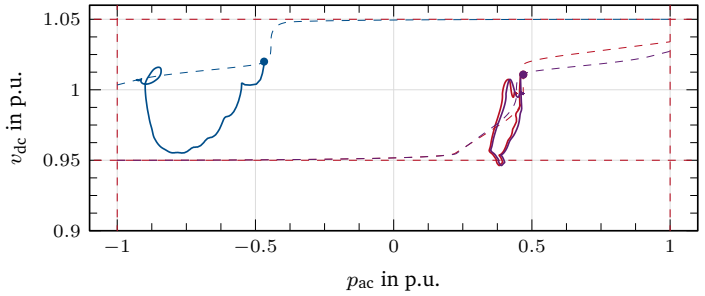

(c) Locus in P-V plane

Figure 6.3.: Results for the converters, grid 202r, outage of C_{NE}.

6.2.2.3. Impact on the Ac Grid for Outage of C_{NE}

A significant effect can be expected, because the outage and the subsequent response of the MTDC system affect the power flow in the ac grid. As none of the converters provides reactive power, the effects in the ac grid will be attributable only to the change in active power flow. In this section, the active and reactive power flow an the ac lines of the system (figure 6.4) and the terminal voltages and generator angles (figure 6.5) are presented.

Figure 6.4a shows the active power flow of the lines. The effect of the tiered control concept is very nicely observable here. There is almost no change in the dc line $L_{dc,\,N\text{-}S}$ and only a very slight increase is observed on the eastern lines $L_{ac,\,E1}$ and $L_{ac,\,E2}$. The bulk of the power previously absorbed by the outaged converter C_{NE} is transported over the horizontal line $L_{ac,\,N}$ to C_{NW}.

Figure 6.4b shows the reactive power flows on the ac lines. Here, a moderate transient with slight oscillations can be observed (better observable in figure 6.5). There is also a split between the eastern and western lines, as the network is not symmetric anymore, with increased reactive power consumption by $L_{ac,\,E1}$. On the other lines, only slight steady state deviations are present.

In the line flows, the effect of the proposed concept is very well visible. As is one of the aims of the design, the post-fault operation of the ac grid is not significantly altered. The line that is impacted the most is short compared to the lines in transmission direction, showing also in the low additional needed reactive power. The increase in active power over the long transmission lines and consequently the needed additional reactive power is kept at a minimum. This is expected to have a positive influence on the stability of the system, which is shown later in the comparison to the equal power sharing in conventional control.

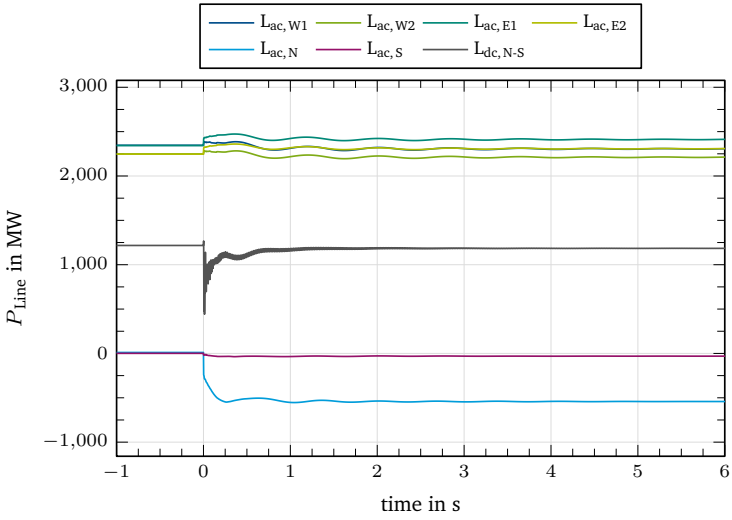

(a) Timeplot of P_{Line}

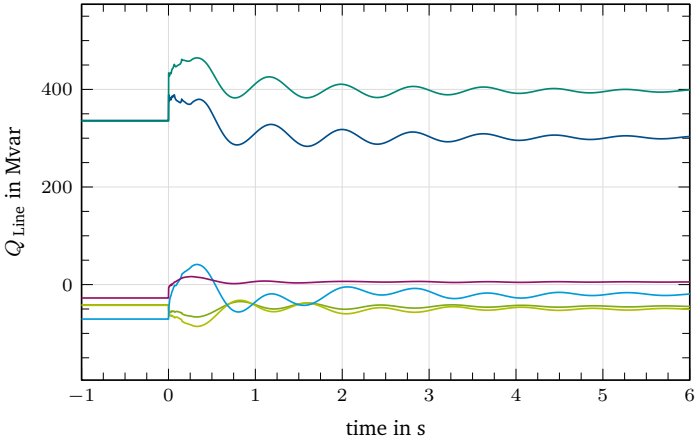

(b) Timeplot of Q_{Lines}

Figure 6.4.: Active P_{Line} and reactive Q_{Line} power for all lines of grid 202r for the outage of C_{NE}. Active power transmission is maintained at the same levels with weak reactive power response.

Looking at the ac terminal voltages and the generator speed gives an estimate on system stability. One has to keep in mind that there is no active power imbalance or direct fault in the ac system, as the load and generation stays constant during and after the fault. All oscillations visible here come from the changed power flow due to the outage. For both V_{Term} and ω_{G}, the oscillations visible in figure 6.5 show oscillatory modes identified in chapter 4 for the model.

Figure 6.5a shows the ac terminal voltages V_{Term}. The voltages show oscillations, which are still in effect at 6s. However, there are no major voltage drops after the fault. The terminals most affected are T_{ME} and T_{MW} at the midpoints of the transmission line. This is expected, as there are no voltage controlling elements, as the shunt compensation units are stationary only.

Figure 6.5b shows the angular speed ω_{G} of the generators. The frequency of the oscillations corresponds to the largest oscillatory modes associated with the generators (see 4.4.4), especially mode 1, i.e. the northern generators oscillating against the southern. Initially, there is a very prominent spike for G_{NE}, which is the generator at the terminal connected to the faulted converter. The excited oscillatory modes show in the further course a diminishing effect of the vertical modes, i.e. the eastern and western modes. It can also be observed, that initially, all modes are present. The least damped mode 1 with a period of approximately $0.8\,\text{s}$ is active in the later course of the simulation.

The analysis of the oscillatory modes shows, that the outage of a converter in an embedded MTDC has a profound effect on the ac grid. While the small benchmark grid has no critical mode, in a real system, existing modes could be excited by the outage of (in a worst case) an entire converter station. While the operating point will be adjusted by the global control levels, it can be seen, that the first second already has a big influence, making a quick reaction desirable, that keeps the excitation of these modes at a minimum.

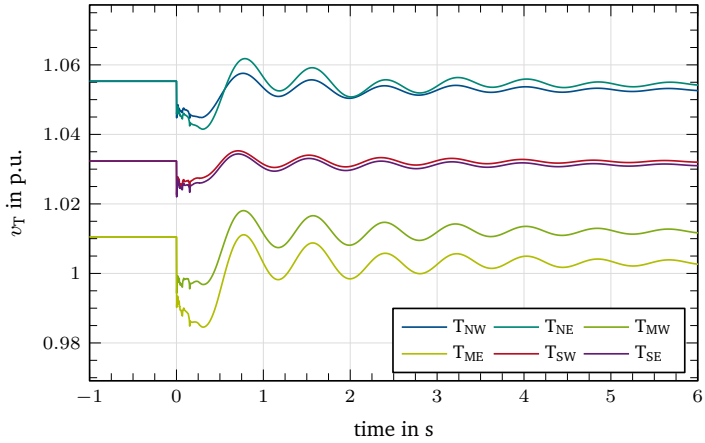

(a) Timeplot for terminal voltages V_{Term}

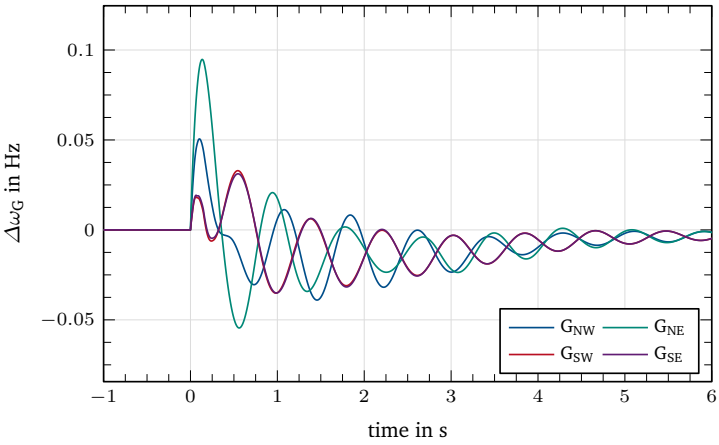

(b) Timeplot for generator angular speed ω_G

Figure 6.5.: Terminal voltages V_{Term} and generator angular speed ω_G in grid 202r for the outage of C_{NE}. Excitation of system oscillatory modes can be observed.

6.2.2.4. Converter Results for Outage of C_{SE}

The design shall – corresponding to the requirements – be able to be directional. For this, the control should react differently to the outage of an inverter in the southern region. We thus analyze the outage of the converter C_{SE}, which is additionally not part of Tier-0 and Tier-1 voltage control. Because the influence on the ac grid is very similar, we will only look at the converter values to assess the effectiveness of the control concept.

The converter values are presented in figure 6.6 in the same fashion as before.

Figure 6.6a shows the dc voltage. The deviations are positive, as expected, with a peak at 1.1 p.u.. The response to the disturbance settles in roughly 0.5 s, without significant oscillations.

Figure 6.6b shows, that converter C_{SW} is responsible for most of the power share. This is in contrast to negative deviation and corresponds to the desired design. As before, the converters, which are not part of the responsible control tier are controlled back to almost the pre-fault value, with only a slight deviation for the steady state voltage controller C_{NW}.

Figure 6.6c shows the locus. The control action is clearly visible and the new operating point according to the characteristic is achieved.

The investigation of the outage in the other control region is crucial for the verification of the control concept. The results show very good compliance with the objective of the design and prove the directional operation is working as intended.

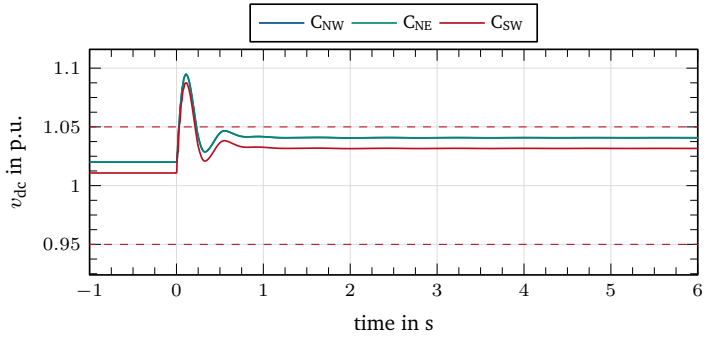

(a) Timeplot of converter V_{dc}

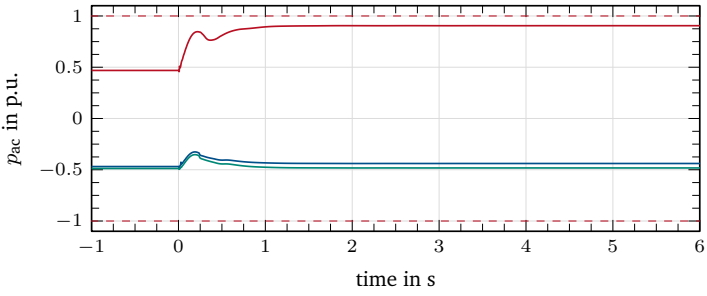

(b) Timeplot of converter P_{ac}

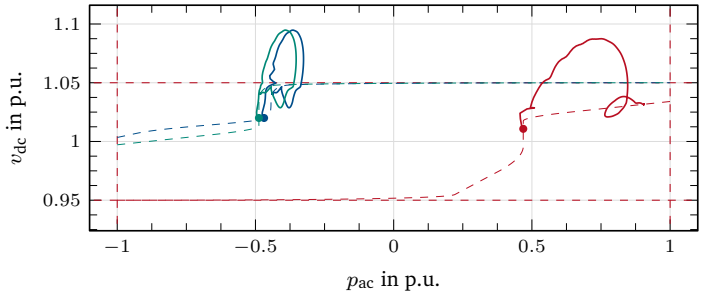

(c) Locus in P-V plane

Figure 6.6.: Results for the converters, grid 202r, outage of C_{SE}.

6.2.2.5. Comparison to Symmetric Droop Concept

In order to evaluate the performance of the proposed tiered grid control concept, the effects need to be compared to some baseline. When looking at the setup present in the benchmark systems, we can see that the basic and advanced conventional concepts more or less have the same challenge: When parameterized to achieve voltage control for the outage in one region, the same response will be done in the other region. To have the most generic benchmark, a voltage droop concept with equal power sharing is selected. The converter controls are parameterized to achieve similar dynamics and comparable steady state voltage deviations, choosing a control angle $\gamma = 0.2\,\mathrm{p.u.}$ for all converters.

To evaluate the difference in power transmission profile, the relevant data needs to be defined. Here, the data collected for both outages are the steady state deviations for converter active power P_{ac} as well as active and reactive power flow at the lines. These values give the information needed in order to benchmark the system. The deviations for the proposed and conventional droop control concept are presented in figure 6.7. The results allow the following observations for the outages:

Converter active power: the failed converter is obviously characterized by a deviation of full pre-fault power for both cases. This power is taken over by the power sharing implemented by the distributed grid control concept. For the conventional concept, the response is the same for both cases. As expected, the converters have more or less equal power share, with very slight more delivered by the converter at the faulted region, which is attributed to the changed power flow and lower voltage drop. In the proposed tiered control concept, we see almost all power taken by the responsible converter (as discussed previously).

Line active power: In conventional control, the power, which is not transmitted over the MTDC system consequently increases the loading of the eastern and western line. In the proposed control, only the horizontal connections are more loaded. For the proposed control, especially for outages at the load end, the power transmission does not change significantly.

Line reactive power: The changed power transmission causes additional reactive power flows, with significantly increased values on the vertical lines with the conventional concept.

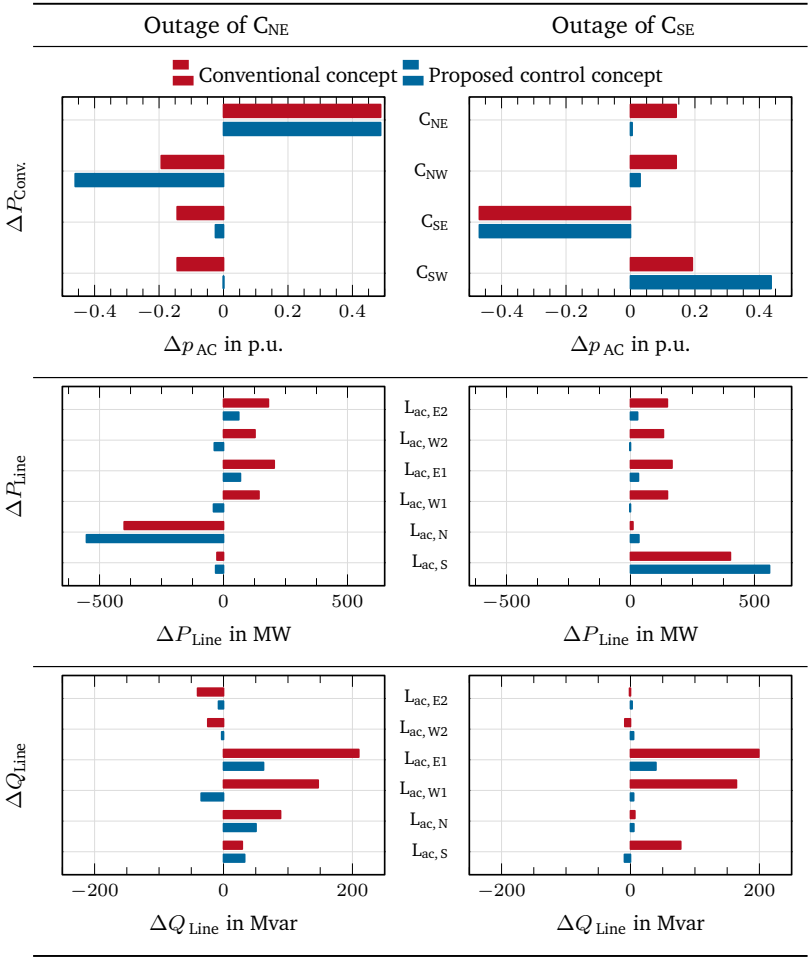

Figure 6.7.: Comparison of steady state deviations of conventional and proposed grid control concepts for both outages in grid 202r.

Comparing the power flow, we can clearly see the differences for the ac system in terms of post-fault power transmission. The reactive power deviation shows one of the key observations. In contrast to dc transmission, ac long-distance transmission is always also associated with reactive power consumption of the overhead lines. When the loading of the line becomes higher, so does the reactive power consumption. This becomes visible here: As the transmission distance over the vertical path is very long compared to the horizontal, the additional active power also causes a significant amount of additional reactive power, e.g. for line $L_{ac,\,E1}$ to more than $200\,\text{Mvar}$ for conventional as compared to about $50\,\text{Mvar}$ for the proposed concept. The benchmark system is disadvantageous for the ac grid, as there are no controlling generators in the middle part. On the other hand, the transmission distance can be larger than the distance chosen here, i.e. 400 km. With the transmission distance increasing, this effect becomes more prominent. Overall, the proposed concept equates to significant lower stress to the grid compared to conventional, symmetric grid control.

Analyzing the oscillatory behavior of the system yields a similar picture, as shown in figure 6.8:

Figure 6.8a shows the terminal voltages, with the same ordering as in figure 6.5a. As expected, there are significantly higher voltage deviations, especially at the middle terminals. In addition, the oscillatory modes are excited to a greater degree.

Figure 6.8b shows the comparison of generator angle. While the initial peak for C_{NE} is very similar, the oscillation is a lot more pronounced at the other generators, reflected also by longer lasting oscillations against each other. Additionally, the conventional concept exhibits a longer transient phase. This is caused by the disturbed active power balance in the ac system and the corresponding necessary primary control action by the generators.

Concluding the comparison, the proposed concept achieves its design objectives, and the hypothesis for improvement could be verified for this benchmark grid.

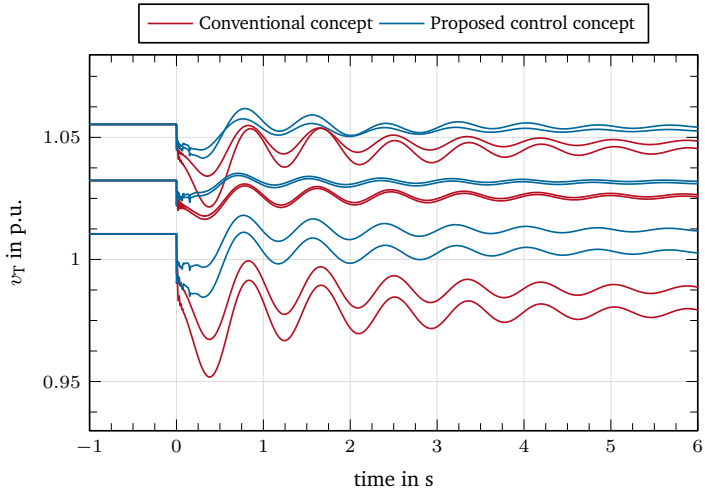

(a) Timeplot for terminal voltages V_{Term}

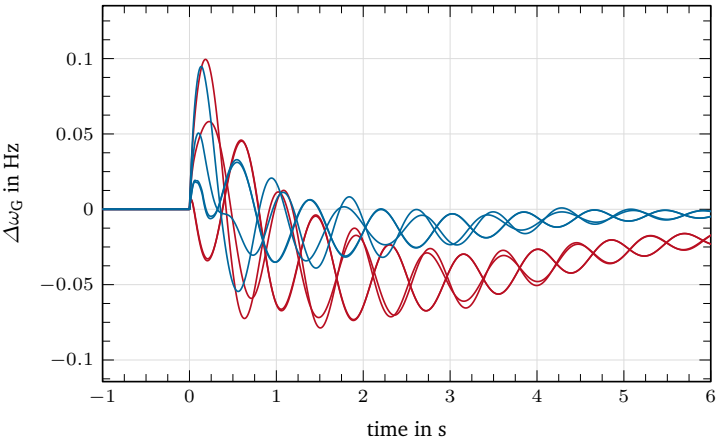

(b) Timeplot for generator angular speed ω_{Gen}

Figure 6.8.: Comparison of terminal voltages V_{Term} and generator angular speed ω_G in grid 202r for the outage of C_{NE} for the proposed and conventional control concept. Excitation of system oscillatory modes is decreased significantly for the proposed concept.

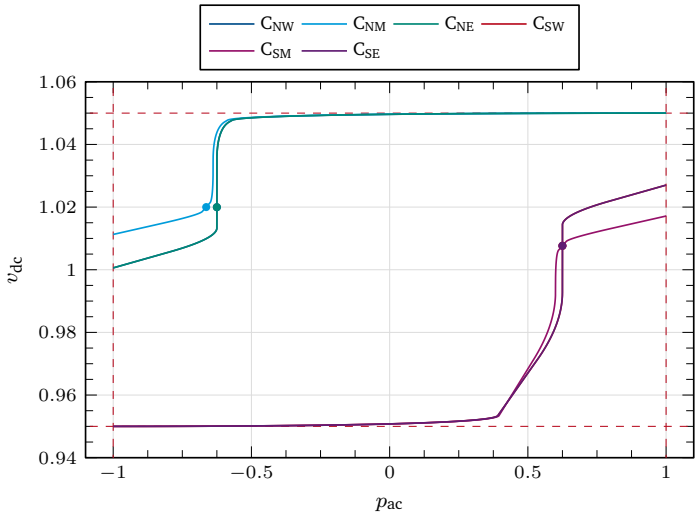

Figure 6.9.: Tiered converter characteristics for grid 333r resulting from parameters in table 6.3.

6.2.3. Grid Concept for Grid 303r

A tiered solution is the goal of the proposed grid control concept. If a first tier cannot provide all power needed to achieve power balancing in the system, the back-up system shall be activated. When there is no active tier, the voltage limitation acts as a back-up level similar to conventional control. However, if there are more than two remaining converters in a region, horizontal tiering is an option available to the operator (see section 6.1). In grid 303r, this is the case. As described in chapter 4, the grids layout features three converters for the southern and northern regions each. Furthermore, the base loading of the converters is increased to more than 70 %, so that no individual converter can achieve voltage control in the event of an outage. For the analysis, we will first describe the parameterization to achieve the desired control concept. We will then analyze the results of the simulation looking at the converter timeplots for one outage and by again comparing outages in the northern and southern region to the conventional concept. The detailed plots shown previously as well as the plots for the outage of C_{SE} will be omitted to avoid redundancy.

Table 6.3.: Parameter set for grid 303r. All values are in %. Converters are parameterized for tiered directional voltage control, relevant parameters (i.e. achieving the active power control) marked in bold for each dead-band.

		C_{NM}	C_{NE}	C_{NW}	C_{SM}	C_{SE}	C_{SW}
db^0	V_{db}^0	**0.25**	0.25	0.25	**0.25**	0.25	0.25
	P_{db}^0	**2.5**	0	0	**2.5**	0	0
db^{+1}	V_{db}^{+1}	2.5	2.5	2.5	**1**	1	1
	P_{db}^{+1}	2.5	0	0	**40**	0	0
db^{+2}	V_{db}^{+2}	5	5	5	**2**	**2**	**2**
	P_{db}^{+2}	50	50	50	**60**	**40**	**40**
db^{-1}	V_{db}^{-1}	**-1**	-1	-1	-2,5	-2.5	-2,5
	P_{db}^{-1}	**-40**	0	0	-2,5	0	0
db^{-2}	V_{db}^{+2}	**-2**	**-2**	**-2**	-5	-5	-5
	P_{db}^{+2}	**-60**	**-40**	**-40**	-20	-20	-20

6.2.3.1. Parameter Sets

The parameters for this set are chosen to allow for horizontal tiering, i.e. the converters in one region to do sequential power sharing. The aim is to have one converter be in the first tier and the second picking up as a backup. The tier could also be built up as distributed. The voltages for the dead-bands are chosen equal to those for grid 202r (see section 6.2.2). The parameters are given in table 6.3, with the parameters responsible to achieve the tiered control again marked in bold. The corresponding control characteristics are given in figure 6.9.

Tier-0 is achieved by the converters at the middle terminal in both the northern and southern region. Tier-1 for both negative and positive dead-bands is achieved by the converter at the middle terminal, with an absolute voltage dead-band of $1\,\%$ and $40\,\%$ power contribution. Tier-2 for both positive and negative dead-bands is achieved by the eastern and western converters using an absolute voltage dead-band of $2\,\%$ and a power contribution of $40\,\%$.

6.2.3.2. Converter Results for Outage of C_{NE}

First, the converter values for the outage at C_{NE} are analyzed. The plots in figure 6.10 are arranged as before.

Figure 6.10a: The voltage profile shows the typical profile. As the total power sharing is achieved in the second tier, the steady state voltage deviation is noticeable after the outage.

Figure 6.10b: The converter powers show the desired effect. First, C_{NM} acts in Tier-1, and provides power up to its limit. Tier-2 voltage control is effective for C_{NW}, which provides the missing power and achieves power balance in the system.

Figure 6.10c: The locus shows, how the Tier-1 voltage controller approaches its final value, which is actually not on the characteristic, as an additional voltage drop is in effect. On the other hand, the Tier-2 voltage controller C_{NW} converges to the appropriate point on its characteristic. The other converters converge back to the same power level according to their characteristic.

The plot values show, that the horizontal tiered grid control is effective and is able to not only keep the system stable but achieve the power sharing works as designed.

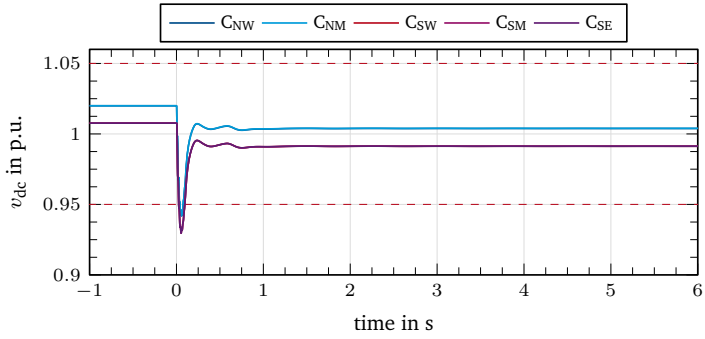

(a) Timeplot of converter V_{dc}

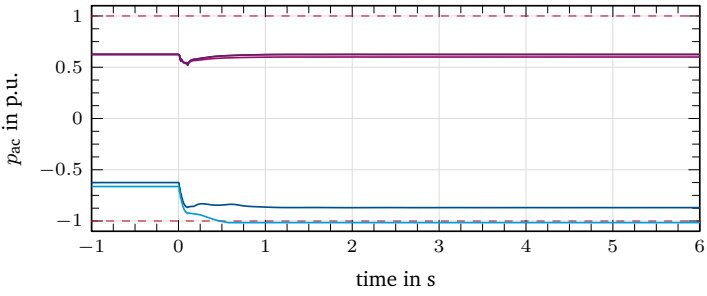

(b) Timeplot of converter P_{ac}

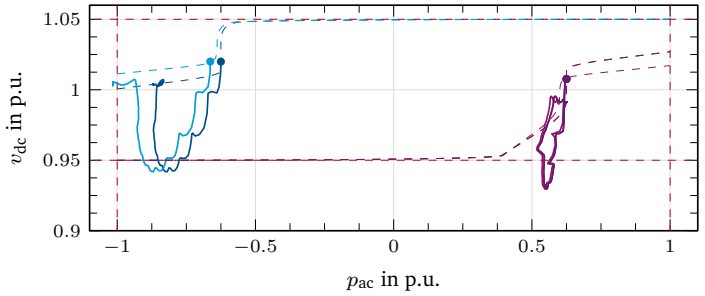

(c) Locus in P-V plane

Figure 6.10.: Results for the converters, grid 303r, outage of $\mathrm{C_{NE}}$.

6.2.3.3. Comparison to Symmetric Droop Concept

The comparison is presented in the same way as before in figure 6.11. The conventional concept is run with parameters identical to grid 202r. The values in the figure are again based on the respective steady state deviations.

Converter active power: Similar to the results from grid 202r, the conventional concept distributes the required power over all converters for both outages. The proposed control shifts the power primarily to the Tier-1 voltage controller, and afterwards to the back-up in Tier-1.

Line active power: For the conventional concept, the vertical lines take additional active power, as expected. The proposed concept avoids this, and the power is transferred over the horizontal lines.

Line reactive power: As before, the active power shift causes a significant amount of extra reactive power, almost all of which is consumed on the vertical lines for the conventional concept. For the proposed tiered concept, the lines are short, causing minimum additional reactive power.

The comparison again shows the advantage of using a directional control concept. As the line to the Tier-1 controller C_{NM} is only half the length, the effect of avoiding the power shift and the associated reactive power is even more pronounced than in grid 202r. Also the multi-tier operation could be verified for both outages.

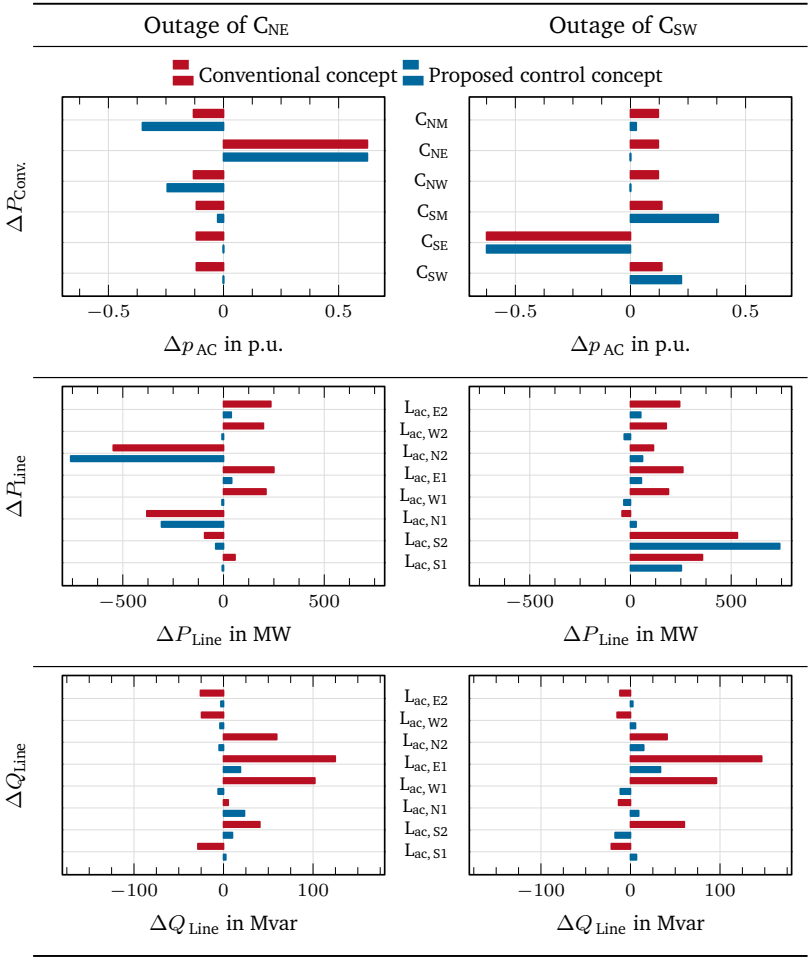

Figure 6.11.: Comparison of steady state deviations of conventional and proposed grid control concept for both outages in grid 303r.

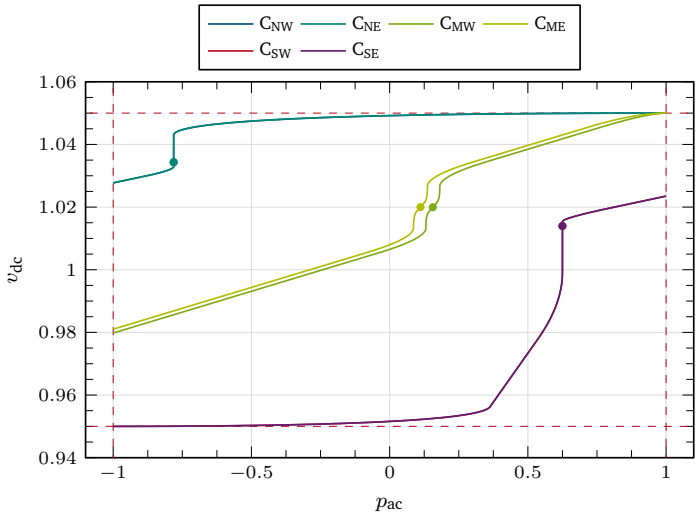

Figure 6.12.: Tiered converter characteristics for grid 222r resulting from parameters in table 6.4.

6.2.4. Grid Concept for Grids 222r

The vertical tiered concept has not been the focus of the grids 202r and 303r, which do not benefit from a vertical concept, as there are no intermediate converters at the vertical middle terminals T_{MW} and T_{ME}. The fall-back voltage control is only done by the voltage limits. In this grid, converters at these terminals are incorporated, and the vertical tiered concept is implemented by integrating both C_{MW} and C_{ME} into the Tier-2 control level. The northern and southern converter setpoints are set to high values in order to see the effect of the second tier. The middle converters have a small pre-fault contribution to the active power transmission.

6.2.4.1. Parameter Sets

The parameters are assigned to a similar methodology as in grid 202r and 303r. The dead-bands are chosen the same[2]. The converters C_{MW} and C_{ME},

[2]Due to stability considerations, the gain for the voltage part has been decreased to $K_V = 0.2$.

Table 6.4.: Parameter set for grid 222r. All values are in %. Converters are parameterized for tiered directional voltage control, relevant parameters (i.e. achieving the active power control) marked in bold for each dead-band.

		C_{ME}	C_{MW}	C_{NE}	C_{NW}	C_{SE}	C_{SW}
db^0	V_{db}^0	**0.25**	**0.25**	0.25	0.25	0.25	0.25
	P_{db}^0	**2.5**	**2.5**	0	0	0	0
db^{+1}	V_{db}^{+1}	1	1	2.5	2.5	**1**	**1**
	P_{db}^{+1}	2.5	2.5	0	0	**40**	**40**
db^{+2}	V_{db}^{+2}	**2**	**2**	5	5	**2**	**2**
	P_{db}^{+2}	**40**	**40**	50	50	**60**	**60**
db^{-1}	V_{db}^{-1}	-1	-1	**-2.5**	**-2,5**	-2.5	-2,5
	P_{db}^{-1}	-2.5	-2.5	**-40**	**-40**	0	0
db^{-2}	V_{db}^{+2}	**-2**	**-2**	**-2**	**-2**	-5	-5
	P_{db}^{+2}	**-40**	**-40**	**-60**	**-60**	-20	-20

which shall be implemented as vertical tiered voltage back-up are symmetrically parameterized, so both can equivalently work as (distributed) back-up for both the northern and the southern regions. In addition, they are assigned as the Tier-0 voltage controllers also in a distributed manner. The parameters chosen are given in table 6.4, with the parameters responsible to achieve the tiered control marked in bold. The corresponding characteristics are shown in figure 6.12. In this figure, around the setpoint of the middle converters, the three tiers for steady state, Tier-1 and Tier-2 operation can be nicely seen, in this case in a symmetrical manner. The converters have the transition from voltage droop to constant power to a sharp voltage droop in a voltage dead-band of only 2 %.

6.2.4.2. Converter Results for Outage of C_{NE}

The results for the converters are presented in the same way as before, with the values given in figure 6.13.

Figure 6.13a: The voltage profile shows the typical profile. Again, the total power sharing is achieved in the second tier, the steady state voltage deviation is noticeable.

Figure 6.13b: The converter powers show the desired effect. In this case, C_{NW} acts in Tier-1, and provides power up to its limit. Tier-2 voltage control is effective for both C_{MW} and C_{ME}, who take over the distributed voltage control and provide the remaining power in equal share.

Figure 6.13c: The locus visualizes the two tiered operation, the primary tier controller ends up at the limits of its characteristic, the Tier-2 controllers shift their power and converge to the appropriate operating point, while the unaffected controllers in the southern region converge back to the constant power part of their characteristic.

The converter plots show, how vertical tiers can be used to separate the individual regions according to the operators choice. Here, both Tier-2 converter effectively operate as distributed voltage controllers.

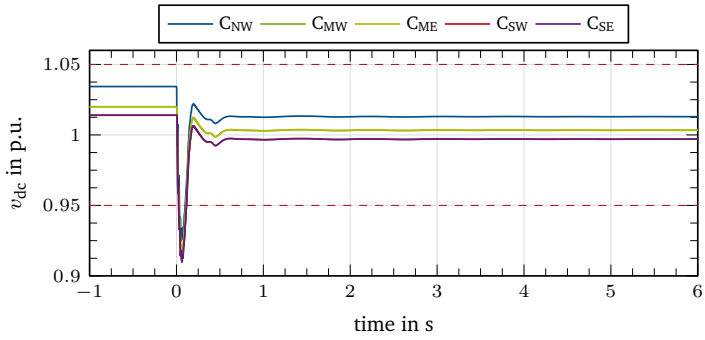

(a) Timeplot of converter V_{dc}

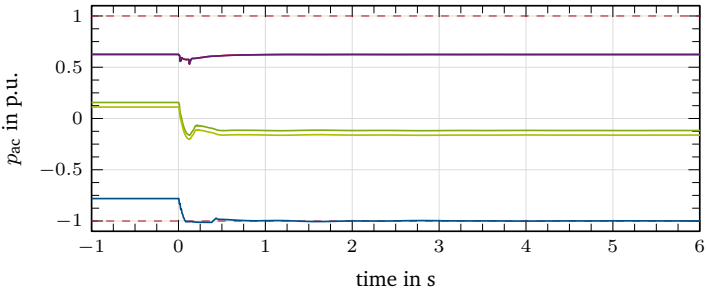

(b) Timeplot of converter P_{ac}

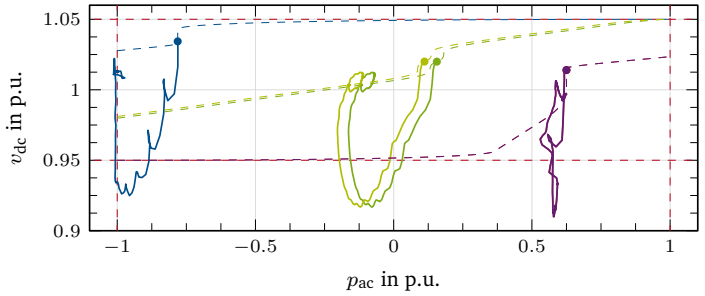

(c) Locus in P-V plane

Figure 6.13.: Results for the converters, grid 222r, outage of $\mathrm{C_{NE}}$.

6.2.4.3. Converter Results for Outage of C_{SE}

The vertical tiered concept has proven effective in the investigation of the outage of C_{NE}. Investigation of the outage of C_{SE} gives us an additional insight (see figure 6.14):

Figure 6.13a: Here we see, that the converters at the northern end, which are already operating at high dc voltage are affected by the voltage limit in place. The voltage is effectively limited and no steady state violation occurs.

Figure 6.13b: The effect of the voltage limitation is seen in the power provision. In order to limit the voltage, the converters lower their power provision to the dc network (increase the negative value). That way, they take part in the power sharing, despite not being part of Tier-2 voltage control.

Figure 6.13c: This voltage limitation is also very nicely observable in the locus of the converters. As the voltage limitation is defined smoothly by the characteristic, the voltage converges to the characteristic at roughly 1.045 p.u..

This case shows, how voltage limits can affect the tiered operation of the control concept. The voltage limitation, however, is an integral part of the concept as well. If the operator would like to avoid this behavior, it is necessary to operate the whole MTDC system at a lower dc voltage. This is necessary to give the voltage tiers enough degree of freedom to operate. Lowering the dc voltage, on the other hand, increases the losses in normal operation, presenting the operator with a trade-off between steady state and contingency operation.

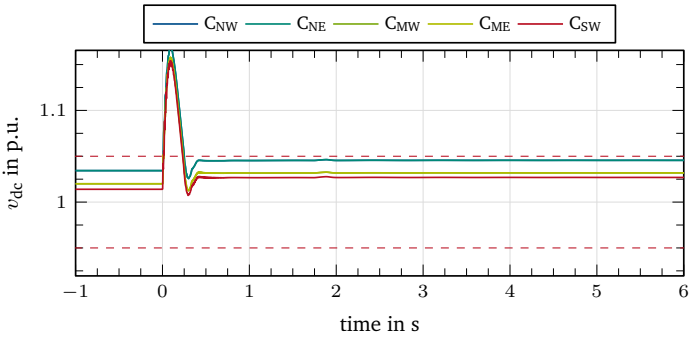

(a) Timeplot of converter V_{dc}

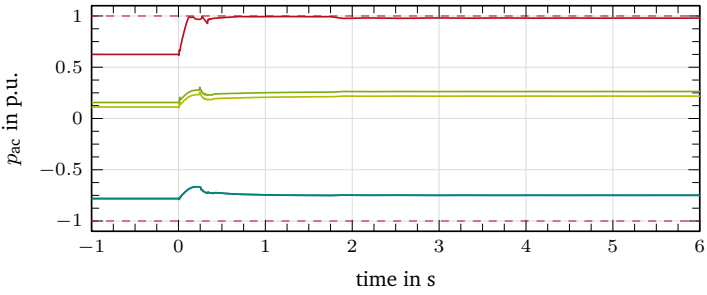

(b) Timeplot of converter P_{ac}

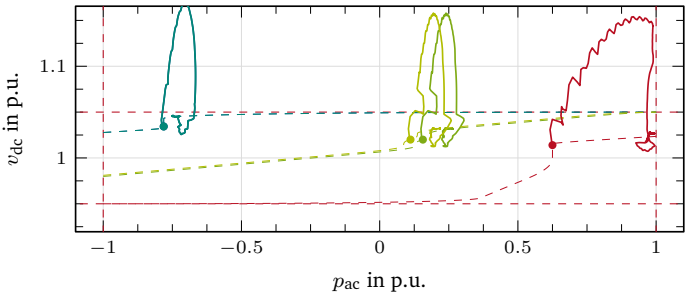

(c) Locus in P-V plane

Figure 6.14.: Results for the converters, grid 222r, outage of C_{SE}.

6.2.4.4. Comparison to Symmetric Droop Concept

The overview over the results as well as the comparison with the conventional voltage droop is shown in figure 6.15.

Converter active power: The conventional concept operates as before. Here, the effect of the changed power flow in the dc system is very well observable, causing the converters on the middle terminals to have an increased power share for an outage of C_{SE}. For the proposed tiered concept, the effects described can be seen here.

Line active power: When compared to the horizontal tiered concepts, a change in power transmission in the ac grid cannot be fully avoided, as the second tier is not located near the outage. This causes an increased power flow over the lines that leads from the outage to the middle terminals, e.g. especially the lines $L_{ac,\,E1}$ and $L_{ac,\,E2}$ for the outage of C_{NE} and C_{SW} respectively.

Line reactive power: Because of the effect described for the active power flow, increased reactive power flows can be observed for the proposed concept as well. Still, the effect is still significantly reduced compared to the conventional concept.

The comparison again shows the advantage of using a directional control concept. The effect for vertical tiered voltage control is not as pronounced as for horizontal, because there is a relevant distance between the converters and the outage. Additionally, the analysis for this grid variant shows that the voltage limit can interfere with the tiered control, when the grid is operated with high voltages and there is an inverter fault further increasing the voltage in the MTDC system.

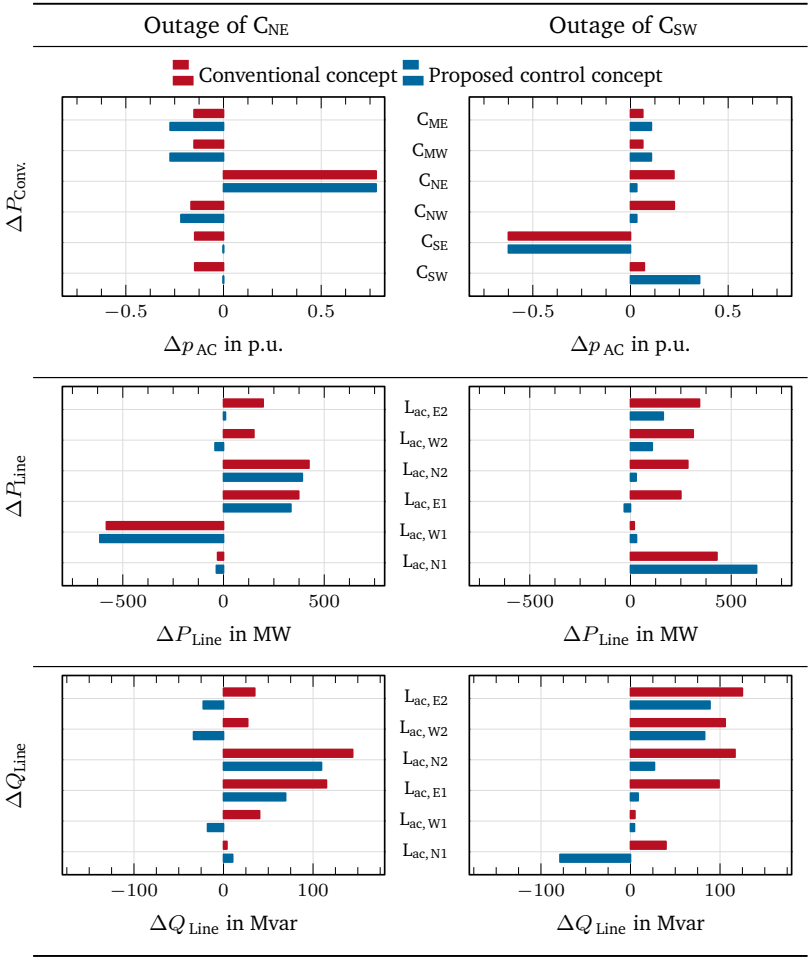

Figure 6.15.: Comparison of steady state deviations of conventional and proposed grid control concept for both outages in grid 222r.

6.3. Summary for Dc Grid Control Strategies

This section provides a design method for active power balancing of embedded MTDC systems. For this, requirements for the control of dc grids are defined and a tiered voltage control system is introduced. The proposed concept follows the design principles *selectivity*, *directionality* and *flexibility*. A concept for MTDC grid control using voltage control tiers is introduced.

The proposed tiered control concept is tested on three benchmark systems, which verify the desired function of control regarding the design principles. For this, the converters are parameterized to achieve a tiered voltage control, followed by time simulation of the grid. The results are analyzed regarding converter control, active and reactive power flow of the ac grid and the excitation of oscillatory nodes. The deviations between pre- and post-contingency operation are compared against a conventional distributed voltage control concept with equal power sharing for the considered outages.

The results show the effectiveness of the control concept. Basic operation is proven for grid 202r in section 6.2.2, while horizontal and vertical tiers are analyzed for grid 303 (section 6.2.3) and grid 222r (section 6.2.4) respectively.

7. Conclusions

7.1. Key Points

This work has analyzed the current state of the art for active power balancing of embedded multi-terminal dc systems. The analysis has shown, that while there is plenty of research directed to this topic, the following key points should be addressed:

1. Consolidation: Beyond Cigré's published basic and advanced methods for converters and dc grids, there are many approaches to the topic, which try to tackle the challenges. This work consolidates some of them into one control concept.

2. Directionality: The analysis has shown the need for a directionally selective control concept, which can avoid power transmission shifts in case of an outage.

3. Selectivity: The proposed concept is able to incorporate several converters in a hierarchical, tiered control. In this way, the operator gains a degree of freedom in the parameterization of the system.

7.2. Summary of Results

For the scope of this work, existing active power balancing methods have been introduced and discussed in chapter 3. Based on this, possible improvements have been identified. These have been used to develop a control design, which can tackle some of the challenges.

The proposed control design is able to achieve arbitrary, continuous control characteristics based on a generalized continuous droop concept. This is achieved by continuously controlling the setpoints for both voltage and power based droop for the characteristic, while scheduling the gains of the corresponding loops and also the gain of the PI controller responsible for the generation

of the current reference. The gain scheduling is performed based on a newly introduced control angle γ, which normalizes the domain between constant voltage, droop and constant power control on a linear and continuous scale. Continuous characteristics are achieved by introducing a continuity factor c_r and construction of the characteristics based on interpolation based on this factor.

Based on this controller concept, a hierarchical tiered control concept for primary control of MTDC systems is proposed, incorporating three control principles *selectivity*, *directionality* and *flexibility*. The concept aims to provide easy and intuitive parameterization, maintaining the prevalent direction of active power transmission and finely controlled tiered power sharing.

Simulations on benchmark systems specifically designed for embedded MTDC investigations have shown, that the proposed concept achieves the requirements set before. Ac power flow deviations after outages can be reduced to a minimum and tiered power sharing works as intended. The simulations also show, that this concept has an effect on the excitation of existing oscillatory modes in the system. While the effect is small, in the very simple benchmark system, the effect on real power systems is much more relevant.

7.3. Propositions and Future Works

The concept proposed here is promising. Still, further steps need to be taken. First and foremost, the concept will have to be applied to real world problems. An example could be simulations regarding realistic topologies and surrounding ac systems including underlying generation and load profiles.

An interesting possibility would be the combination of existing droop base research with the proposed concept. As the characteristics shown here are, fundamentally, based on the basic droop characteristics, methods such as the pilot node concept or the optimization of droop parameters can be easily applied here.

Last and certainly not least, the concept needs to achieve a better level of the standardization, which is one of the key challenges in MTDC, especially for multi-vendor installations.

A. Simulation Model Component Data

This appendix lists the parameters used in the simulation models used in this work. The model data used for the main components, i.e. generators, transmission lines and HVDC converters, is described in the following and shown in the corresponding tables.

Generators The generators used in the model are synchronous machines of type turbo generator. The generators are connected via transformer to the transmission system. The electrical data used for the generator models is given in table A.1. All generators are equipped with an AVR of type AC1A responsible for terminal voltage control and a turbine governor responsible for active power control. The governor is of type IEEEG1, modeling a gas turbine as energy source. The parameters of the AVR are given in table A.2, the parameters of the governor in table A.3.

Transmission lines The transmission lines in the simulation model are of two types. For the ac transmission part, OHL of type *Donaumast* are used, encompassing two circuits per transmission path, each consisting of bundles of four subconductors. These lines use a geometric modeling approach, yielding realistic results based on the actual transmission tower type. The data for the OHL is given in table A.4. For the dc transmission part, XLPE copper cables with a rated voltage of $320\,\mathrm{kV}$ and a cross section of $2500\,\mathrm{mm}^2$ are used. The corresponding data is given in table A.5.

HVDC Converters The HVDC converters are modeled as MMC units with half-bridge submodules connected to the transmission grid by converter transformers. The corresponding data for the converters is given in table A.6.

Table A.1.: Electrical data used for the generator models.

Parameter Name	**Parameter Symbol**	**Value**	**Unit**
Rated Power	S_r	592	MVA
Rated Voltage	V_r	18	kV
Rated Power Factor	$\cos\varphi_\mathrm{r}$	0.9	
Rotor Type		Round Rotor	
Acceleration Time Constant (base S_r)	T_a	7	s
Stator Resistance	r_Str	0.001	p.u.
Leakage Reactance	x_l	0.15	p.u.
d-axis Reactance	x_d	2.3	p.u.
q-axis Reactance	x_q	2	p.u.
Transient d-axis Reactance	x'_d	0.4	p.u.
Transient q-axis Reactance	x'_q	0.6	p.u.
Transient d-axis Time Constant	T'_d0	8	s
Transient q-axis Time Constant	T'_q0	1.8	s
Subtransient d-axis Reactance	x''_d	0.25	p.u.
Subtransient q-axis Reactance	x''_q	0.25	p.u.
Subtransient d-axis Time Constant	T''_d0	0.05	s
Subtransient q-axis Time Constant	T''_q0	0.03	s

Table A.2.: Control parameters of the AVR AC1A used for the generator models.

Parameter Name	**Parameter Symbol**	**Value**	**Unit**
Measurement Delay	T_r	0.025	s
Filter Derivative Time Constant	T_c	0.3	s
Filter Delay Time	T_b	0.1	s
Controller Gain	K_a	100	p.u.
Controller Time Constant	T_a	0.01	s
Exciter Constant	K_e	1	p.u.
Exciter Time Constant	T_e	0.5	s
Stabilization Path Delay Gain	K_f	0	p.u.
Stabilization Path Delay Time	T_f	1	s
Rectifier Regulation Constant	K_c	0.65	p.u.
Exciter Armature Reaction Factor	K_d	0.2	p.u.
Saturation Factor 1	E_1	3.9	p.u.
Saturation Factor 2	S_e1	0.1	p.u.
Saturation Factor 3	E_2	5.2	p.u.
Saturation Factor 4	S_e2	0.5	p.u.
Controller Minimum Output	$V_\mathrm{r,min}$	-10	p.u.
Controller Maximum Output	$V_\mathrm{r,max}$	10	p.u.

Table A.3.: Parameters of the governor IEEEG1 used for the generator models.

Parameter Name	Parameter Symbol	Value	Unit
Controller Gain	K	20	p.u.
Governor Time Constant	T_1	0.25	s
Governor Derivative Time Constant	T_2	0	s
Servo Time Constant	T_3	0.1	s
High Pressure Turbine Factor	K_1	0.3	p.u.
High Pressure Turbine Factor	K_2	0	p.u.
Intermediate Pressure Turbine Time Constant	T_5	10	s
Intermediate Pressure Turbine Factor	K_3	0.4	p.u.
Intermediate Pressure Turbine Factor	K_4	0	p.u.
Medium Pressure Turbine Time Constant	T_6	0.4	s
Medium Pressure Turbine Factor	K_5	0.3	p.u.
Medium Pressure Turbine Factor	K_6	0	p.u.
High Pressure Turbine Factor	T_4	0.3	s
Low Pressure Turbine Time Constant	T_7	0	s
Low Pressure Turbine Factor	K_7	0	p.u.
Low Pressure Turbine Factor	K_8	0	p.u.
High Pressure Turbine Rated Power	$P_{\mathrm{r,hp}}$	$P_{\mathrm{r,Gen,hp}}$	MW
Low Pressure Turbine Rated Power	$P_{\mathrm{r,lp}}$	$P_{\mathrm{r,Gen,lp}}$	MW
Valve Opening Time	V_{o}	0.1	p.u./s
Valve Closing Time	V_{c}	-0.1	p.u./s
Minimum Gate Limit	P_{min}	0.1	p.u.
Maximum Gate Limit	P_{max}	1	p.u.

Table A.4.: Electrical data used for the ac overhead transmission lines.

Parameter Name	Parameter Symbol	Value	Unit
Tower Type		Donaumast	
Number of Line Circuits	n_{sys}	2	
Nominal frequency	f_{n}	50	
Subconductor Material		Aluminium	
Thermal Current	I_{th}	2, 72	kA
Rated Voltage	V_{r}	380	kV
Number of Subconductors	$n_{\mathrm{Subcond.}}$	4	
Bundle Spacing	$d_{\mathrm{Subcond.}}$	0.4	m
Subconductor Resistance	R'	0.108	Ω/km
Equivalent Radius	GMR	9.138	mm

Table A.5.: Electrical data of used for the dc transmission cable.

Parameter Name	Parameter Symbol	Value	Unit
Thermal Current	I_{th}	$1,825$	kA
Rated Voltage	V_{r}	320	kV
Cross section	d	2500	mm^2
Resistance (20°C)	R'	0.0072	Ω/km
Reactance	L'	0.117	mH/km
Capacitance	C'	0.3	µH/km

Table A.6.: Electrical data used for the HVDC converter models.

Parameter Name	Parameter Symbol	Value	Unit
Rated Power	S_{r}	1280	MVA
Rated Ac Voltage	$V_{\text{r,ac}}$	110	kV
Rated Dc Voltage	$V_{\text{r,dc}}$	320	kV
Arm Reactor, Resistance	R_{arm}	7	Ω
Arm Reactor, Reactance	L_{arm}	0.001	mH
No-load Losses	$P_{\text{loss},0}$	3000	kW
Switching Losses	$P_{\text{loss},1}$	0	kW/A
Conducting Losses	$P_{\text{loss},2}$	0	Ω
Commutation Reactance	L_{c}	0.01	Ω
Submodule Capacitance	C_{SM}	20	mF
Number of Submodules per Arm	N_{SM}	100	

B. Load Flow Simulation Scenarios

This appendix gives details on the steady state load flow scenarios that make up the basis for the dynamic verification of the proposed converter and grid control concepts. For reference, the generalized ac benchmark system introduced in section 4.4 on page 52 is shown in figure B.1.

B.1. Parameterization of the Ac Grid Components

The components that make up the ac grid are parameterized to cause a power transfer from the northern to the southern region. The resulting load flow is constant over all dc grid cases, i.e. there is only one scenario regarding the ac grid. The parameters for the components active and reactive power provision is given in table B.1. The ac grid is asymmetric, with a significant transfer of almost 3000 MW between the regions. The bulk of the reactive power is provided by the generators, with most by the southern, which is due to the voltage drop over the long ac lines.

B.2. Parameterization of the Dc Grid Components

The dc system's steady state load flow is solely defined by the operating points of the converters. The different simulation grids are parameterized to show a particular scenario. Thus, all three cases have a different dc-side load flow. The load flow for all grids and all active converters is shown in table B.2. For each converter, the steady state reference points for active power P_{ac} and dc voltage V_{dc} is shown. The converters have a rated power $S_{\mathrm{r}} = 1280\,\mathrm{MVA}$.

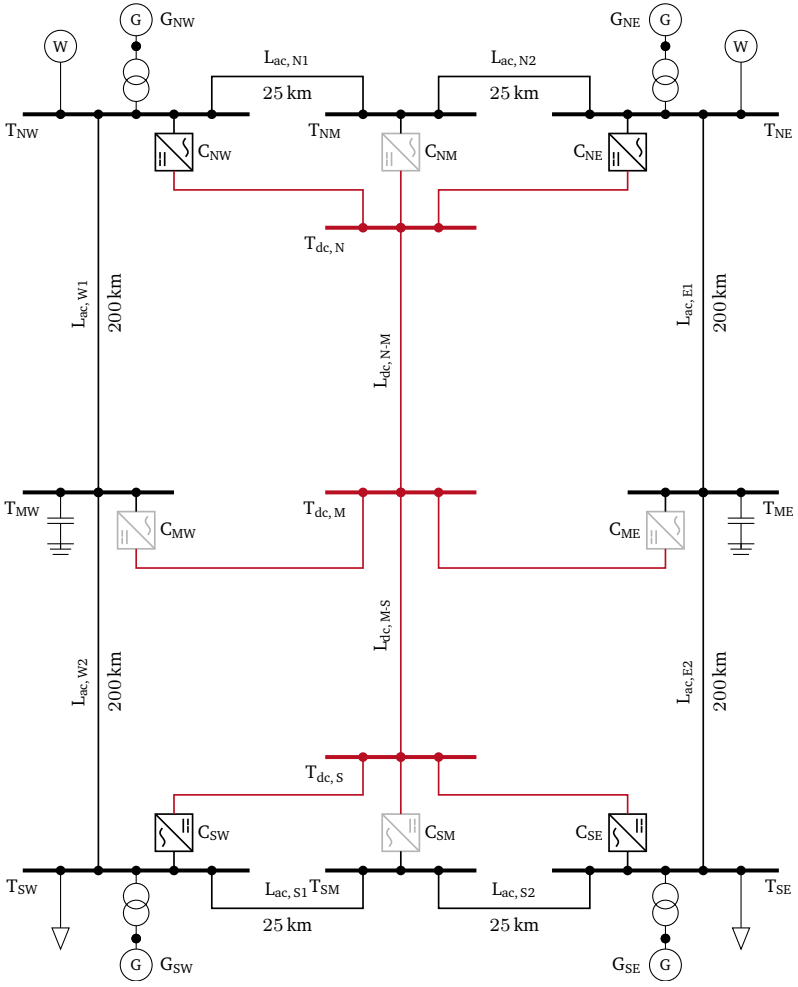

Figure B.1.: General model of the power system used in this work including line lengths. The gray units represent the optional converters of the MTDC.

Table B.1.: Steady state load flow parameters of the ac components

Type	**Component**	$\boldsymbol{P}$ MW	$\boldsymbol{Q}$ Mvar
Generator	G_{NW}	$658,4$	$324,5$
	G_{NE}	$658,4$	$323,2$
	G_{SW}	$658,4$	$719,4$
	G_{SE}	$658,4$	$719,4$
Load	L_{SW}	$3410,3$	0
	L_{SE}	$3410,3$	0
RES	W_{NW}	$2300,0$	0
	W_{NE}	$2300,0$	0
Compensation	C_{MW}	0	$-272,3$
	C_{ME}	0	$-272,3$

Table B.2.: Steady state load flow parameters of the dc converters for each grid. The steady state slack is marked bold.

Grid	**Reference points**	**Converter**							
		C_{NW}	C_{NM}	C_{NE}	C_{MW}	C_{ME}	C_{SW}	C_{SM}	C_{SE}
202r	P_{ac} in MW	**-624**		-600			600		600
	V_{dc} in pu	**1,02**		1,02			1,011		1,011
303r	P_{ac} in MW	-1000		-1000	200	**143**	800		800
	V_{dc} in pu	1,034		1,034	1,02	**1,02**	1,014		1,014
222r	P_{ac} in MW	-800	**-849**	-800			800	800	800
	V_{dc} in pu	1,02	**1,02**	1,02			1,007	1,007	1,007

C. Bibliography

References for Chapter 1

[1.1] International Energy Agency. *World Energy Outlook 2020*. Paris.: IEA. URL: https://www.iea.org/reports/world-energy-outlook-2020.

[1.2] ENTSO-E Transmission System Operators. *Ten-Year Network Development Plan 2020*. ENTSO-E, 2020. URL: https://consultations.entsoe.eu/system-development/tyndp2020/.

[1.3] Übertragungsnetzbetreiber. *Netzentwicklungsplan Strom 2035 (2021). zweiter Entwurf*. CC-BY-4.0. URL: https://www.netzentwicklungsplan.de/de/netzentwicklungsplaene/netzentwicklungsplan-2035-2021.

[1.4] JWG C4/B4/C1 - 604. *Influence of Embedded HVDC Transmission on System Security and AC Network Performance*. Cigré, 2013.

[1.5] Working Group B4.58. *Control Methodologies for Direct Voltage and Power Flow in a Meshed HVDC Grid*. Cigré, 2017.

References for Chapter 2

[2.1] D. van Hertem, O. Gomis-Bellmunt, and J. Liang. *HVDC Grids*. John Wiley & Sons Inc, 2016. ISBN: 1118859154.

[2.2] K. Sharifabadi, L. Harnefors, et al. *Design, Control and Application of Modular Multilevel Converters for HVDC Transmission Systems*. John Wiley & Sons Inc, 2016.

[2.3] JWG C4/B4/C1 - 604. *Influence of Embedded HVDC Transmission on System Security and AC Network Performance*. Cigré, 2013.

[2.4] Cigré Working Group B4.57. *Guide for the Development of Models for HVDC Converters in a HVDC Grid*. Cigré, 2014.

[2.5] L. Zhang, L. Harnefors, and H. P. Nee. "Power-Synchronization Control of Grid-Connected Voltage-Source Converters." In: *IEEE Transactions on Power Systems* 25.2 (2010), pp. 809–820. DOI: 10.1109/TPWRS.2009.2032231.

[2.6] Cigré Working Group B4-52. *HVDC grid feasibility study*. 2011.

[2.7] L. Harnefors, N. Johansson, et al. “Interarea Oscillation Damping Using Active-Power Modulation of Multiterminal HVDC Transmissions.” In: *IEEE Transactions on Power Systems* 29.5 (2014), pp. 2529–2538. DOI: 10.1109/TPWRS.2014.2306826.

[2.8] Joint Working Group B4/B5.59. *Protection and local control of HVDC-grids*. Cigré, 2018.

References for Chapter 3

[3.1] J. P. Torreglosa, P. García-Triviño, et al. “Control strategies for DC networks. A systematic literature review.” In: *Renewable and Sustainable Energy Reviews* 58 (2016), pp. 319–330. DOI: 10.1016/j.rser.2015.12.314.

[3.2] J. J. Justo, F. Mwasilu, et al. “AC-microgrids versus DC-microgrids with distributed energy resources: A review.” In: *Renewable and Sustainable Energy Reviews* 24 (2013), pp. 387–405. DOI: 10.1016/j.rser.2013.03.067.

[3.3] M. S. Mahmoud, N. M. Alyazidi, and M. I. Abouheaf. “Adaptive intelligent techniques for microgrid control systems. A survey.” In: *International Journal of Electrical Power & Energy Systems* 90 (2017), pp. 292–305. DOI: 10.1016/j.ijepes.2017.02.008.

[3.4] H. Kakigano, Y. Miura, and T. Ise. “Distribution Voltage Control for DC Microgrids Using Fuzzy Control and Gain-Scheduling Technique.” In: *IEEE Transactions on Power Electronics* 28.5 (2013), pp. 2246–2258. DOI: 10.1109/TPEL.2012.2217353.

[3.5] N. L. Diaz, T. Dragičević, et al. “Intelligent Distributed Generation and Storage Units for DC Microgrids—A New Concept on Cooperative Control Without Communications Beyond Droop Control.” In: *IEEE Transactions on Smart Grid* 5.5 (2014), pp. 2476–2485. DOI: 10.1109/TSG.2014.2341740.

[3.6] A. Maknouninejad, Z. Qu, et al. “Optimal, Nonlinear, and Distributed Designs of Droop Controls for DC Microgrids.” In: *IEEE Transactions on Smart Grid* 5.5 (2014), pp. 2508–2516. DOI: 10.1109/TSG.2014.2325855.

[3.7] K. Rouzbehi, A. Miranian, et al. “Optimized control of multi-terminal DC GridsUsing particle swarm optimization.” 2013 15th European Conference on Power Electronics and Applications (EPE). In: *15th European Conference on Power Electronics and Applications (EPE)*. 2013. DOI: 10.1109/EPE.2013.6634326.

[3.8] H. Abdi, S. D. Beigvand, and M. La Scala. “A review of optimal power flow studies applied to smart grids and microgrids.” In: *Renewable and Sustainable Energy Reviews* 71 (2017), pp. 742–766. DOI: 10.1016/j.rser.2016.12.102.

[3.9] Working Group B4.58. *Control Methodologies for Direct Voltage and Power Flow in a Meshed HVDC Grid*. Cigré, 2017.

[3.10] K. Rouzbehi, J. I. Candela, et al. “Multiterminal DC grids. Operating analogies to AC power systems.” In: *Renewable and Sustainable Energy Reviews* 70 (2017), pp. 886–895. DOI: 10.1016/j.rser.2016.11.270.

[3.11] A. Egea-Alvarez, J. Beerten, et al. “Hierarchical power control of multiterminal HVDC grids.” In: *Electric Power Systems Research* 121 (2015), pp. 207–215. DOI: 10.1016/j.epsr.2014.12.014.

[3.12] K. Rouzbehi, A. Miranian, et al. “A hierarchical control structure for multi-terminal VSC-based HVDC grids with GVD characteristics.” In: *2013 International Conference on Renewable Energy Research and Applications (ICRERA)*. International Conference on Renewable Energy Research and Applications (ICRERA) (Madrid, Spain). 2013, pp. 996–1001. ISBN: 978-1-4799-1464-7. DOI: 10.1109/ICRERA.2013.6749897.

[3.13] D. van Hertem, O. Gomis-Bellmunt, and J. Liang. *HVDC Grids*. John Wiley & Sons Inc, 2016. ISBN: 1118859154.

[3.14] F. Sass, T. Sennewald, et al. “System security of hybrid AC-HVDC-systems challenges and new approaches for combined security assessment, preventive optimization and curative actions.” In: *Global Energy Interconnection* 1.5 (2018), pp. 585–594.

[3.15] M. Baradar, M. R. Hesamzadeh, and M. Ghandhari. “Modelling of multi-terminal HVDC systems in optimal power flow formulation.” In: *IEEE Electrical Power and Energy Conference*. DOI: 10.1109/EPEC.2012.6474944.

[3.16] M. Baradar, M. R. Hesamzadeh, and M. Ghandhari. “Second-Order Cone Programming for Optimal Power Flow in VSC-Type AC-DC Grids.” In: *IEEE Transactions on Power Systems* 28.4 (2013), pp. 4282–4291. DOI: 10.1109/TPWRS.2013.2271871.

[3.17] M. Baradar. “Modeling of Multi Terminal HVDC Systems in Power Flow and Optimal Power Flow Formulations.” KTH Royal Institute of Technology, 2013.

[3.18] J. Rimez. “Optimal operation of hybrid AC/DC meshed grids.” TU Eindhoven, The Netherlands, 2014.

[3.19] J. Rimez and R. Belmans. “A combined AC/DC optimal power flow algorithm for meshed AC and DC networks linked by VSC converters.” In: *International Transactions on Electrical Energy Systems* 25.10 (2015), pp. 2024–2035. DOI: 10.1002/etep.1943.

[3.20] R. Wiget and G. Andersson. “Optimal power flow for combined AC and multi-terminal HVDC grids based on VSC converters.” In: *IEEE Power and Energy Society General Meeting*. DOI: 10.1109/PESGM.2012.6345448.

[3.21] V. Saplamidis, R. Wiget, and G. Andersson. “Security constrained Optimal Power Flow for mixed AC and multi-terminal HVDC grids.” In: *IEEE Eindhoven PowerTech*. 2015. DOI: 10.1109/PTC.2015.7232616.

[3.22] T. Sennewald, F. Linke, and D. Westermann. “Preventive and Curative Actions by Meshed Bipolar HVDC-Overlay-Systems.” In: *IEEE Transactions on Power Delivery* 35.6 (2020), pp. 2928–2936. DOI: 10.1109/TPWRD.2020.3011733.

[3.23] M. Aragüés-Peñalba, J. Beerten, et al. “Optimal power flow tool for hybrid AC/DC systems.” In: *11th IET Int. Conf. AC and DC Power Transmission*. 2012. DOI: 10.1049/cp.2015.0077.

[3.24] M. Aragüés-Peñalba, A. E. Alvarez, et al. “Optimal power flow tool for mixed high-voltage alternating current and high-voltage direct current systems for grid integration of large wind power plants.” In: *IET Renewable Power Generation* 9.8 (2015), pp. 876–881. DOI: 10.1049/iet-rpg.2015.0028.

[3.25] N. Meyer-Huebner, F. Gielnik, et al. “Dynamic optimal power flow in AC networks with multi-terminal HVDC and energy storage.” In: *IEEE Innovative Smart Grid Technologies - Asia (ISGT-Asia)*. 2016. DOI: 10.1109/ISGT-Asia.2016.7796402.

[3.26] N. Meyer-Huebner, M. Suriyah, and T. Leibfried. “N-1-Secure Optimal Generator Redispatch in Hybrid AC-DC Grids with Energy Storage.” In: *IEEE PES Innovative Smart Grid Technologies Conference Europe (ISGT-Europe)*. 2018, pp. 1–6. ISBN: 978-1-5386-4505-5. DOI: 10.1109/ISGTEurope.2018.8571779.

[3.27] N. Meyer-Huebner, M. Suriyah, and T. Leibfried. “Distributed Optimal Power Flow in Hybrid AC–DC Grids.” In: *IEEE Transactions on Power Systems* 34.4 (2019), pp. 2937–2946. DOI: 10.1109/TPWRS.2019.2892240.

[3.28] N. Meyer-Huebner, S. Weck, et al. “N-1-Secure Dispatch Strategies of Embedded HVDC Using Optimal Power Flow.” In: *IEEE Power & Energy Society General Meeting (PESGM)*. 2018, pp. 1–5. ISBN: 978-1-5386-7703-2. DOI: 10.1109/PESGM.2018.8586478.

[3.29] F. Bennewitz, S. Weck, et al. “Determination of optimal converter operating points regarding static voltage stability and system losses in hybrid transmission systems.” In: *11th IEEE International Conference on Compatibility, Power Electronics and Power Engineering (CPE-POWERENG)* (Cadiz, Spain). 2017, pp. 16–21. ISBN: 978-1-5090-4963-9. DOI: 10.1109/CPE.2017.7915138.

[3.30] F. Bennewitz, S. Weck, et al. “Evaluation of master control for connection of wind farms to multiple asynchronous power systems with HVDC systems.” In: *52nd International Universities Power Engineering Conference (UPEC)* (Heraklion). 2017, pp. 1–6. ISBN: 978-1-5386-2344-2. DOI: 10.1109/UPEC.2017.8231872.

[3.31] W. Feng, L. A. Tuan, et al. “A New Approach for Benefit Evaluation of Multiterminal VSC –HVDC Using A Proposed Mixed AC/DC Optimal Power Flow.” In: *IEEE Transactions on Power Delivery* 29.1 (2014), pp. 432–443. DOI: 10.1109/TPWRD.2013.2267056.

[3.32] S. Rodrigues, R. T. Pinto, et al. “Optimal power flow control of VSC-based multiterminal DC network for offshore wind integration in the north sea.” In: *IEEE Journal of Emerging and Selected Topics in Power Electronics* 1.4 (2013), pp. 260–268.

[3.33] A. Fuchs, J. Garrison, and T. Demiray. “A security-constrained multi-period OPF for the locational allocation of automatic reserves.” In: *IEEE Manchester PowerTech*. IEEE Manchester PowerTech (Manchester, United Kingdom). IEEE, 2017, pp. 1–6. ISBN: 978-1-5090-4237-1. DOI: 10.1109/PTC.2017.7981181.

[3.34] R. Wiget. “Combined AC and Multi-Terminal HVDC Grids – Optimal Power Flow Formulations and Dynamic Control.” en. ETH Zurich, 2015.

[3.35] D. Kourounis, A. Fuchs, and O. Schenk. “Toward the Next Generation of Multiperiod Optimal Power Flow Solvers.” In: *IEEE Transactions on Power Systems* 33.4 (2018), pp. 4005–4014. DOI: 10.1109/TPWRS.2017.2789187.

[3.36] J. Kardos, D. Kourounis, and O. Schenk. “Two-Level Parallel Augmented Schur Complement Interior-Point Algorithms for the Solution of Security Constrained Optimal Power Flow Problems.” In: *IEEE Transactions on Power Systems* 35.2 (2020), pp. 1340–1350. DOI: 10.1109/TPWRS.2019.2942964.

[3.37] M. Schanen, F. Gilbert, et al. “Toward Multiperiod AC-Based Contingency Constrained Optimal Power Flow at Large Scale.” In: *Power Systems Computation Conference*. 2018, pp. 1–7. DOI: 10.23919/PSCC.2018.8442590.

[3.38] M. Baradar and M. R. Hesamzadeh. “A stochastic SOCP optimal power flow with wind power uncertainty.” In: *IEEE PES General Meeting | Conference & Exposition* (National Harbor, MD, USA). 2014, pp. 1–5. DOI: 10.1109/PESGM.2014.6939790.

[3.39] C. D. Barker and R. Whitehouse. “Autonomous converter control in a multi-terminal HVDC system.” In: *9th IET International Conference on AC and DC Power Transmission (ACDC 2010)*. 9th IET International Conference on AC and DC Power Transmission (ACDC 2010). 2010, pp. 1–5. DOI: 10.1049/cp.2010.0988.

[3.40] T. K. Vrana, J. Beerten, et al. “A classification of DC node voltage control methods for HVDC grids.” In: *Electric Power Systems Research* 103 (2013), pp. 137–144. DOI: 10.1016/j.epsr.2013.05.001.

[3.41] K. Sharifabadi, L. Harnefors, et al. *Design, Control and Application of Modular Multilevel Converters for HVDC Transmission Systems*. John Wiley & Sons Inc, 2016.

[3.42] F. Thams, J. A. Suul, et al. “Stability of DC voltage droop controllers in VSC HVDC systems.” In: *2015 IEEE Eindhoven PowerTech*. 2015 IEEE Eindhoven PowerTech. 2015, pp. 1–7. DOI: 10.1109/PTC.2015.7232614.

[3.43] A.-K. Marten, D. Westermann, et al. “Factors Influencing Oscillations within Meshed HVDC Grids and Implications for DC Voltage Control.” In: *Critical information infrastructures security. 9th International Conference, CRITIS 2014, Limassol, Cyprus, October 13-15, 2014, Revised selected papers / Christos G. Panayiotou, Georgios Ellinas, Elias Kyriakides, Marios M. Polycarpou (eds.)* (Cham). Ed. by C. G. Panayiotou, G. Ellinas, et al. LNCS sublibrary. SL 4, Security and cryptology 8985. Cham: Springer, 2016, pp. 178–189. ISBN: 978-3-319-31664-2.

[3.44] A.-K. Marten, F. Sass, and D. Westermann. “Continuous DC node voltage control characteristic for multi-terminal and meshed HVDC grids.” In: *IEEE Int. Energy Conf. (ENERGYCON)*. 2016. DOI: 10.1109/ENERGYCON.2016.7513927.

[3.45] K. Rouzbehi, A. Miranian, et al. “A novel approach for voltage control of multi-terminal DC grids with offshore wind farms.” In: *IEEE ECCE Asia Downunder*. 2013 IEEE ECCE Asia Downunder (ECCE Asia 2013) (Melbourne, VIC). 2013, pp. 965–970. DOI: 10.1109/ECCE-Asia.2013.6579223.

[3.46] B. Berggren, R. Majumder, and N. Johansson. "A generic VSC HVDC primary control structure suitable for stability studies." In: *EPRI HVDC & FACTS Conference*. 2013.

[3.47] B. Berggren, K. Linden, and R. Majumder. "DC Grid Control Through the Pilot Voltage Droop Concept —Methodology for Establishing Droop Constants." In: *IEEE Transactions on Power Systems* 30.5 (2015), pp. 2312–2320. DOI: 10.1109/TPWRS.2014.2360585.

[3.48] K. Rouzbehi, A. Miranian, et al. "Optimized Control of Multi-Terminal DC Grids Using Particle Swarm Optimization." In: *EPE Journal* 24.2 (2014), pp. 38–49. DOI: 10.1080/09398368.2014.11463883.

References for Chapter 4

[4.1] Cigré Working Group B4.57. *Guide for the Development of Models for HVDC Converters in a HVDC Grid*. Cigré, 2014.

[4.2] ABB. "XLPE Land Cable Systems. User´s Guide." In: (). (Visited on 06/21/2020).

[4.3] P. Kundur. *Power System Stability and Control*. McGraw-Hill Professional, 1994.

[4.4] T. K. Vrana, Y. Yang, et al. "The CIGRÉ B4 DC Grid Test System." In: (2013).

[4.5] Working Group B4.72. *DC grid benchmark models for system studies*. Cigré, 2020.

[4.6] F. Sass, T. Sennewald, et al. "Mixed AC high-voltage direct current benchmark test system for security constrained optimal power flow calculation." In: *Transmission Distribution IET Generation* 11.2 (2017), pp. 447–455. DOI: 10.1049/iet-gtd.2016.0993.

References for Chapter 5

[5.1] Working Group B4.58. *Control Methodologies for Direct Voltage and Power Flow in a Meshed HVDC Grid*. Cigré, 2017.

[5.2] B. Berggren, R. Majumder, and N. Johansson. "A generic VSC HVDC primary control structure suitable for stability studies." In: *EPRI HVDC & FACTS Conference*. 2013.

[5.3] H. Prautzsch, W. Boehm, and M. Paluszny. *Bézier and B-spline techniques*. Mathematics and visualization. Berlin and New York: Springer, 2002. xiv, 304. ISBN: 3540437614.

Own publications

[1] S. Weck, I. Talavera, and J. Hanson. “Behaviour of Mechanically Switched Capacitors with Damping Network (MSCDN) during Energization.” In: (2015). URL: https://www.semanticscholar.org/paper/Behaviour-of-Mechanically-Switched-Capacitors-with-Weck-Talavera/c75254e4b9932ca826707f2476e722262464a106.

[2] S. Weck, J. Hanson, et al. “Planning and design of a European HVDC grid divided into feasible protection zones.” In: *IEEE Electrical Power and Energy Conference (EPEC). 12-14 Oct. 2016*. 2016 IEEE Electrical Power and Energy Conference (EPEC) (Ottawa, ON, Canada). IEEE Electrical Power and Energy Conference et al. Piscataway, NJ: IEEE, 2016, pp. 1–6. ISBN: 978-1-5090-1919-9. DOI: 10.1109/EPEC.2016.7771777.

[3] S. Weck, S. Rüberg, and J. Hanson. “Planning and Design Methodology for a European HVDC Overlay Grid.” In: *13th IET International Conference on AC and DC Power Transmission (ACDC 2017). 14-16 Feb. 2017*. 13th IET International Conference on AC and DC Power Transmission (ACDC 2017) (Manchester, UK). IET International Conference on AC and DC Power Transmission, Institution of Engineering and Technology, and ACDC. Stevenage: IET, 2017, 26 (6 .)–26 (6 .) ISBN: 978-1-78561-421-7. DOI: 10.1049/cp.2017.0026.

[4] I. Talavera, S. Weck, and J. Hanson. “Sensitivity analysis of the Electrical Stresses in Mechanically Switched Capacitors with Damping Network due to Components’ Tolerances.” In: (2015). URL: https://doi.org/10.24084/repqj13.437.

[5] I. Talavera, S. Weck, and J. Hanson. “Sensitivity analysis of the Electrical Stresses in Mechanically Switched Capacitors with Damping Network due to Components’ Tolerances.” In: (2015). URL: https://www.semanticscholar.org/paper/Sensitivity-analysis-of-the-Electrical-Stresses-in-Talavera-Weck/4d66eb67040623952b4cd63aa4487dc0bec73cf6.

[6] Ignacio Talavera, Sebastian Weck, et al. “Influence of the Quality Factor and Tuning Frequency on the Behaviour and Investment Costs of Mechanically Switched Capacitors with Damping Network.” In: (2015).

[7] F. Bennewitz, S. Weck, et al. “Determination of optimal converter operating points regarding static voltage stability and system losses in hybrid transmission systems.” In: *11th IEEE International Conference on Compatibility, Power Electronics and Power Engineering (CPE-POWERENG)* (Cadiz, Spain). 2017, pp. 16–21. ISBN: 978-1-5090-4963-9. DOI: 10.1109/CPE.2017.7915138.

[8] F. Bennewitz, S. Weck, et al. “Evaluation of master control for connection of wind farms to multiple asynchronous power systems with HVDC systems.” In: *52nd International Universities Power Engineering Conference (UPEC)* (Heraklion). 2017, pp. 1–6. ISBN: 978-1-5386-2344-2. DOI: 10.1109/UPEC.2017.8231872.

[9] N. Meyer-Huebner, S. Weck, et al. “N-1-Secure Dispatch Strategies of Embedded HVDC Using Optimal Power Flow.” In: *IEEE Power & Energy Society General Meeting (PESGM)*. 2018, pp. 1–5. ISBN: 978-1-5386-7703-2. DOI: 10.1109/PESGM.2018.8586478.

[10] P. Krasselt, S. Weck, and T. Leibfried. “Voltage-based harmonic compensation using MCCF state estimation.” In: *2014 IEEE Innovative Smart Grid Technologies - Asia (ISGT ASIA)*. 2014 IEEE Innovative Smart Grid Technologies - Asia (ISGT ASIA). 2014, pp. 284–289. ISBN: 2378-8542. DOI: 10.1109/ISGT-Asia.2014.6873804.

[11] M. Böhringer, S. Choudhury, et al. “Sizing and Placement of Community Energy Storage Systems using Multi-Period Optimal Power Flow.” In: *2021 IEEE Madrid PowerTech*. 2021 IEEE Madrid PowerTech. 2021, pp. 1–6. DOI: 10.1109/PowerTech46648.2021.9494820.

[12] L. Steinhaeuser, M. Coumont, et al. “Comparison of RMS and EMT Models of Converter-Interfaced Distributed Generation Units Regarding Analysis of Short-Term Voltage Stability.” In: *NEIS 2019; Conference on Sustainable Energy Supply and Energy Storage Systems*. NEIS 2019; Conference on Sustainable Energy Supply and Energy Storage Systems. 2019, pp. 1–6.